Application of Label-free Microfluidic Technologies for the Enrichment, Expansion and

Characterization of Circulating Tumor Cells in Pancreatic Cancer

by

Lianette Rivera Báez

A dissertation submitted in partial fulfillment
of the requirements for the degree of
Doctor of Philosophy
(Chemical Engineering)
in The University of Michigan
2017

Doctoral Committee:

      Professor Sunitha Nagrath, Chair
      Professor Ronald G. Larson
      Professor Shuichi Takayama
      Professor Greg Thurber

Lianette Rivera Báez

lianette@umich.edu

ORCID iD: 0000-0003-0696-2959

DEDICATION

To my parents, Linda A. Báez and Victor M. Rivera, for their unconditional love and
encouragement throughout my academic journey.

ACKNOWLEDGEMENTS

It is through the support, mentorship, and love of so many individuals that I am blessed to fulfill my goal of earning my Ph.D. degree. It is my great privilege to acknowledge all the people and resources that made this dissertation possible.

First and foremost, I would like to thank my advisor, Dr. Sunitha Nagrath. I was fortunate to have a mentor who encouraged my intellectual curiosity and guided me throughout the completion of my Ph.D. She helped me grow as a scientist in ways that I never thought possible. I am eternally grateful for her support and advice along every step of my graduate school journey. I thank her for believing in me and encouraging me to realize my fullest potential. She is a role model for me in both my personal and professional career.

I would like to give a special thanks to my committee members, Dr. Ronald Larson, Dr. Greg Thurber and Dr. Shuichi Takayama, for providing me with guidance throughout this entire process. I appreciate all of their valuable feedback as well as their investment of time to help me further my research.

I am also grateful to my collaborators, Dr. Diane Simeone, Dr. Kyle Cuneo, Dr. Vaibhav Sahai, Dr. Max Wicha, Dr. Geeta Mehta, Dr. Ebrahim Azizi, and Dr. David Lubman for helping me translate my research and provide clinical meaning to my projects. Thank you for providing me with the necessary resources and support as well as the meaningful feedback.

I am very thankful to have been a part of the Nagrath Lab family. This is where I received immense support and guidance over the course of my Ph.D. They were instrumental in the completion of my projects and provided me with meaningful feedback every step of the way. Thank you to the members of the Takayama Lab for providing me with guidance and support as well. I would also like to acknowledge the Lurie Nanofabrication Facility (LNF), the Microscopy and Image Analysis Lab (MIL), the DNA Sequencing Core, and the Unit for Laboratory Animal Medicine (ULAM) at the University of Michigan.

I am grateful for the opportunity to work with a great team of researchers in the pancreatic CTC field: Mina Zeinali, Chris Dunlay, Kara Schradle, Anisha Patel, Heather Cameron, Lidong Wang, Meredith Morgan, and Mackenzie Goodwin. I also would like to thank Ines Lohse, Ramdane Harouaka, Shreya Raghavan, and Shamileh Fouladdel for their scientific input towards my work.

Special thanks to the cancer patients who donated their blood for my studies. Without their help, none of this work would have been possible. Thank you for putting your trust in my research and giving a personal meaning to it.

Words cannot express how thankful I am to the College of Engineering Office of Graduate Education, specifically Kim Elliot, Shira Washington, and Mike Nazareth. As a Latina in STEM, my development as a professional goes hand-in-hand with my desire to promote diversity and equality, which are key to innovation and greater societal contributions. The Office of Graduate Education allowed me to pursue this personal commitment. I was able to help inspire underrepresented minorities to pursue STEM by participating in various recruiting events over the past five years. These events served as a

TABLE OF CONTENTS

LIST OF TABLES

LIST OF FIGURES

LIST OF APPENDICES

ABSTRACT

Pancreatic cancer is a devastating disease with a 5-year survival rate of less than 6%. This poor outcome is heavily associated with the resistance of pancreatic tumors to chemotherapy and radiation therapy. The profound heterogeneity of pancreatic tumors is speculated to be one key reason for this intense resistance. To improve treatment outcome, it is crucial to evaluate the characteristics of pancreatic adenocarcinoma for each patient and to select or adapt tumor-specific therapy accordingly. Over the past ten years, evidence has pointed to the importance of circulating tumor cells (CTCs) in the spread of cancer through the metastatic process. These cells are shed by the primary tumor into the circulation and are now known to be key players in metastasis. CTCs are believed to be a good surrogate biomarker for not only prognosis, but also for cancer detection and development of personalized treatment.

This thesis outlines the use of a microfluidic device that allows for the isolation, expansion, and characterization of pancreatic CTCs. This device, named the Labyrinth, allows for the label free isolation of CTCs at a high throughput of 2.5mL/min, offering a biomarker independent CTC characterization platform to study heterogeneity among CTC subpopulations in pancreatic cancer. This Labyrinth allows for a high CTC recovery of 92%, while having a WBC removal of 89%.

The Labyrinth technology was used to investigate the use of CTCs for clinical prognosis. This was performed through a clinical study, where CTCs were isolated and enumerated for over 150 treatment naïve patient samples. CTC counts were then correlated

with treatment efficacy (surgery, chemotherapy or radiotherapy). Our results show for all treatment options there is a statistically significant decrease in CTC counts. Lastly, a trend was observed between the decrease of CTC count and higher overall survival among all treatment options.

The employment of the Labyrinth for heterogeneity studies was then explored in this thesis. CTCs isolated from pancreatic cancer patients were monitored for markers associated with the cancer EMT cell population including CK, CD24, and CD90. We found that there were cells that were CK+, which were then characterized as CTCs, that also had CSC markers associated with them in most cases. Tissue analysis (IHC) from one of the patients showed the existence of this CTC subpopulation close to the tumor vasculature, suggesting their aggressiveness and ability to travel to the bloodstream to invade other organs.

This thesis also describes *in vitro and in vivo* characterization performed on expanded CTCs. CTCs were isolated from ten pancreatic cancer patients with locally advanced disease using the Labyrinth and expanded *in vitro* for over 30 days. Expansion of CTCs was successfully achieved for 3 of the samples, giving a 30% success rate. CTC cultures were then characterized in both 2D (adherent) and 3D (spheroid) *in vitro* conditions. Furthermore, an *in vivo* study model (NOD SCID mice) was created, being the first ever pancreatic CDX model. This model displayed metastasis across several organs after only 3 weeks of CTC injection.

CTCs could serve as a potential avenue for a non-invasive alternative to diagnosing and treating pancreatic cancer and thereupon preventing the development of the disease. The isolation and expansion of CTCs, the heterogeneous population of cells that promote metastasis, can provide meaningful information to elucidate the process of pancreatic tumorigenesis to preempt its fatal result.

CHAPTER 1. CIRCULATING TUMOR CELLS (CTCs) IN PANCREATIC CANCER: UNDERSTANDING THEIR CLINICAL UTILITY AND ISOLATION TECHNOLOGIES

1.1 Abstract

The study of circulating tumor cells (CTCs) has been made possible by many technological advances in its isolation. Their isolation has seen many fronts, but each technology brings forth a new set of challenges to overcome. Microfluidics has been a key player in the capture of CTCs and their downstream analysis, with the aim of shedding light into their clinical application in cancer and metastasis. Researchers have taken diverging paths to isolate such cells from blood, ranging from affinity-based isolation targeting surface antigens expressed on CTCs, to label free isolations taking advantage of the size differences between CTCs and other blood cells. For both major groups, many microfluidic technologies have reported high sensitivity and specificity for capturing CTCs. However, the question remains as to the superiority among these two isolation techniques, specifically to identify different CTC populations. This chapter highlights the key aspects of affinity and label free microfluidic CTC technologies, and discusses which of these two would be the highest benefactor for the study of CTCs.

1.2 Pancreatic Cancer

Pancreatic cancer is the fourth leading cause of cancer death in the United States. The overall 5-year survival rate among patients with pancreatic cancer is only 6%. This year, an estimated 46,420 new cases and 39,590 deaths from pancreatic cancer are expected to occur in the United State[1]. For all stages combined, the 1- and 5-year relative survival rates of pancreatic cancer are 27% and 6%, respectively. Surgery, chemotherapy, and radiation therapy are treatment options for pancreatic cancer patients. Even for these 20% patients with a tumor that has been surgically removed, the 5-year survival is about 20% to 25%. Although no evidence of metastatic is observed at the time of diagnosis, the median overall survival of those patients ranges only from 9 to 10 months [2].

The poor outcome of pancreatic cancer treatment could partly be due to the resistance of pancreatic tumors to chemotherapy and radiation therapy[3]. Even if pancreatic tumors initially respond to treatment, they will eventually become resistant to the conventionally used agents. The profound heterogeneity and ongoing genetic instability of pancreatic tumors is speculated to be the key reason for this intense resistance. To improve treatment outcome, it is crucial to evaluate the characteristics of pancreatic adenocarcinoma for each patient and to select or adapt personalized tumor-specific therapy accordingly. Early identification of treatment response would provide valuable information for clinicians to select the most appropriate therapy and potentially limit toxicity in non-responding patients.

1.3   Circulating Tumor Cells (CTCs)

Emerging evidence has pointed to the importance of circulating tumor cells (CTCs) in the spread of cancers [4]. Circulating tumor cells (CTCs), suspected of being precursors of metastasis [5] have been in the spotlight as a liquid biopsy [6-9] and are being investigated as surrogate biomarkers for clinical trials [10-12]. These are cells shed by a primary tumor into the blood circulation, and can potentially form secondary tumors en route (**Figure 1.1**) [13]. Being intermediaries between the primary and metastatic tumors, they offer insights into both; additionally, they can reveal key aspects of the metastatic cascade. Indeed, there have been studies showing that CTCs have distinct identities, consisting of a heterogeneous mix of populations similar to both the primary tumor and the metastatic tumor [14-17]. CTCs can be detected from the peripheral blood of patients and hold the promise of being a real-time biomarker for cancer detection and management [18]. The utility of CTCs as a predictive and prognostic marker has been explored in various cancers like breast cancer, prostate cancer, liver cancer and colorectal cancer [19-22]. For example, in patients with metastatic breast cancer, the number of CTCs before and during treatment is an independent predictor of progression free and overall survival [21,23]. Nagrath *et al.* surveyed patients from different cancers in advanced stages over their treatment course and showed that changes in CTC numbers could predict changes in the tumor burden [24]. Elevated CTC numbers during treatment have also been shown to be associated with disease progression [23,25]. Furthermore, it is possible to monitor treatment resistant mutations and telomerase activity in CTCs, thereby demonstrating their clinical utility in therapeutic monitoring [26,27].

The current gold standard for CTC isolation is the CellSearch (Veridex, USA) system, which is the only FDA approved system for CTC detection [22]. This test separates

epithelial cells using magnetic beads functionalized with antibodies against the epithelial cell adhesion molecule (EpCAM) [28]. Using the CellSearch system it has been shown that CTCs have prognostic utility in breast, prostate and colon cancers [22]. However, there is considerable cell loss (~20-40%) caused by the inability of the platform to detect cancer cells with a reduced EpCAM expression, such as those that have gone through or are in the process of going through epithelial to mesenchymal transition (EMT) [29,30]. Currently, CTC studies are geared toward finding genetic signatures that could guide treatment decisions [31].

The major challenge toward accomplishing more with these entities lies in their rarity; CTCs are detected at a frequency of tens among billions of blood cells [32,33]. The vast majority of the background cells (blood cells) contribute to not only challenges in enriching for the target cells (CTCs), but purity issues during downstream molecular analyses [4]. Attempts at increasing CTC concentrations by expanding them after isolation are hardened by viability issues [33]. Hence, the key aspects of any CTC isolation technology should be a high recovery rate without compromising on purity and viability [33]. A plethora of microfluidic technologies have risen to these challenges with promising results. With their help, scientists are now analyzing complex fluids such as blood *in vitro,* as a means to investigating non-invasive alternatives for cancer detection, patient prognosis and therapeutic monitoring [18].
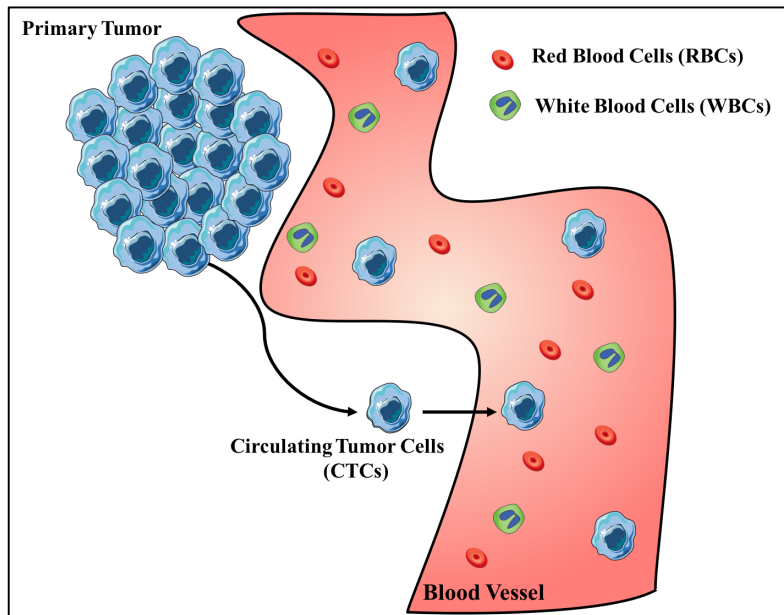
Figure 1.1 Circulating Tumor Cells (CTCs)

1.4 Microfluidic Technologies for CTC Isolation

Microfluidic devices have had a major impact on the field of CTC research [34]. Such efforts have been facilitated by the automation of labor-intensive experimental processes involved in isolating and characterizing CTCs. Consequently, the microfluidic field has been gaining pace especially in the handling of rare cells [33,35]. Different materials ranging from traditional silicon and glass to elastomers have been used for making these devices. The use of poly-dimethylsiloxane (PDMS), an elastomer, has made rapid prototyping an easy and preferred method, leading to widespread use of microfluidic technologies for investigating CTCs [32,36]. Their smaller dimensions allow precise manipulation of fluid flow in the devices, translating to better control over the cells. The smaller volumes also demand lesser reagents [4]. Microfluidics for CTC isolation gained popularity with the reporting of the CTC-chip [24]. Over the years, many similar and innovative microfluidic platforms have come up, each exploiting specific properties of CTCs to separate them from blood cells. The different properties may be biological such as target antigens, or physical such as size,

density, deformity [32,37]. This review compares the two most widely-used methodologies, namely affinity-based (biological) and size-based (physical) techniques of CTC isolation.

Microfluidic technologies are mainly categorized by their exploitation of CTCs' distinctive (i) biochemical properties or (ii) biophysical properties. The former is based on the expression of cell surface markers, while the latter includes size, deformability, density, and electric charge [38]. For either of these strategies, it is imperative that developing an optimal CTC isolation method meet the following criteria: (i) high recovery, (ii) high purity of CTCs by removal of contaminating blood cells, and (iii) high system throughput to ensure handling of large sample volumes as expected for clinical settings [33]. Capture or retrieval of CTCs is followed by identification by immunocytochemical staining demonstrating positive signals for Cytokeratin(s) and the nuclear stain DAPI (4',6-diamidino-2-phenylindole), with the absence of the leukocyte marker CD45 [24]. Although there are multiple methods in each category of isolation, this chapter will focus on two of the most prevalent methods for CTC isolation- affinity, and size based or label free isolation (Figure 1.2). Here, new progress and emerging technologies are highlighted for each isolation method. Furthermore, the advantages and disadvantages based on their downstream applications for studying subpopulations and heterogeneity, genomic characterization, cell expansion, *in vivo* studies, and single cell analysis of CTCs will be elucidated (Table 1.1).
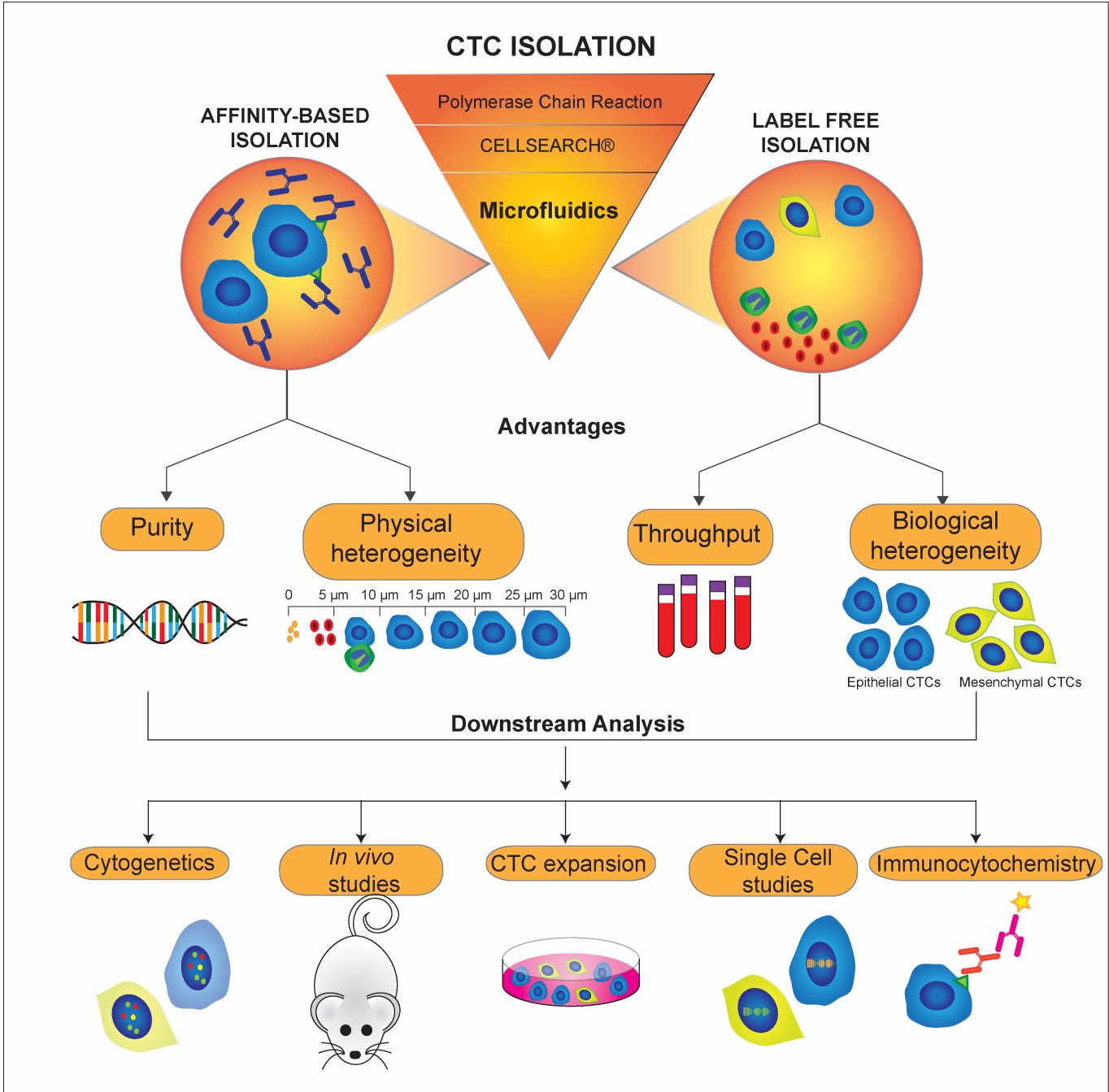
Figure 1.2 Strategies for CTC isolation

1.5 Immunoafinity Based Technologies

Affinity-based isolation, the main principle of technologies such as CellSearch and the CTC-chip [24], make use of the affinity of an antigen to its corresponding antibody. Antigens or surface markers present on the membrane of CTCs are targeted by specific antibodies that can be immobilized onto a solid surface [39]. The antigens (and hence the cell) can grab on to the target antibodies under ideal conditions of affinity-binding. The bound cells can then be separated and/or identified for further assays, depending on their method of capture. The commonly used antigen for CTC capture is the Epithelial Cell Adhesion Molecule (EpCAM), and is considered to be expressed by epithelial cancers [18]. While recent findings have brought into question the utility of EpCAM in identifying the aggressors [40], it still remains the most widely adopted choice of capture antibodies. Combinations of antibodies are also being employed to widen the capture net [41].

The first immuno-capture microfluidic technology for CTCs, the CTC-chip [24] consists of a series of 100 μm tall microposts coated with antibodies against EpCAM, which can interrogate whole blood for capturing CTCs expressing the antigen. The novelty of this technology lay in its ability to capture CTCs from whole blood with high sensitivity and viability [24]. Following this, a number of technologies with varying degrees of sensitivity and purity were developed. The high-throughput microsampling unit (HTMSU) [42], Cell Enrichment and Extraction (CEE) channel [43], Herringbone HB-chip [36], the graphene oxide chip [44], all performing EpCAM-based CTC capture, improved upon the above parameters. The NanoVelcro CTC chip, another recently developed immuno-capture device, makes use of nano-sized structures coated with EpCAM for CTC capture [45,46]. Other nanomaterial based devices for CTC interrogation include the incorporation of

carbon nanotubes (CNTs), the porous nature of which provides a high surface area for cell interaction [47,48], and the use of TiO_2 nanofibres (TINFs) produced by electrospinning techniques for anti-EpCAM capture of CTCs [49]. The GEDI chip developed in 2010 [50] has a similar approach and enabled CTC isolation with an antibody against prostate specific membrane antigen (PSMA). They showed an improved purity over the CTC-chip and also opened the arena for achieving CTC capture with antibodies other than EpCAM. Different antibodies or antibody cocktails have since been explored to capture different populations that may have been otherwise missed. Galletti *et al.* demonstrated the use of anti-Her2 for studying CTCs from breast and gastric cancer [51]. Yu *et al.* used a mixture of EpCAM, EGFR and Her2 to capture CTCs from breast cancer [15]. Pecot *et al.* used an interesting approach wherein the cells are tagged with a cocktail of antibodies, followed by capture by functionalized microchannels [41,43]. Aptamers, which can be synthesized to specifically recognize target molecules on the surface of cells, have also been incorporated for CTC capture [52]. An example of a microfluidic aptamer-based affinity capture device was demonstrated by Sheng et al. for capture of colorectal CTCs from whole blood [52].

Immuno-magnetic capture is also a popular method of affinity isolation wherein magnetic beads coated with antibodies are made to bind to cells in order to separate CTCs from WBCs [4]. MACS (magnetic activated cell sorter) is one such technology, that operates by separating cells bound to magnetic beads through a target antibody followed by purification under a magnetic field [53]. Magnetic nanoparticles are also used to label cancer cells through anti-EpCAM to separate them from blood cells with high efficiency at a high flow rate of 10 ml hr^{-1} [54]. Another novel immunological approach was developed by Shi *et al.* in which microbubbles enveloped with anti-EpCAM were used for CTC isolation [46].

Affinity-based capture also holds negative selection under its umbrella, in which the target cells are made to pass through while leukocytes (WBCs) are targeted by antibodies against CD45 [55,56], and/or CD15 [56]. The advantage of negative selection lies in its capability of isolating CTCs that may or may not express epithelial markers [56]. This approach has been used in the CTC-iChip [56], and by Wu *et al.* [57]. Casavant *et al.* used magnetic beads coated with anti-CD45 as a means of depleting white blood cells as a precursor to CTC enrichment [55].

Recently, the limitation of throughput for immuno-affinity isolation of CTCs has been addressed by several devices operating at high flow rates. Of note are the demonstrations of the CTC-iChip [56] which is a combination of affinity and size-based isolation, an integrated high-throughput device by Liu *et al.* [58], immunomagnetic isolation at 10 ml hr^{-1} [54], and the OncoBean Chip, a purely affinity isolation device operating at 10 ml hr^{-1} developed in our lab [59]. An *in-vivo* CTC detection technology, the GILUPI CellCollector, employing anti-EpCAM to capture CTCs in venous blood flow is also an example of a system that demonstrates CTC isolation even under high physiological shear stresses (20 ml min^{-1}) present in the circulation [60].

1.5.1   Advantages of immune-affinity based approaches

CTC enumeration, albeit a very important part of CTC studies, is only one aspect of the clinical utility of these cells. And while CTC numbers have been correlated to prognosis [22], characterization of these cells is still an unmet and essential demand. With numerous technologies for CTC enrichment and enumeration in development, studies are now shifting gear toward addressing what these cells are capable of. With this in mind, a number of recent findings have been published showing CTCs' ability to metastasize [61],

their tumor forming potential [15,62], their potential utility as agents showing drug response [15] and their clonal heterogeneity [16]. Baccelli *et al.* showed that CTCs are a diverse pool of cells, and may contain a certain population of metastasis initiating cells (MICs) which would be the aggressive cells [61].

Because of the principle of capture, affinity-based isolation offers very high specificity of the recovered CTCs since the target CTCs are validated by the capture antigen in addition to identification by immunostaining procedures. The method also enables recovery of an assorted pool of CTCs, regardless of morphological considerations such as size. Whilst many size-based technologies may capture CTCs with high yields, the wide variability of CTC sizes previously reported [13,32,63] makes the smaller CTCs highly probable to be missed in size based techniques which are usually biased towards the larger cells. Affinity-based methods can indiscriminately capture such populations, and are also capable of doing the same without the need for preprocessing steps such as dilution or red blood cell lysis, invariably required by physical separation techniques [63]. The specificity also allows for better downstream analysis which may have clinical utility. One such application was demonstrated by Maheswaran *et al.* who performed downstream sequencing studies on CTCs captured on an affinity platform (the CTC-chip) from lung cancer patients [26].

Affinity capture also allows high purity of the recovered CTCs [50]. Since these cells are rare, any downstream applications are dictated by the accompaniment of contaminating blood cells. The specificity of CTC capture by affinity techniques is also reflected in the retained background cells. The targeted capture not only allows for low non-specific retention but also washes away most red blood cells, eliminating the need for red blood cell lysis as a

precursor to blood analysis. The highly specific and pure CTC yield facilitated by immuno-capture combined with the viability is also conducive to CTC culture and expansion [64].

In order to efficiently study the diverse properties of CTCs, their isolation needs to be tailor-made to answer the relevant biological questions. Immuno-affinity offers a beautiful platform for this purpose as antibody-based capture techniques can be customized to target different subpopulations of CTCs. A combination of antibodies consisting of the traditional anti-EpCAM with another marker, or successive captures with the respective individual antibodies can yield the desired populations [41,65]. For instance, Riethdorf *et al.* utilized HER2 as a target agent to identify CTCs among patients undergoing neoadjuvant treatment for a HER2 inhibitor [11]. Pecot *et al.* used an interesting cocktail of antibodies to target both epithelial cells and potential CTCs undergoing epithelial-mesenchymal transition (EMT) [41]. Affinity-based capture techniques are thus widely capable of specific targeting of cell subpopulations, an area requiring deeper attention as more and more studies illuminate tumor cell heterogeneity [17].

Affinity based methods also offer high utility with respect to capturing rare events such as CTC clusters [4,16]. These clusters may sometimes be larger than the detection range of physical separation techniques and/or may clog the channels [66]. CTC clusters are believed to have more metastasizing capability than single cells in the circulation [16,67]. Larger clusters containing a heterogeneous mix of cells may also be captured if some of the cells in the cluster express the target antigen, thereby achieving capture of potentially "unfamiliar" populations using "known" targets. Furthermore, the generally lower shear experienced by cells in immuno-affinity capture [59] also enables collection of CTCs that are possibly circulating in conjunction with platelets. Platelets are believed to be implicated in

metastasis and platelet-enveloped CTCs may be important in disease progression as they are able to evade immune surveillance [16,68-70].

1.5.2 Disadvantages of affinity-based approaches

Traditionally preferred for CTC isolation [18], affinity methods have validated their utility in a number of CTC analyses studies. However, they suffer from a few limitations. Throughput is a major concern with antibody-based CTC recovery chips such as the CTC-chip and HB-chip [56]. This is due to the limited shear conditions under which affinity binding occurs [59]. Microfluidic flow-based affinity capture requires optimal velocity and shear conditions for antibody-antigen binding [24,39]. A very high shear may disrupt any bonds if formed, while a very low shear is conducive to non-specific cell binding [59]. An optimal binding condition would provide adequate capture of target cells, with minimal amount of blood cells retained; in other words, a high efficiency with minimal contamination. These optimal conditions limit the velocity of flow during capture. The CTC-chip and its successors operating on similar principles therefore had an operating flow rate of 1-3 ml hr^{-1} [59]. In the CTC-chip itself, increasing the flow rate from 1 to 3 ml hr^{-1} diminished the capture efficiency [24]. This limits the blood volume that can be analyzed due to the time constraints it places on the experiments. Of late, a number of technologies have overcome the throughput limitation by introducing novel designs to circumvent the issue of optimal binding conditions [59].

Epithelial-to-mesenchymal (EMT) transition, a process in which cells lose their epithelial characteristics and become more mesenchymal, is believed to be an important process hampering the study of CTCs on the basis of EpCAM alone [13]. As these cells undergo the change, their EpCAM expression decreases, and they may be missed by

EpCAM targeted capture [13,71]. These EMT-undergoing cells are believed to be important players in metastasis [71] and may be able to provide useful information about the dissemination of tumor cells [13]. Combinations of antibodies are therefore being employed to capture not only epithelial cells, but also the mesenchymal ones [41].

Many microfluidic affinity based technologies employ surface modifications for antibody conjugation and immobilization [24]. This poses problems as many of the bonds are irreversible and cannot be easily degraded and/or may affect the viability of these rare cells themselves in the process [72]. Subsequent assays such as single cell analysis and CTC derived xenografts may not be feasible in such cases due to cell release difficulties [72]. Many genetic analyses performed on CTCs thus depend on nucleic acid extraction from the pool of cells captured on these devices, which may create background noise as the captured populations contain impurities such as blood cells [4].

1.6   Biomarker independent technologies for the isolation of CTCs

The use of physical properties allows a label-free isolation, aimed to overcome biased cell selection using biological-based separation methods. This approach allows the isolation of intact cells without stressing their plasma membrane through antibody binding, which is a vital aspect for further downstream characterization of CTCs. This method tends to exploit the size differences among CTCs and other blood components. More specifically, CTCs have been shown to have a diameter of 13 to 25 μm in diameter [35], larger than the rest of the blood cells such as leukocytes with diameter ranges from 8 to 11μm [73], and red blood cells (RBCs) with diameters in the range of 5–9 μm [74]. Label-free approaches can be classified into three main categories- filtration, hydrodynamic chromatography, and

dielectrophoresis (DEP). In addition, other novel methods exploiting the physical properties of CTCs including acoustic separation have also been recently developed [75-77].

Compared to immuno-affinity based approaches, the biomarker independent CTC isolation technologies are still evolving. While many of these have been optimized with cancer cell lines, few have been validated with clinical specimens. The use of cancer cell lines as a CTC model makes an ideal model for the optimization of a new technology. However, cell lines do not represent the heterogeneous morphology found in clinical specimens [78]. Some subpopulations of CTCs will indeed be more deformable and smaller than cancer cell lines. Therefore, using cell lines to optimize new technologies may not serve as a true test of efficiency as their clinical utility will only be determined by testing clinical samples [79]. Here, the recent label free microfluidic technologies that have been (i) characterized using cancer cell lines and (ii) clinically proven to work by isolating CTCs from patient samples over the past 5 years are summarized.

Filtration Methods

Membrane-based filtration is one of the first methods used for isolating CTCs, being a relatively straightforward and low cost technique. This method captures target cells using constrictions based on cell size and deformability [79]. Most of the reported membranes have pore sizes around 7–8 μm diameter, with few reporting on membranes with pore size diameters up to 11 μm [80]. Vona *et al.* proposed ISET (Isolation by Size of Epithelial Tumor Cells), a commercially available technology that uses a polycarbonate membrane-filter [81]. This is a filtration method that uses 8 μm cylindrical pores to capture CTCs. However, its large variability in CTC capture efficiency and low purity caused by membrane clogging left opportunities for further improvement. Integrating microfabricated filtration

membranes into microfluidic devices has since emerged as an optimized approach for CTC separation. Materials such as polycarbonate [82-84], parylene-C [85-87], nickel [88] and silicon [89] have demonstrated to provide the appropriate membrane surface area and porosity to enhance CTC capture.

In 2010, Lin *et al.* published one of the first label free methods to be tested using clinical samples [86]. With a total of 57 human samples from various cancer types, this parylene membrane microfilter identified CTCs in 51 out of 57 patients compared to only 26 patients with the CellSearch method. Tan *et al.* published a label free biochip that uses physical structures or pillars to trap single cells without having cell buildup [90]. Lim *et al.* developed a silicon microsieve that contains a dense array of pores to isolate CTCs at a flow rate of 1 ml min^{-1} [89]. Zhou *et al.* designed a device that aims for the filter-based capture of viable cells with the use of a design that incorporates a low mechanical stress, termed the separable bilayer (SB) microfilter [91]. The high viability of enriched CTCs using the SB microfilter allows for functional analysis and on-chip expansion of CTCs, further discussed in the next section of this review.

Hydrodynamic Methods

Hydrodynamic based approaches have shown the highest throughput capability [80]. Recently, inertial migration of particles has been introduced and applied in various studies to achieve high throughput separation based on particle size [92]. Briefly, the particles migrate and are focused in microchannels due to the equilibrium of two inertial lift forces which act on the particles in opposite directions- shear gradient lift force and wall lift force [92]. Some other technologies exploit a secondary flow called Dean flow that takes place in curvilinear channels [93]. In addition, hydrophoresis is another approach that makes use of

rotational flow for separating particles based on size [94]. Another approach, termed deterministic lateral displacement (DLD), in which microposts are strategically placed to divide the flow into several laminar streams, are also used for separation of CTCs from blood cells [95]. Regardless of the type of hydrodynamic based technologies, the goal is to impart different flow velocities based on cell size differences to separate the target cells with high efficiency. Lee *et al.* developed a lab-on-a disc platform that utilizes centrifugal force to rapidly transfer unprocessed whole blood samples from one chamber to another [96]. The selective isolation of CTCs was achieved through the use of a commercially available track-etched polycarbonate membrane filter on a lab-on-a-disc system. Hou *et al.* developed a spiral microchannel for separation of CTCs using centrifugal forces, a principle known as Dean Flow Fractionation [63]. Using this device, they were able to detect a subpopulation of CTCs that were positive for CD133, a phenotypic marker characteristic of stem-like behavior in lung cancer cells [97]. Furthermore, this device was the first inertial device to demonstrate the capacity to process blood samples with a high hematocrit. Our group also demonstrated theoretical investigation of inertial separation of CTCs using cascaded spiral microfluidics [98]. Sollier *et al.* developed the Vortex Chip, which uses micro-scale vortices and inertial focusing to isolate CTCs [99]. Hyun *et al.* developed a parallel multi-orifice flow fractionation (p-MOFF) device in which contraction/expansion microchannels were placed in a parallel configuration for CTC separation [100]. This device was shown to use inertial forces to isolate CTCs from 24 breast cancer patients at a high throughput [100]. Warkiani *et al.* developed the trapezoid chip, which uses a trapezoidal design and exploits Dean forces and lift forces to isolate CTCs [101]. More recently, Warkiani *et al.* reported an ultra-high-throughput spiral device [102] consisting of three stacked spiral

17

microfluidic chips with two inlets and two outlets, in which the combination of the inertial and Dean forces focuses the cells at certain equilibrium positions of the channel cross-section. Khoo *et al.* published an improved version of this technology with clinical validation using a large number of clinical samples, and also performed downstream immunophenotyping and molecular analyses from isolated CTCs [103], further discussed in the next section.

Dielectrophoresis Methods

DEP methods are used for isolating CTCs based on cell membrane and cell dielectric properties. Using this approach CTCs are generally separated by their response to non-uniform electrical fields, since the polarizability of a cell relies on its composition, morphology and the frequency of the applied electric field [104]. Therefore, using DEP based devices allows the identification of cells with different phenotypes. However, compared to the two previously described approaches, DEP-based technologies do not show high selectivity and have low throughputs (<1 ml hr^{-1}) [79].

Shim *et al.* used a continuous flow microfluidic processing chamber into which CTCs are isolated from clinical samples using a combination of DEP, sedimentation and hydrodynamic lift forces [105]. Choi *et al.* designed a novel DC (direct current) impedance-based microcytometer that detects changes in DC impedance and exploits size differences between CTCs and blood cells [106].

1.6.1 Advantages of label free approaches

Physical CTC separation methods have the potential to address the shortcomings involved in biological marker based separation methods. Overcoming biased cell selection using molecular markers permits heterogeneity studies on CTCs, where different

subpopulations can be analyzed. As previously mentioned, CTCs that have undergone EMT are associated with a loss of expression for epithelial markers, such as EpCAM and Cytokeratin (CK). As a result, the most aggressive cancer cells could potentially be the least likely to be captured and identified using EpCAM based technologies [35,41].

Isolated CTCs can be collected without compromising cell viability or gene expression, which in turn enables their molecular characterization. For instance, Shim *et al.* used continuous flow dielectrophoretic field flow fractionation (DEP-FFF) method and also performed molecular studies on isolated CTCs [105]. For a colon primary tumor, 10% of the stained cells had the KRAS G13D mutation, which also reflected the number of cells that were stained positive for Cytokeratin. Warkiani *et al.* performed DNA fluorescence *in situ* hybridization (FISH) to evaluate the HER2 status of isolated CTCs from breast cancer patients using their trapezoid chip [101,102]. Their results showed that the presence of HER2+ CTCs varied across samples and was also observed in samples derived from patients with HER2- tumors (2 out of 5). A later spiral technology by Warkiani *et al.* characterized CTCs that were isolated from lung and breast cancer patients by immunophenotyping using cell markers such as Pan-cytokeratin, CD45, CD44, CD24 and EpCAM, fluorescence in-situ hybridization (FISH) for EML4-ALK fusion or targeted somatic mutation analysis [102]. They also demonstrated the ability to find matching mutations of the EGFR gene in CTCs, cell-free DNA and tumors biopsy specimens [103].

Unlike most immuno-affinity based isolation systems which only allow on-chip growth of CTCs [64] due to difficulties in post-separation retrieval [72], inertial-based technologies simplify CTC culture by using off-chip standard cell culture techniques since cells can be recovered in suspension. This advantage gives rise to multiple CTC expansion approaches,

such as the use of extracellular matrix (matrigel or collagen) for CTCs growth or a 3D culture system [64]. Sollier *et al.* showed that A549 cells processed with the Vortex Chip and collected in a well-plate proliferate over 3 days [99]. Similarly, Hou *et al.* used their device to demonstrate this advantage by successfully culturing sorted MCF-7 cells for 5 days [63]. Moreover, they also show the retrieval of intact MCF-7 cell clusters. Despite the high throughput of the label free devices, these technologies are still able to preserve cell clusters, which are of greater interest to study the metastatic ability of CTCs [16,107].

In vivo application of label free technologies is still very limited. In one study Zhou *et al.* used their SB microfilter device to perform the only *in vivo* study currently published using a label-free microfluidic device [91]. This group demonstrated capture and expansion of CTCs originated from two mouse model systems from 4T1 and 4T07 cells. They demonstrated tumor formation after injection of 4T1 CTCs and 4T07 CTCs into BALB/C mice. Their study also showed similar tumorigenicity for both CTCs recovered by the SB microfilter.

1.6.2 Disadvantages of label free approaches

Although on average CTCs are shown to be larger than leukocytes, there is a significant overlap in the size of CTCs and leukocytes that may hinder label-free separation efforts. The FDA approved CellSearch system has detected CTCs with cell diameters ~4 μm [28]. Marinnucci *et al.* also reported findings on CTCs that were the same size or smaller than leukocytes [108]. This variability in size can cause the loss of CTCs or, to overcome such problem, low sample purity. Although greatly studied, filter-based approaches encounter clogging difficulties when processing large sample volumes [109]. This results in flow rate discrepancies, which could endanger important performance characteristics ranging from

device reproducibility to cell viability for post-processing analysis. Regarding the use of

DEP, one concern is the effect on the viability of CTCs due to the generation of gases like

hydrogen and oxygen. Moreover, elevated temperatures may also affect cell viability [110]

Table 1.1 Summary of microfluidic technologies for CTC isolation

AFFINITY BASED ISOLATION						
Technology	Capture Method	Flow Rate	Capture Efficiency details	Purity	Clinical utility	Reference
CTC-chip	Affinity (EpCAM)	1 ml hr^{-1}	>60% with different concentrations of NCI-H1650 cells (lung)	50%	Tested with 116 patient samples (lung, prostate, pancreatic, breast and colon cancers)	[24]
HB-chip	Affinity (EpCAM)	1.2 ml hr^{-1}	92% with PC3 cells (prostate)	14%	Tested with 15 prostate cancer patient samples	[111]
GEDI chip	Affinity (PSMA)	1 ml hr^{-1}	85% in blood with LNCaP cells (prostate)	68%	Tested with 20 prostate cancer patient samples	[50]
NanoVelcro Chip	Affinity (EpCAM)	0.5 ml hr^{-1}	>80% with LNCaP, PC3, C4-2 cells (prostate)	------	Tested with 40 prostate cancer patient samples	[45]
Graphene oxide chip	Affinity (EpCAM)	1 ml hr^{-1}	>85% with MCF7 cells (breast)	------	Tested with 20 patient samples (breast, pancreatic and lung cancer)	[44]
OncoBean Chip	Affinity (EpCAM)	10 ml hr^{-1}	>80% with H1650 (lung) and MCF7 (breast) cancer cell lines	------	Tested with 6 patient samples (lung, breast and pancreatic cancer)	[59]
LABEL FREE ISOLATION						
Device Name	Capture Method	Flow Rate	Capture Efficiency details	Purity	Clinical utility	Reference
p-MOFF	Size-based (Hydrodynamic)	0.6 ml min^{-1}	93.75% with MCF-7 91.60% with MDA-MB-231	------	Tested with 24 breast cancer patient samples	[100]
N/A	Size-based (Filter Pilar type)	Operating pressure of 5 KPa	80% with AGS, N87, HepG2, Huh7, CAL27, and FADU	89% mean purity	Tested with 5 metastatic lung cancer patient samples	[90]

N/A	Size-based (Hydrodynamic)	3 ml hr^{-1}	>85% with MCF-7	-----	Tested with 20 metastatic lung cancer patient samples	[63]
SB microfilter	Size-based (Filter Pore type)	Gravity driven flow	83±3%with MCF-7 78±4% with MDA-MB-231	-----	Tested with 6 metastatic breast cancer mouse model and 1 metastatic colorectal cancer patient samples	[91]
N/A	Size-based (Filter Pore type	>225 ml hr^{-1}	>90% with RT4, T24, HT-1080, LNCaP, MCF-7, SK-BR-3 and MDA-MB-231	------	Tested with 51 patient samples (prostate, colorectal, breast and bladder cancer)	[86]
Vortex Chip	Size-based (Hydrodynamic)	7.5mL/20min	15.9 % A54816.8% OVCAR5 17.7% MCF-7 17.7%M395 18.2% PC3	57-94%	Tested with 12 patient samples (breast and lung cancer)	[99]
N/A	Size-based (Centrifugal Force)	3mL whole blood in 20 s (2400 rpm)	61% with MCF-7	------	Tested with 23 patient samples (lung and gastric cancer)	[96]
N/A	Size-based (DEP)	10 ml hr^{-1}	70-80% With MDA-MB-435 and MDA-MB-231	-----	Tested with late stage colon cancer patients	[105]
N/A	Size-based (DC-Impedance)	13 µl min^{-1}	88% with OVCAR-3	---	Tested with 24 breast cancer patients samples	[106]
Dean Flow Fractionation	Size-based (Hydrodynamic)	7.5 mL blood/ 8 min	>80 % withMDA-MB-231, MCF-7 and T24	~4 log depletion	Tested with 10 patient samples (breast and lung cancer)	[101]
N/A	Size-based (Hydrodynamic)	7.5mL/10min	87.6% with MCF-7 76.4% with T24	------	Tested with 10 patient samples	[102]

N/A	Size-based (tilted-angle standing surface acoustic waves (taSSAWs)	20 μL min^{-1}	>83% with MCF-7, HeLa, UACC903M-GFP, LNCaP	~90% removal rate of WBCs	(breast and lung cancer)	
					Tested with 3 metastatic breast cancer patients	[75,76]

1.7   The future of microfluidic technologies for the study of CTCs

The field of microfluidics and CTCs is rapidly evolving. In fact, last year the journal Lab on a Chip published a complete CTC-themed issue that highlights some of the new technologies along with review papers targeting different aspects, both technical and clinical [112]. Both affinity and size-based methods of CTC isolation need dramatic improvements to their systems to enable highly efficient CTC recovery [4]. Affinity isolations have the potential to provide key information that may be missed by size-based techniques as outlined in their advantages above. Refinements such as increasing throughputs, targeting multiple populations with the use of multiple antibodies may be the important steps needed to further improve these technologies. Use of novel materials and reversible conjugation of antibodies that may enable CTC release will offer more robust CTC analysis modules, as these CTCs can then be utilized for downstream assays [72,113]. Using immuno-capture methods, different populations of CTCs can be segregated for further analysis that may be able to identify tumorigenic CTCs, such as xenograft studies [114]. As for label free technologies, their future is driven by exploiting the physical differences between CTCs and leukocytes, with the goal of achieving selective separation of CTCs. For example, cell deformability can be combined with CTC size properties to develop new label free technologies [79]. Regardless of the technological approach, emerging technologies should not compromise throughput or sensitivity, while still targeting heterogeneous CTCs.

Past the improvement upon current microfluidic technologies, we predict an increase in effort on the molecular understanding of CTCs, encompassing multiple downstream analyses that advances personalized treatment. The comprehensive investigation of CTCs

25

is hampered by their low numbers, making this one of the biggest challenges in this field [33]. For better understanding of CTCs, we expect to see an increase in technologies that not only aim for the isolation of such cells, but also to perform *in situ* expansion on such devices. For example, Zhang *et al.* expanded CTCs from early lung cancer patients using a 3D co-culture device that used cancer associated fibroblasts and a combination of collagen and matrigel to resemble the tumor microenvironment [64]. Moreover, we predict an increase of label free methods for straightforward retrieval of CTCs from microfluidic chips, leading to *ex vivo* expansion. Recently, several groups have successfully performed *ex vivo* expansion of CTCs from breast cancer [115] and from colon cancer [116]. Overcoming the limitation of low numbers of CTCs by expanding them will allow for phenotypic and genomic characterization of CTCs, which in turn will lead to personalized treatment strategies. The establishment of cell lines from cancer patients could guide the course of drug therapy at an individual level to ensure optimal treatment outcome.

Heterogeneity among CTCs makes their isolation and characterization a challenging task. The molecular characterization of CTCs has exposed information on the genotype and phenotype of these tumor cells and demonstrated a striking heterogeneity of CTCs [117]. Thus, the present setback is the identification of the functional properties of the different CTC subsets. This could be achieved through the use of functional assays that reveal the biology of CTCs, with particular emphasis on the discovery of the most aggressive subset of CTCs. At present, such assays are limited by the very low concentration and yield of CTCs. Single cell studies could serve as an essential tool to assess the heterogeneity among CTCs. The study of single CTCs by their molecular characterization provides high clinical

relevance by potentially aiding in early cancer detection and revealing new therapeutic targets for personalized medicine [118,119].

While CTC enumeration has shown tremendous potential in terms of clinical utility [120], researchers are now exploring their validity as more than just an enumerable measure of disease intensity or spread. The prognostic and diagnostic utilities of CTCs are now an area of extensive focus through analysis of gene expression profiles [121], single cell analysis [14], RNA and DNA studies [5,26], and cytogenetics to detect gene amplifications or rearrangements [122,123]. Examining epigenetic modifications and their after effects on the metastatic cascade may be a useful tool for determining therapeutic efficacy. Chimonidou *et al.* analyzed CTCs and cell-free DNA in breast cancer for methylation of a tumor suppressor gene SOX17 promoter [124]. In another study of breast cancer, methylation of a metastasis suppressor gene was studied in primary tumor and CTCs, and the authors investigated its effect on survival [125]. Whilst the rarity of CTCs offers challenges in enrichment and downstream assay feasibilities, cell free DNA suffer from similar limitations with respect to available amounts [126]. Malara *et al.* identified CTC subpopulations that are enriched for methylated DNA using folate receptors. Methylation of cancer cells is believed to be implicated in metastasis, and the authors found that patients with high methylation of CTCs had a risk of relapse [126]. Albeit CTC enumeration has seized attention as a possible endpoint in clinical trials due to their prognostic utility [127], a comprehensive analysis of the genome and epigenome will likely compliment traditional diagnostic methods and open the arena for more frequent patient monitoring, leading to timely decision making. This also has the potential to circumvent invasive tissue biopsies [24]. CTCs also offer a means of personalized therapeutics through their tumorigenic

capabilities [114]. CTC expansion on in vitro microfluidic models, one of which has recently been demonstrated by our group [64] propose a method for testing of drugs or drug combinations [114,128], which can be used to make quicker decisions for therapeutic management. Resistance to treatment can be monitored similarly by analyzing CTCs [26]. The idea that all of the above could possibly be accomplished through venipuncture, a relatively low discomfort means to achieving a higher end, in a field as vast and challenging as cancer management, is both an exciting and formidable notion. The future of CTCs thus looks promising toward patient-specific tumor monitoring.

CHAPTER 2. DEVELOPMENT, OPTIMIZATION AND VALIDATION OF LABYRINTH AS A MICROFLUIDIC TECHNOLOGY FOR THE ISOLATION OF PANCREATIC CTCs

2.1 Abstract

Circulating tumor cells (CTCs) present in the blood are the instruments of metastasis and are of high biological and clinical relevance. Single-cell technologies are playing an increasing role in profiling CTCs in the peripheral blood for detection and real time monitoring of cancer metastasis. CTCs also help in identifying its distinct drivers. However, current approaches are limited to manual selection of CTCs, which hinders the unbiased comprehensive study of CTCs on a single cell level. A unique label-free microfluidic "Labyrinth" device is presented in this chapter. This device isolates CTCs at a high throughput of 2.5mL/min, offering the first biomarker independent single cell isolation and genomic characterization platform to study heterogeneous CTC subpopulations in cancer patients. The Labyrinth takes advantage of inertial forces on the microscale in curved geometries to differentially focus cells based on their size. This novel strategy of multi-course path traversing across inner loops to outer loops yielding highest hydrodynamic path length enabling focusing of white blood cells (WBCs), leading to high recoveries (> 90%) and efficient separation of WBCs from CTCs, resulting in high purity (~ 200 WBCs/mL), even in whole blood samples without any pre-processing. The Labyrinth platform allows a thorough molecular understanding of the heterogeneity among CTCs. This platform also shows CTCs potential as a biomarker to non-invasively evaluate tumor progression and response to treatment in cancer patients.

2.2 Introduction

Circulating tumor cells (CTCs) found in the peripheral blood of cancer patients are often indicators of metastasis[21,28]. The study of CTCs has clinical potential as a prognostic biomarker to predict treatment efficacy, progression-free survival, and overall survival in patients[10,30,129-131]. Additionally, molecular analysis of CTCs using single cell technologies may facilitate the selection of molecularly targeted therapies and assess the efficacy of these treatments.

The clinical and biological relevance of CTCs makes their isolation an active area of research, bolstered by several technological developments over the past 15 years[132]. Technologies taking advantage of microfluidic principles to manipulate cells are establishing their niche and are an active area of research[110]. These approaches are mainly categorized by their exploitation of either CTCs' distinctive biological or physical properties (Table 1.1). The most widely used microfluidic approach for isolation of CTCs is immune-affinity capture using distinct antibodies targeting molecules that are expressed exclusively on tumor cells and are absent in blood cells. The most commonly used antibody for isolation of CTCs is against the epithelial cell adhesion molecule (EpCAM). This strategy has been successfully validated for use in prognosis, therapeutic monitoring and molecular diagnosis[15,24,26,36,111]. However, it is now widely accepted that CTCs can have heterogeneous expression of cell surface markers, including EpCAM, and that some CTCs might not express EpCAM at all. Furthermore, these technologies cannot achieve downstream single cell analysis due to their inability to release CTCs that are captured on the device[24,36,111].

In an attempt to move away from affinity based isolation approaches, researchers have turned toward size based technologies. CTCs derived from solid tumors show larger

30

sizes compared to the majority of cells in circulating blood. Although these size differences are small, this finding makes it an attractive strategy for separating CTCs from blood cells. In fact, size based filtration techniques are now emerging[10,19,86,133]. The issues encountered with these approaches include pore clogging, high-pressure drop, pre-fixation to prevent CTC loss, low throughput, and excessive non-specific cell retention. Other label free separation techniques reported in the literature include deterministic lateral displacement separation method[134], microfluidic flow fractionation approach[100], and acoustic based separation[75]. However, one of the common limitations among these techniques is the limited flow rate or yet to successfully isolate CTCs from clinical specimens. Recently, inertial migration of particles has been introduced and applied in various studies to achieve high throughput particle separation based on particle size[92]. Sun *et al.*, inspired by single spiral channel, developed a double spiral microchannel for label-free tumor cell separation and enrichment[135]. Ozkumur *et al.* applied the inertial focusing in a relatively short sinusoidal channels along with lateral displacement and immunomagnetic selection in the integrated microfluidic system known as the "CTC-iChip"[56]. Although this technology is promising, an unbiased molecular study of CTCs cannot be achieved due to insufficient purity to overcome the ultimate manual selection of CTCs based on a EpCAM+/CD45- phenotype[136]. Hence, we developed a completely label-free and surface expression independent microfluidic Labyrinth (Figure 2.1a) to isolate CTCs from blood cells with high recovery, while achieving the highest purity among all label-free technologies (Table 1.1). The Labyrinth platform can facilitate a thorough biological understanding of CTCs and their subpopulations, having a direct impact upon patient care for early detection, monitoring treatment response, and developing personalized therapy.
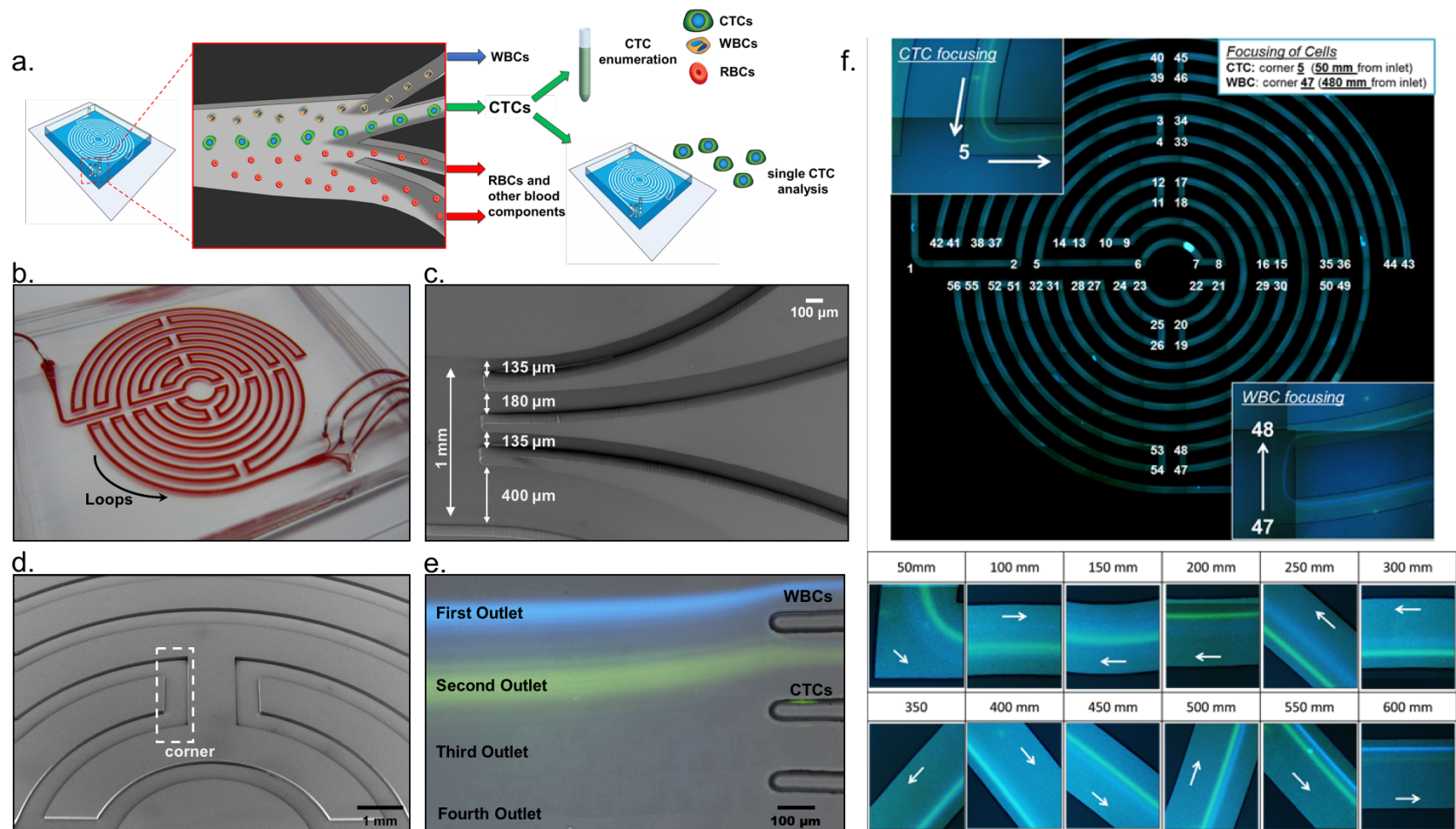
Figure 2.1 Device design and mechanism of Labyrinth. A) Workflow of the Labyrinth system. CTCs are separated through Labyrinth, and can be used for downstream analysis or further purified by applying second Labyrinth for single cell analysis. B) Labyrinth loaded with red dye and the indication of "loops". C) SEM image of the outlet design. D) SEM image of the channel and the indication of "corners". E) The separation of labeled WBC/MCF-7 cell line into individual outlets. F) Focusing and separation of labeled WBCs and MCF-7 GFP cells along Labyrinth. Cancer cells are focused after traveling for 50 mm from inlet in Labyrinth, while WBCs are focused after 480 mm. Streams of cancer cells and WBCs are well separated at outlet.

2.3   Methods

2.3.1   Fabrication of SU-8 mold for Labyrinth

The mold for the polydimethylsiloxane (PDMS) device is formed from a negative photoresist SU-8 100 patterned using soft lithography. Using a spin-coater, the negative photoresist layer, SU-8 100, is deposited onto silicon wafer rotating at 2450 rpm for 1 minute. The wafer is then soft-baked for 10 minutes at 65 °C and 70 minutes at 95°C. The mask is aligned to the wafer and is exposed to UV light for 20 seconds. Post-exposure-baking is applied for 3 minutes at 65 °C and 10 minutes at 95°C. Then, the wafer is developed by soaking in developer for 6 minutes and in IPA for 1 minute to remove the inactivated photoresist. It is hard baked for 4 minutes at 150-180 °C. The height of the mold built on silicon wafer is 100 μm, and the width of the channel is 500 μm.

2.3.2   Fabrication of PDMS device

The flow chamber for labyrinth is made from PDMS. 30 mL Sylgard polymer base and 3 mL curing agent are well-mixed and poured onto a silicon mold. The mixture is put in a desiccator for 2 hours to remove bubbles from the mixture. It is then heated at 65 °C overnight to harden the polymer. The polymer is cut into the desired shape, and punched with needle for tubing. The PDMS device is then bonded to standard sized glass slides via plasma surface activation of oxygen. The bonded device is tubed with 0.66 mm diameter tubes.

2.3.3   Sample preparation for spike cell experiments

A pancreatic cancer cell line with green fluorescent protein (PANC-1/GFP) was cultured and mixed with white blood cells (stained with DAPI) in buffer solution (PBS).

33

The MCF-7 breast cancer cell line was stained with Green Cell Tracker (Life Technologies, USA) and mixed with a portion of a healthy control blood sample.

2.3.4 Experimental Protocol for labyrinth.

The device was pre-flowed with 1% Pluronic acid solution (diluted in 1X PBS) at 100 μL/min for 10 minutes and then incubated for 10 minutes to prevent cell clotting on channel walls. Cell sample suspended in buffer was flowed through the labyrinth at different flow rates (1000, 2000, and 3000 μL/min) and was observed under a microscope. Product from outlets was collected after 1 minute duration of flow stabilization. Waste from each outlet of labyrinth was collected for cell counting to calculate the recovery percentage. To observe the isolation of cancer cells from other blood components, images and movies were taken using both a high-speed camera and a fluorescence microscope under brightfield, FITC, and DAPI filters.

2.3.5 Measuring cell viability for Labyrinth-processed cell line

Cell viability was assessed using the MTT ((3-(4,5-Dimethylthiazol-2-yl)-2,5-diphenyltetrazolium bromide) colorimetric assay. In principle, MTT is taken up into cells by endocytosis or a protein-facilitated mechanism and is reduced by mitochondrial enzymes to yield a purple formazan product. The ability of cells to reduce MTT provides an indication of the mitochondrial integrity and activity, which, in turn, may be interpreted as a measure of cell viability [5]. After labyrinth processing, PANC-1 cells were seeded in a 96 well plate for 6 days and compared with unprocessed cells (control). Data points were taken every 24 hours by adding 8 μL of a 5mg/mL solution of MTT powder in PBS to the desired well. Once violet crystals were formed, media was aspirated and 150 μL of

isopropanol/0.1% 4mM HCL solvent was added to each well. Absorbance was measured at 520 nm using a Microplate reader (Bio-Tek, Winooski, VT).

2.3.6   Patient Sample Processing

Labyrinth was pre-flowed with 1% Pluronic acid solution (diluted in 1X PBS) to prevent cell clotting on channel walls. Blood samples were then processed through the device at a flow rate of 2.5mL/min. Blood samples from pancreatic cancer patients were collected into EDTA tubes and processed through Labyrinth with 1:5 dilution with PBS, and without any further pre-processing steps. A typical run involves processing of 7.5 mLs of whole blood in 15 minutes.Blood samples from metastatic breast cancer patients were collected in EDTA tubes and processed through the Labyrinth within 4 hours of collection. When samples were processed to ultimately undergo downstream single cell analysis, RBCs in blood samples were removed using density separation (6% dextran solution, M.W. 250,000) prior to the Labyrinth process. The blood sample with dextran solution was kept still in room temperature for 45 minutes to bring down the RBCs driven by density difference. The supernatant, which includes everything in whole blood except RBCs, was carefully taken out using pipettes, and was diluted to 25 mL with PBS.

2.3.7   Immunostaining protocol of cytoslides

Samples were permeabilized by applying 0.05% Triton X-100 (PBST) solution for 15 minutes. Slides were then blocked using 20% donkey serum for 30 minutes at room temperature (RT). A cocktail of primary antibodies were added and left in a humidified chamber overnight. The next day, cytoslides were washed thrice with 0.05% PBST for 5 minutes. Samples were incubated in the dark with secondary antibodies for 45 minutes at RT. Finally, samples were washed thrice with 0.05% PBST for 5 minutes and mounted

with Prolong Gold with DAPI. Table S7-8 shows the different primary and secondary antibodies used in this study.

2.3.8   Processing of samples using the Double Labyrinth

Processing samples through LL involves collecting samples from second outlet and processing it again through a second Labyrinth device. In cell line experiments, MCF-7 was pre-labelled with cell tracker and spiked into blood (200/mL) from healthy donors. 10 mL of spiked blood samples was diluted to 25 mL with PBS buffer solution. The diluted samples were processed through first Labyrinth at 2500 µL/min and product from second outlet was collected (6 mL). The collected product from first Labyrinth was processed through second Labyrinth at the same flow rate (2500 µL/min) and product from second outlet was collected as final product.

2.3.9   Calculation of Log Depletion

The log depletion for single Labyrinth is calculated based on the initial number of WBCs spiked into the samples. After single Labyrinth an average of 96.6% (n = 9) of WBCs were depleted into outlet 1, hence resulting in an average of 1.78 log depletion (range 1.49-2.23). The log depletion for double Labyrinth is based on the initial number of WBCs per mL ($\sim 0.7 \times 10^7$). The average of 350 WBCs/mL (n = 5) results in a log depletion of 4.3 in average (range 3.9-4.5).

2.3.10   Preparation of Cytospin slides

Second outlet product was processed using Thermo Scientific™ Cytospin 4 Cytocentrifuge. 300 µL of sample is added into each cytospin funnel and cytocentrifuged at a speed of 800 rpm for 10 minutes. Samples are fixed on the cytoslides using 4% PFA

and cytocentrifuged at the same conditions described above. Cytoslides are stored at 4o C until further staining.

2.4 Results

2.4.1 Labyrinth design and physical principle of separation

The design of our device is inspired by the Labyrinth in Greek mythology, an elaborate structure with numerous turns and corners built to hold the Minotaur. We applied a similar structure for the size-based enrichment of CTCs by bulk depletion of hematopoietic cells using inertial microfluidics based separation.

Particle Focusing

The inertial microfluidics based particle separation relies on the equilibrium between inertial lift forces and Dean flow that results in the migration of particles during laminar flow in microfluidic devices with curved channels (Figure 2.2). Particles in a straight channel experience stresses that act over the entire channel surface, including shear stress that yields drag forces and normal stress that yields lift forces perpendicular to the direction of flow. The migration of particles due to lift forces was first observed by Segré and Silberberg in the 1960s[137,138]. Di Carlo reported that particles would be maintained at specific positions due to the combination of inertial lift forces where shear gradient lift pushes the particles toward the wall and the wall lift effect pushes the particles toward the center[139]. These forces will confine the particles in a straight channel to several equilibrium positions, where the number of equilibrium positions is related to the geometry of the channel.

A relation describing the magnitude of lift force (F_z) was reported by Asmolov[140]:

$$F_z = \frac{\mu^2}{\rho} Re_p{}^2 f_c(\text{Re}_c, x_c) \tag{1}$$

37

where $\mathrm{Re_p}$ is the particle Reynolds number, Re_c is the channel Reynolds number, and x_c is the position of the particle within the channel.

Particle Separation

The Dean flow, on the other hand, occurs in the flow in curved channels. Dean flow is secondary flow due to the centrifugal effects that will affect the particle equilibrium positions[141]. Dean flow is characterized by counter-rotating vortices where the flow at the midline of the channel is directed outward around a curve, while the flow at top and bottom of the channel is directed inward[141]. The drag force due to Dean flow (F_D) is correlated with the particle size and curvature of the channel, and this drag force will also affect the equilibrium position of the particles. Therefore, the equilibrium between inertial lift forces and the drag force from Dean flow can be utilized for size-based sorting[135].

In the presence of inertial lift forces that keep a particle in a stationary position, an expression of drag force F_D is raised by Di Carlo[92]:

$$F_D \sim \rho U_m{}^2 a D_h{}^2 r^{-1} \tag{2}$$

where U_m is the maximum channel velocity, a is the particle diameter, D_h is the hydraulic diameter, and r is the radius of curvature of the channel.

The lift forces stabilize particles at positions located along the centerline of a channel cross section, while Dean flow drag forces cause particles to migrate around the cross section. A new equilibrium position can be estimated from the ratio of F_z to F_D [92]:

$$\frac{F_z}{F_D} = \frac{1}{\delta}\left(\frac{a}{D_h}\right)^3 \mathrm{Re}_c{}^n, \ (n < 0) \tag{3}$$

where δ is the curvature ratio, $\delta = \frac{D_h}{2r}$ (4).

Cell Separation

CTCs can be isolated from other blood cells in curved microfluidic devices by focusing different sized cells into different streamlines and collecting them into individual outlet channels. The inertial force can be considered as the driving force that focuses the particles, while the drag force from Dean flow is the force that causes particle migration away from the center of the channel, leading to size-based separation (Figure 2.2).

Giving the fact that F_z is proportional to the square of particle size (Eqn. 1), blood cells are more difficult to focus in microfluidic channels due to their smaller size compared to CTCs. It has been proposed that sharp curves enhance the focusing of smaller particles[135,142]. To focus the relatively smaller cells found in blood such as WBCs, a microfluidic device must contain curves with a high curvature ratio.

Besides the focusing of particles, it is also crucial to have the proper curvature for sized separation (Figure 2.2). In the situation of high curvature ratio where F_D dominates, particles could be dispersed and lose their focusing due to the insufficiency of F_z, or all the particles with different sizes could be pushed to the same focusing position due to the strong migration force (F_D)[142]. In a curve with extremely low curvature ratio where F_z dominates, particles with different sizes remain at the same equilibrium positions similar to a straight channel due to the limited migration force[142]. An accurate design of curves in the microfluidic structure would lead to the focusing of cells while separating CTCs and blood cells by size.
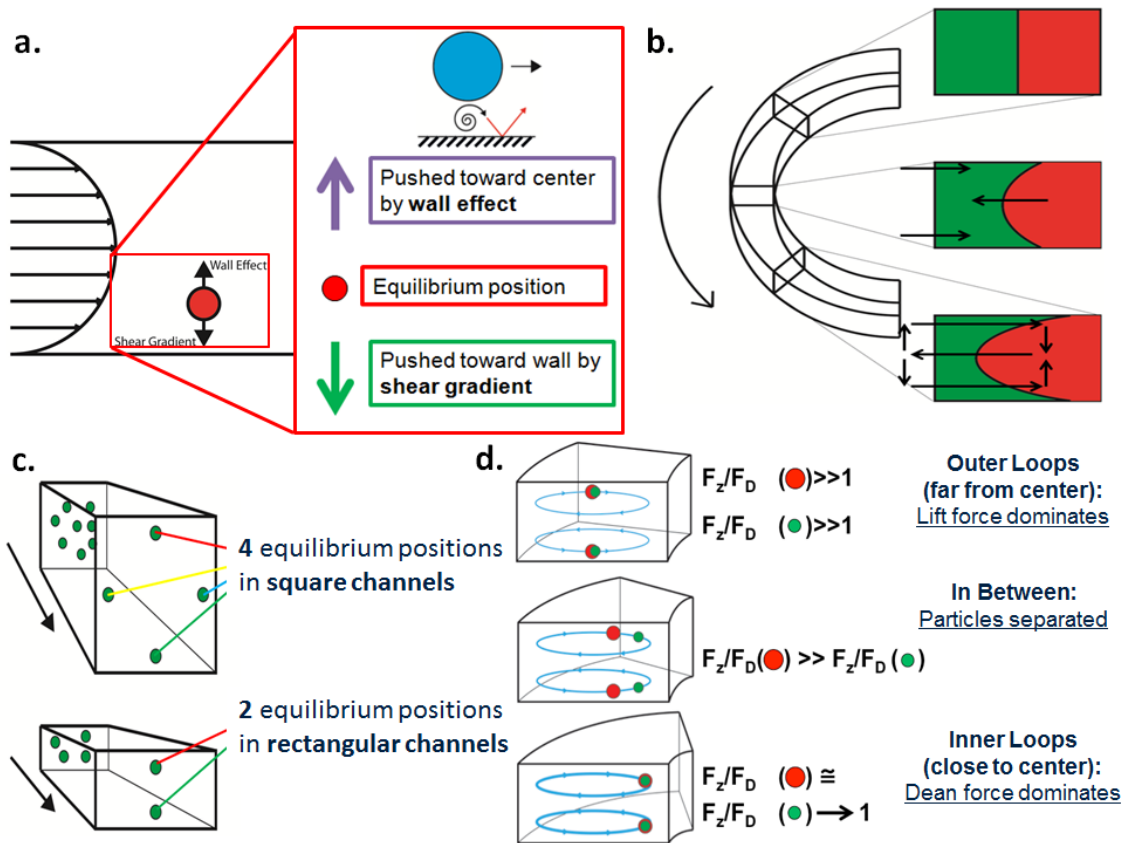
Figure 2.2 Physics of the Labyrinth. Physics of Labyrinth. **a,** Particle on a channel is focused by lift forces, which includes the force from shear gradient and from wall effect. When the two forces are balanced, the particles reach their equilibrium position. **b,** In a curved channel, the fluid close to the inner wall will be drawn away from the center of curvature by centrifugal force, causing two vortices to appear at top and bottom, accordingly. **c,** Particles will be focused to several equilibrium positions in microfluidic channels. For square channels, there will be 4 equilibrium positions and for rectangular channels, there will be 2. **d,** Desired focusing position occurs when ratio for the larger particle is greater than the ratio for small particle, and the ratios are not too close to 1 nor too greater than 1. At such position, the particles can be well separated.

2.4.2 Labyrinth Design

The total channel length of Labyrinth is 637 mm. It is 500 μm in width and 100 μm in height. It consists of 11 loops and 56 corners. The loops (Figure 2.1b), which have a small curvature ratio (δ) (Eqn. 4) range from 5.29×10^{-3} to 3.70×10^{-2} m^{-1}, and were incorporated into the Labyrinth to provide enough length of channel to achieve total focusing of cells and to have the proper curvature for the separation between CTCs and

blood cells (Figure 2.1 e, f). The 56 sharp right-angle corners (Figure 2.1d), which have high curvature ratio, further enhance the focusing of smaller cells without the need for positive or negative selection. The channel width expands to 1000 μm from 500 μm before the streams are diverted into the outlets (Figure 2.1c). The outlets were designed such that the focused individual streams could be collected separately (Figure 2.1e).

2.4.3 Cell Focusing in Labyrinth

To demonstrate cell focusing in the Labyrinth, DAPI-labeled WBCs with GFP-labeled breast cancer cells (MCF-7) were mixed in PBS buffer and flowed through the Labyrinth. Figure 2.1f presents a fluorescent image (green: MCF-7 GFP; blue: WBCs) of the entire device. The corners in the device are numbered in sequential order from inlet to outlet. Cancer cells in the Labyrinth started focusing at corner #5 (50 mm from inlet), whereas WBCs became focused at corner #47 (480 mm from inlet), as shown in Figure 2.1f. The difference in the length needed for the cells to be focused resulted from the magnitude of lift force, which was proportional to the fourth power of particle size (Eq. 1). Given the smaller cells encounter lower lift forces compared to big cells, it is harder to focus the smaller cells in inertial fluidics devices. Smaller cells require longer time to come to the equilibrium positions as the force experienced by them is much smaller compared to bigger cells. Hence the smaller cells need longer travel distance to be able to focus fully. Additionally, Labyrinth design incorporated multiple turns to aid the focusing of smaller cells further. Focused WBCs were sorted out into the first outlet and the CTCs stream was collected through the second outlet as shown in Figure 2.1e.

2.4.4 Testing and optimization of Labyrinth for cell recovery

The Labyrinth was optimized and tested for inertial separation of cancer cells using human breast (MCF-7), pancreatic (PANC-1), prostate (PC-3) and lung (H1650) cancer cell lines. It was determined that the optimal flow rate for maximized recovery and purity was between 2.0-2.5 mL/min (Figure 2.3) after the first 60sec, which are used for the flow to stabilize in the device for optimal collection (Figure A.5). Pre-labeled (Cell Tracker) cancer cells and WBCs were spiked at a high concentration (~100,000/mL and ~500,000/mL, respectively) into buffer and separated using the Labyrinth. Using MCF-7 cells, $91.5 \pm 0.9\%$ of cancer cells were recovered from the second outlet while $91.4 \pm 3.3\%$ of WBCs were removed through the first outlet (Figure 2.4a, n=3). With GFP-labeled PANC-1 cells, a similar separation was achieved, with $92.4 \pm 3.2\%$ recovery of cancer cells with $89.0 \pm 1.1\%$ of WBCs removed in the first outlet (Figure 2.4a, n=3). Labyrinth recovery was further tested with other solid tumor cell type such as lung and prostate and found the yields to be similar (Figure 2.4a). MCF-7 and PC-3 cells were spiked into whole blood and run through Labyrinth without any pre-processing. The recoveries even from whole blood are higher than 90% (Figure 2.4a) demonstrating the ability of Labyrinth to isolate CTCs directly from whole blood. Separation of cancer cells from other blood cells was visualized using a high speed camera and, as shown in Figure 2.4b, the cell streams were physically separate, enabling high purity isolation of the cancer cell population. To further characterize the ability of the Labyrinth to isolate lower concentrations of CTCs (100/mL), MCF-7/GFP cells were spiked into buffer and into healthy donor blood samples, and then processed through the Labyrinth. In this set of experiments, when spiking into blood, blood is treated with Dextran following the spike to remove excess RBCs and see

its effect on recovery. The average recovery in buffer solution was 94.4 ± 3.8%, while in

RBC depleted blood a 95.3 ± 0.7% recovery was obtained (Figure 2.4c). Importantly, an

MTT assay demonstrated that the shear stress experienced by cells processed through the

Labyrinth did not have a significant effect on cell viability or proliferation rates (Figure 2.4

d, e).
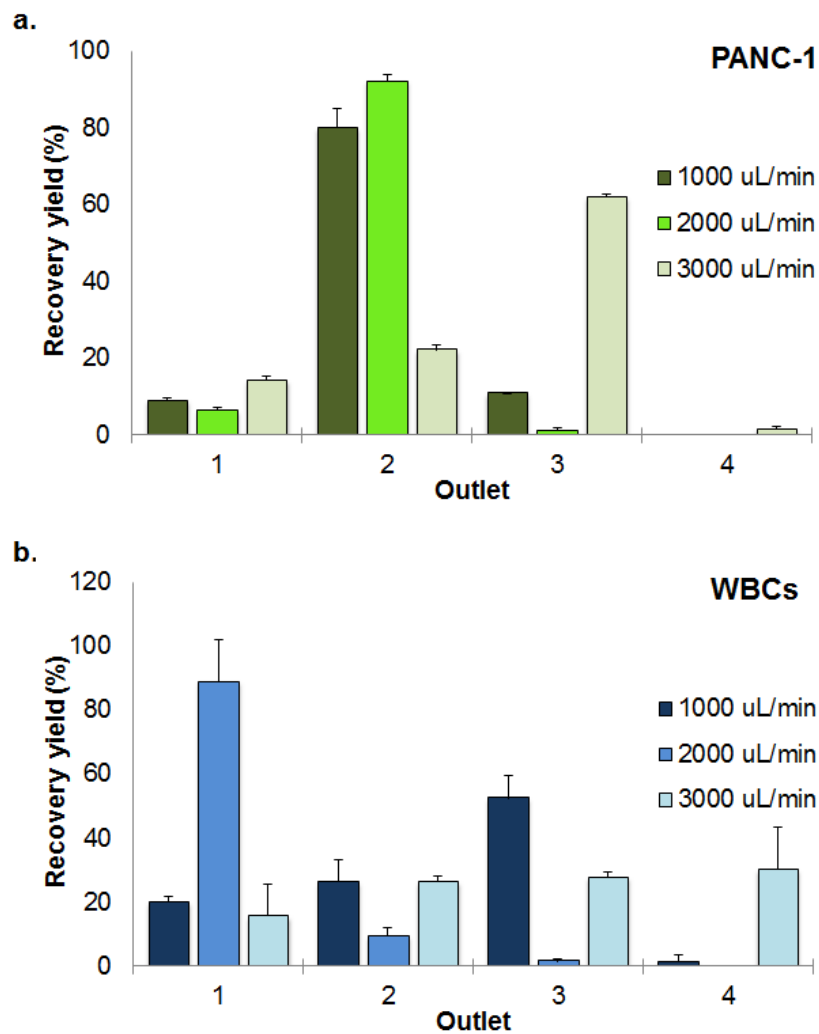
Figure 2.3 Flow rate optimization for pancreatic CTC isolation. PANC1 recovery optimization. a, PANC1 cell line recovery measured at different at flow rates ranging from 1-3 mL/min. b, WBC removal measured at different at flow rates ranging from 1-3 mL/min.

2.4.5 Double Labyrinth Separation for higher specificity

Processing of samples through a single Labyrinth even at a flow rate of 2.5 mL/min, which is considerably greater than the currently available label-free techniques yielded comparable or better purity (13800 WBCs/mL average, n=9, compared to 32,000 WBCs/mL reported[56]). However, to further increase CTC enrichment for high content downstream molecular assays at single cell resolution we adopted the strategy of using a double Labyrinth (LL), two single Labyrinth devices applied in series. This system furthers reduce the WBC contamination yet maintains equivalent CTC viability. As shown in Figure 2.4 f, g, the recovery of MCF-7 cells using a double Labyrinth (91.1 ± 0.7%) was consistent with the results obtained using a single Labyrinth (91.5 ± 0.9%), but with lower WBC contamination (663 ± 647 WBCs/mL), representing a two-log improvement in tumor cell enrichment over the single Labyrinth. This mode of operation yields by far the highest purity reported using the label-free methods. It is to be noted that the additional run through Labyrinth does not significantly add to the processing time (<5 minutes). A detailed comparison of the performance metrics between Labyrinth and other microfluidic technologies and all other technologies (macro or micro) are provided in Table A.6, demonstrating the advantages of Labyrinth in terms of high flow rate, high yields, high purity along with cell viability.
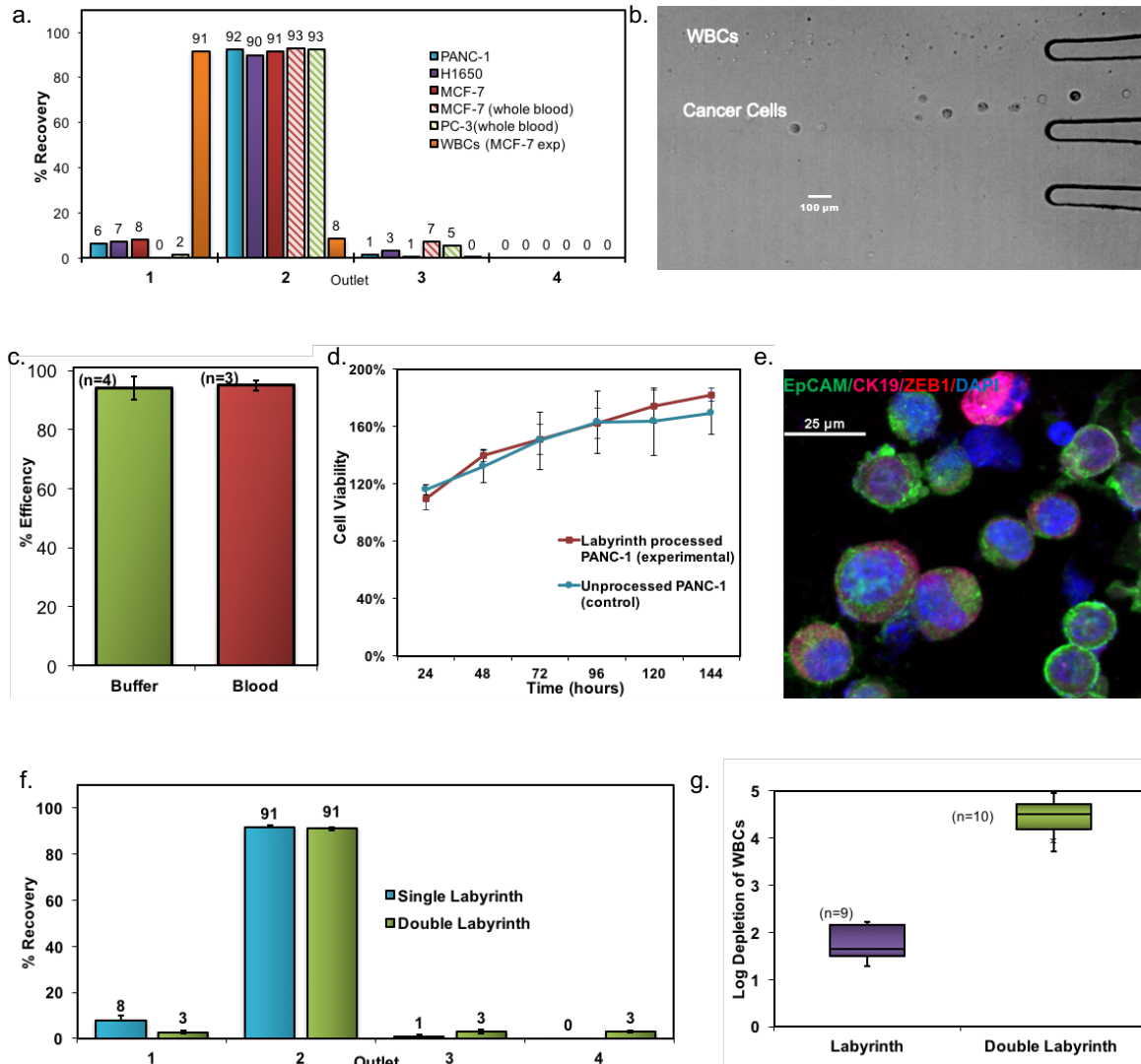
Figure 2.4 Control experiments with spiked cancer cell lines using Labyrinth A) Recovery results from each outlet of the Labyrinth for four different cancer cell lines: breast (MCF-7), pancreatic (PANC-1), prostate (PC-3) and lung (H1650) cancer along with white blood cells (WBCs). PANC-1, H1650, and MCF-7 were spiked into RBC-removed blood, whereas MCF-7 and PC-3 were spiked into whole blood. B) High speed camera image showing Labyrinth's ability to separate WBCs from cancer cells through first and second outlet. C) Recovery results from second outlet using 100 MCF-7 cells for both buffer experiments (n=4) and spiked cells in whole blood (n=3). D) MTT assay results for Labyrinth-processed PANC-1 cells and cultured over a period of 7 days. E) Fluorescence image showing morphology preservation of PANC-1 cells processed at 2.5 mL/min. F) Comparison of recovery efficiency using a single or double Labyrinth for each outlet. Error bars represent the standard deviation of three replicates. G) Log depletion of WBCs using the single (n=9) and double Labyrinth (n=10) to demonstrate high device purity

2.4.6 Isolation of CTCs from pancreatic cancer patients

CTC analysis was performed using blood samples collected from 20 patients with a new diagnosis of pancreatic cancer, as shown in Figure 2.5a. These whole blood samples were all processed without any pre-processing as described in methods. All of the samples had measurable CTCs, identified as DAPI positive nucleated cells staining positive for CK-19 and negative for CD45, as shown in Figure 2.5b. CTC Enumeration in these twenty patients showed a yield of 51.6 ± 25.5 pancreatic CTCs per mL blood, whereas less than 2 CTC-like cells/mL were found in healthy controls. Patient demographics are provided in Table A.7. These results demonstrated that the Labyrinth is capable of isolating patient derived CTCs directly from whole blood with high sensitivity.

Pancreatic CTCs were further evaluated to determine what percentage of the cells displayed epithelial versus mesenchymal-like features. To quantitate epithelial-like cells, expression of EpCAM and CK-19 was assessed, while for quantification of mesenchymal-like cells, the EMT markers ZEB1 and ATDC were used. All patient samples contained not only CK+ CTCs but also EMT marker positive CTCs. An average of $53 \pm 17\%$ of the captured CTCs stained positive for EMT-related markers along with CK-19. Figure 3c presents three CTC subpopulations obtained from the same patient differentially expressing epithelial and mesenchymal markers, demonstrating intra-patient CTC heterogeneity.The molecular characteristics of CTCs were explored by mutational analysis of select genes using the DNA isolated from captured CTCs. DNA was extracted from five pancreatic patient samples, where patient demographics are shown on supplementary table A.9. The qBiomarker Somatic Mutation PCR Array: Human Pancreatic Cancer (Qiagen)

was chosen to represent a comprehensive spectrum of frequently mutated genes in pancreatic cancer. The array includes multiple assays for genes including APC, BRAF, CDKN2A, CTNNB1, KRAS, NRAS, PIK3CA, SMAD4 and TP53. Using this array, mutations were detected in all samples tested involving at least one of the genes (Table A.8). All of the samples tested were positive for KRAS. As expected, no mutations were detected in the healthy control.
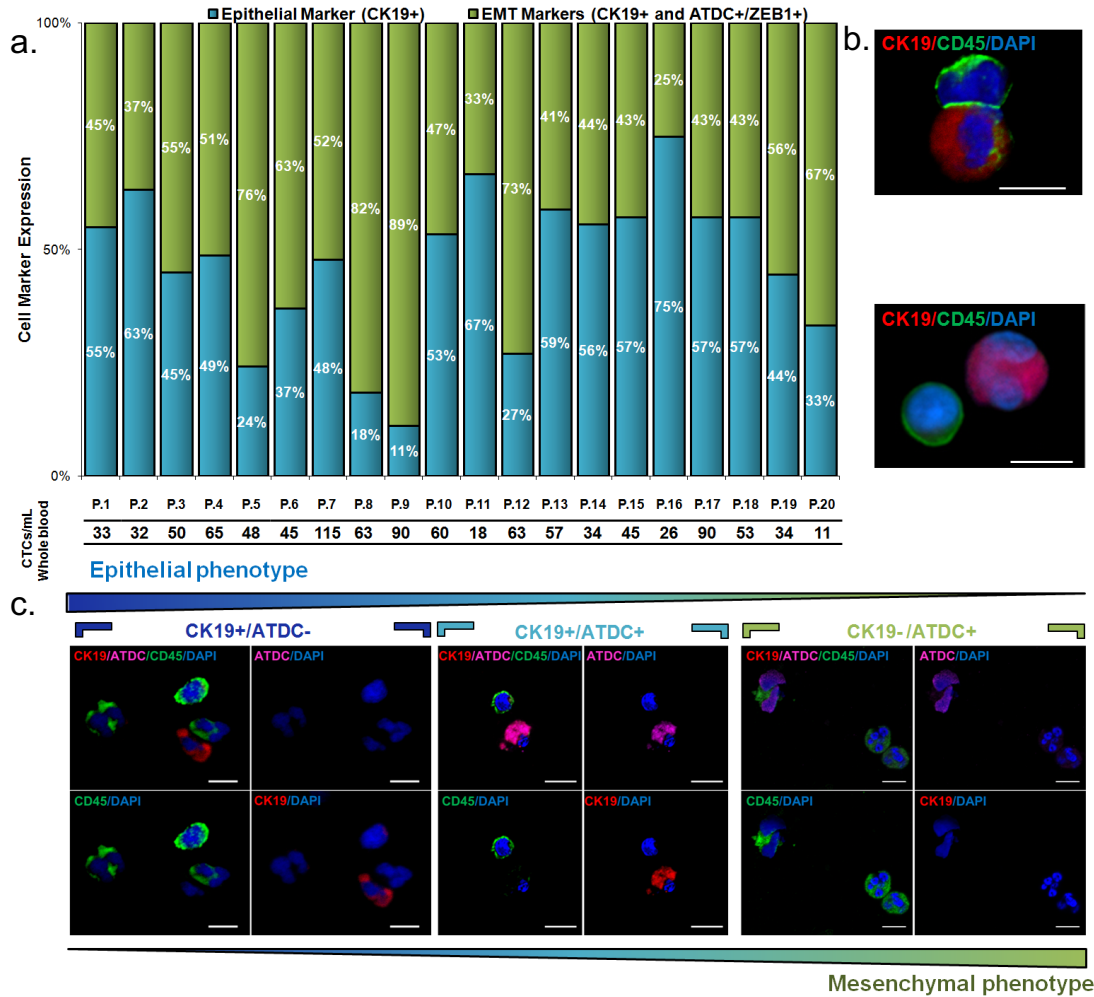
Figure 2.5 Isolation of CTCs directly from whole blood (without any additional pre-processing steps) collected from pancreatic cancer patients using single Labyrinth. A) Percentage of CTCs expressing both EMT and epithelial markers vs only epithelial markers. Column on the bottom indicates the total CTCs (CK+, CD45-, DAPI+) per mL of blood for each patient. B) Fluorescence microscope images of CTCs from patient samples and white blood cells stained with DAPI (blue), cytokeratin (red) and CD45 (green) C) Immunocytochemistry analysis performed on a metastatic sample where both epithelial and EMT-like CTC subpopulations were found. Scale bar 10 μm.

2.5 Discussion

CTCs are critical to understanding the biological process of metastasis and could serve as potential biomarker to noninvasively evaluate tumor progression and response to treatment. There is a substantial evidence that CTCs released from the primary tumor travel through the blood to distant anatomic sites and contribute to the development of lethal metastases. The development of technologies capable of isolating and molecularly characterizing these rare cells at single cell resolution should facilitate studies into their biology and the mechanisms of metastasis. Isolation strategies should not only be efficient and sensitive but also should be unbiased with regard to surface expression. In this respect, microfluidics have allowed for an unprecedented spatio-temporal control of cells[4]. While its application for cancer research is nascent, a number of studies have demonstrated its feasibility in the isolation and characterization of CTCs from clinical samples. In order to sort the WBCs from CTCs in a truly label-free fashion we developed a novel strategy using inertial microfluidics that not only uses the delicate balance of inertial and Dean forces to differentially focus cells, but also induces fluidic path directional shift by incorporating 56 high curvature turns. Unlike other inertial focusing methods, the multi-course path traversing across inner loops to outer loops yields highest hydrodynamic path length (637mm) to enhance the focusing of both CTCs and WBCs resulting highest purity (Table A.6).

With the presented Labyrinth, we were able to demonstrate a high throughput, continuous, and a true biomarker independent (without positive or negative selection) microfluidic separation technology to isolate CTCs from whole blood. Classical genomic analysis techniques use population average readouts. However, these approaches mask

49

cellular heterogeneity and dynamics and are limiting for studying rare and heterogeneous cell populations, including cancer stem cells. We demonstrated that the cells isolated using Labyrinth contain subpopulations of CTCs expressing markers of epithelial and mesenchymal stem-like cells.

Over the past several years, a tremendous amount of effort has been invested in the development of new therapeutic agents that can take advantage of the "Achilles' heel" of CSCs by targeting cell-surface molecular markers or various signaling pathways. A number of agents capable of targeting breast and pancreatic cancer stem cells in preclinical models are currently entering clinical trials[143]. Assessment of the efficacy of the agents will require development of innovative clinical trial designs with appropriate biologic and clinical end points. The lack of proper biomarker endpoints has resulted in difficulty in assessing the effects on CSCs in these studies. The high throughput Labyrinth enables single cell isolation and creates opportunities to monitor heterogeneous subpopulations through treatment. Future research will involve more extensive application of innovative microfluidic systems that target the use of CTCs as a reliable biomarker for early detection, treatment selection, and monitoring of cancer patients

CHAPTER 3. APPLICATION OF LABYRINTH TECHNOLOGY FOR THE ISOLATION OF CTCs IN PANCREATIC PATIENT SAMPLES: A CLINICAL STUDY

3.1 Abstract

Pancreatic cancer has lowest overall survival rate among all types of cancer. One of the major challenges with pancreatic cancer is our inability to detect it in early stages. This is due to the vagueness and non-specificity of its symptoms, which are commonly confused with those of other diseases. Due to the aggressive nature of pancreatic cancer, the likeliness of tumor invasion to other organs at the time of diagnosis is uncharacteristically high (when compared to other solid tumors). While no curative alternative is available for this diagnosis, current treatment options retard tumor progression. Here, we investigate the utility of CTCs as a tool for assessing tumor response to the only three therapy options available for pancreatic cancer. For this study CTCs were isolated using the label free Labyrinth technology, followed by the enumeration of total and EMT-like CTCs. Over 150 treatment naïve samples were tested for CTCs, with 83% of patients displaying an aggressive EMT-like CTC subpopulation. This cohort was further stratified by each patient's treatment options: surgery, chemotherapy, and radiotherapy. CTCs were measured at two time points for each of the treatment courses (pre-/post- treatment). For all treatment cohorts, we observed a statistically significant decrease in CTC count after treatment completion. The use of CTC for predicting overall survival of the patient was also investigated. Results showed a trend toward correlation of a decrease in CTCs with higher survival probability for all treatment options. However, only in chemotherapy

treated patients we could observe a statistically significant p-value. Our work highlights

the clinical utility of CTCs as a biomarker for treatment monitoring in pancreatic cancer.

3.2   Introduction

The incidence of pancreatic adenocarcinoma is increasing and it is projected to be the second most common cause of cancer death by 2030. This projected increase is thought to be secondary to the aggressive biology of the disease in combination with the shifting population demographic created by the aging baby boomers[144]. Patients are often diagnosed with pancreatic cancer at an advanced stage as the diagnosis of pancreatic cancer can be difficult due to absent or ambiguous symptoms, and a lack of screening biomarkers[145]. There is a great need to find an effective and economical tool for diagnosis, prognosis and predictive decision making in the field. Recent advances in endoscopy have made access to pancreatic lesions for tissue diagnosis slightly less challenging, however, the false negative rates is up to 20% for fine needle aspirate and 19-30% for brush cytology[146-148]. The invasive nature of the procedure does not lend this technique to routine repeat biopsies that may be used to assess pharmacodynamic responses during clinical trials or to develop predictive biomarkers.

Recent work focusing on isolation of circulating tumor cells (CTCs) in cancer patients, including pancreatic cancer, holds promise to fill this technological gap. This concept capitalizes on the nature of pancreatic cancer to metastasize hematogenously early in the disease process. Tumor cell dissemination may be as a result of passive shedding or as a result of acquired characteristics by cells through a process of epithelial to mesenchymal transition (EMT)[149,150]. Studies in genetically engineered mouse models of pancreatic cancer have demonstrated that tumor cells can be found circulating in the blood prior to histological evidence of tumor development in the pancreas[151]. This suggests that a similar process may occur in patients, and access to these circulating tumor cells would

provide vital diagnostic information about patients at high risk for developing pancreatic cancer.

Approximately 85% of the patients that undergo surgery for pancreatic cancer will eventually relapse and die of their disease[144]. This information suggests that many of these patients might have circulating tumor cells at the time of surgery, and therefore they may have disease beyond the pancreas, although it cannot be detected with current clinical detection methods, which typically involves CT scan[148]. This observation has led to an increasing popularity in the use of neoadjuvant chemotherapy to treat any systemic disease for some patients prior to surgery, even in the setting of resectable disease[152]. Given the improvement in survival in some subsets of patients with neoadjuvant chemoradation[153] we sought to examine the impact of therapy on circulating tumor cells in patients before and after therapeutic intervention.

Through joint efforts in the field of medicine and bioengineering multiple platforms exist to enrich patient blood samples for CTCs. The number of CTCs in cancer patients are typically quite low in peripheral blood (~1 CTC for every 10^7 blood cells), and thus presents significant technical challenges in detection and isolation from other blood components[149,154-156]. Among the technologies that have been developed to enrich for CTCs from other blood components, the vast majority can be classified as either based on CTC antigenic and immunoaffinity characteristics, or physical properties. Following isolation, the identification of CTCs is typically performed by immunofluorescence staining for cells that are positive for cytokeratin and/or EPCAM (indicating their epithelia origin) and negative for CD45 (ruling out hematopoietic cells) and positive for DAPI (nuclear stain). The overall goal of the many different approaches that have been developed is to facilitate

detection of CTCs from among the millions of other contaminating blood cells and then to employ mechanisms to isolate or immobilize the cells so that cells can be further analyzed. To date there is only one FDA approved for clinical use in the USA. The CellSearch® system, (Janssen Diagnostics, Raritan, NJ, USA) was approved for use by the FDA in 2004 and it involves immunomagnetic capture of CTCs through formation of an EpCAM antibody-antigen complex[157]. CTCs are then identified by negative stains for CD45 and IF staining for nuclear content with DAPI as well as cytokeratins (CK) 8, 18 and 19. This technology has successfully detect elevated levels of CTCs in patients with metastatic cancers of the breast, colon, prostate and lung,[21,158-161] however; in a trail of 79 patients with locally advanced PDA the detection rate was low at 11% using the CellSearch platform[162]. Given to low yield in pancreatic cancer CTCs with an immunoaffnity based approach using EPCAM, we developed a platform that enriches CTCs from patient blood samples based on physical properties. The Labyrinth is a high throughput, label-free microfluidic device that separates cells based on their diameter through the use of inertial forces. The Labyrinth consists of a microfluidic channel that utilizes multiple curves as well as 56 sharp corners to create this separation (Chapter 2). The Labyrinth contains four outlets where the CTCs, which are larger than white blood cells, exit the device in the second outlet with a high recovery of >90%. WBCs are depleted from the first outlet, achieving an 89% WBC removal from the sample. Its high flow rate of 2000 μL/min enables short processing time of 11 minutes for a standard 10mL EDTA tube. To evaluate the utility of the labyrinth as a platform for CTC enrichment in pancreatic ductal adenocarcinoma we prospectively collected over 150 samples from the multi-disciplinary Pancreatic clinic at University of Michigan between 2014 – 2016.

3.3 Methods

3.3.1 Patient sample processing

Labyrinth is pre-flowed with 1% Pluronic acid solution (diluted in 1X PBS) at 100 µL/min for 10 minutes to prevent cell clotting on channel walls. A full tube of whole blood (~7-10mL) was collected for each patient and processed for CTC enumeration. RBCs in blood samples were removed using density separation (6% dextran solution, M.W. 250,000) prior to the Labyrinth process. The blood sample with dextran solution was kept still in room temperature for 1 hour to bring down the RBCs driven by density difference. The supernatant, which includes everything in whole blood except RBCs, was carefully taken out using pipets, and was diluted with PBS buffer at a 1:3 ratio. Blood samples were then processed through the device, at a flow rate of 2 mL/min.

3.3.2 Preparation of cytospin slides

Second outlet product is processed using Thermo Scientific™ Cytospin 4 Cytocentrifuge. 300 µL of sample is inserted into each cytospin funnel and cytocentrifuged at a speed of 800 rpm for 10 minutes. Samples are fixes on the cytoslides using 4% PFA and cytocentrifuged at the same conditions described above. Cytoslides are stored at $4^{\circ}C$ for further staining.

3.3.3 Immunostaining protocol of cytoslides from patient samples

Samples were permeabilized with Phosphate Buffered Saline with 0.05% Triton (PBS-T) solution for 15min and blocked using 10% donkey serum for 30 minutes at RT. Rabbit anti-human Zeb1 (1:500 Santa Cruz sc-25388), Mouse IgG1 anti-human anti-Pan-Keratin (1:500 Biolegend 628601), Mouse IgG2a anti-human anti-Cytokeratin 19 (1:500 Santa Cruz sc-6278) and Rat IgG2b anti-human CD45 (1:500 Santa Cruz sc-70699) in

blocking buffer and applied to samples overnight in a refrigerator at 4oC The next day, samples were washed for five minutes with PBS-T (3X). Donkey anti-rat AF FITC 488 (1:500 Life Technologies A21208), Donkey anti-mouse APC 647 (1:500 Life Technologies A31571) , Donkey anti-rabbit 568 TxRed (1:500 Life Technologies A10042) were diluted in blocking buffer and applied to samples, which were incubated in dark for 45min at RT. Samples were again washed 3 times for 5min with PBS. DAPI (1µg/ml, Thermo Fisher) diluted in PBS was applied for 10min at room temperature to label nuclei. A drop of Prolong® Diamond Antifade Mountant (Thermo Fisher) was then added and coverslips were mounted onto the slides for imaging.

3.3.4   Statistical Analysis

Covariates including CTC total, epithelial CTC, EMT like CTC, stage, age, sex and CA19.9 were collected at different time points of the study. Spearman's rank correlation was used to for correlation analysis because of the non-normality of the covariates. Paired Wilcoxon signed-ranked test (median) and one sided paired t-test (mean) were used to compare the covariates pre-surgery vs post-surgery, pre-chemotherapy vs on-chemotherapy vs post-chemotherapy, and pre-radiation vs post-radiation.

For treatment naïve patients, the overall survival (OS) time was the time of first data collection to death or last follow-up. For the surgery, chemotherapy and radiation patients, the overall survival time was the time of surgery or start of treatment to death or last follow-up. For the surgery patients, the recurrence-free survival was the time of surgery to recurrence or last follow-up. Since some of the overall survival time is right censored, the non-parametric Kaplan-Meier estimator was used to estimate the survival function of patients. Logrank test was used to test the difference in survival curves by different groups.

To estimate the effect of baseline covariates such as stage, CTC and CA19.9, univariate and multivariate cox-ph models were built and compared.

3.4   Results

3.4.1   CTC isolation in pancreatic cancer patients using the Labyrinth

The Labyrinth was tested and optimized for the inertial separation of pancreatic cancer cells (PANC1). It was determined that the optimal flow rate for maximal recovery and purity was 2.0 mL/min and that it took 60 sec for the flow to stabilize in the device for optimal collection (Chapter 2). Under these conditions, PANC1 cells were spiked into whole blood at different cell concentrations ranging from 10-100K. In all cases, recovery was above 88%, proving that the Labyrinth could be used to process clinical samples, where low numbers of CTCs are expected (Figure 3.1b).

To examine the clinical utility of the Labyrinth, CTCs were isolated using size based separation by Labyrinht, and then the isolated CTCs were fluorescently stained and enumerated. Blood samples were collected from 358 patients diagnosed with pancreatic cancer.Taking advantage of the Labyrinth's label free approach, CTCs were enumerated for each patient and classified as either Epithelial-like or EMT-like CTCs. Epithelial-like CTCs were expected to be cancer-specific, panCK positive, DAPI positive, and CD45 (white blood cell marker) negative. EMT-like CTCs were identified by the coexpression of panCK and Zeb1, a commonly reported EMT-related marker in pancreatic cancer[163], in addition to being DAPI positive and CD45 negative. The total number of CTCs was equal to the sum of the two subpopulations as per the classifications described. Patients from the treatment naïve cohort underwent commonly-used treatments for pancreatic cancer, such as surgery, chemotherapy, and radiotherapy. These patients were used to study the correlation of CTC counts with treatment monitoring and efficacy, as shown in Figure 3.1a.
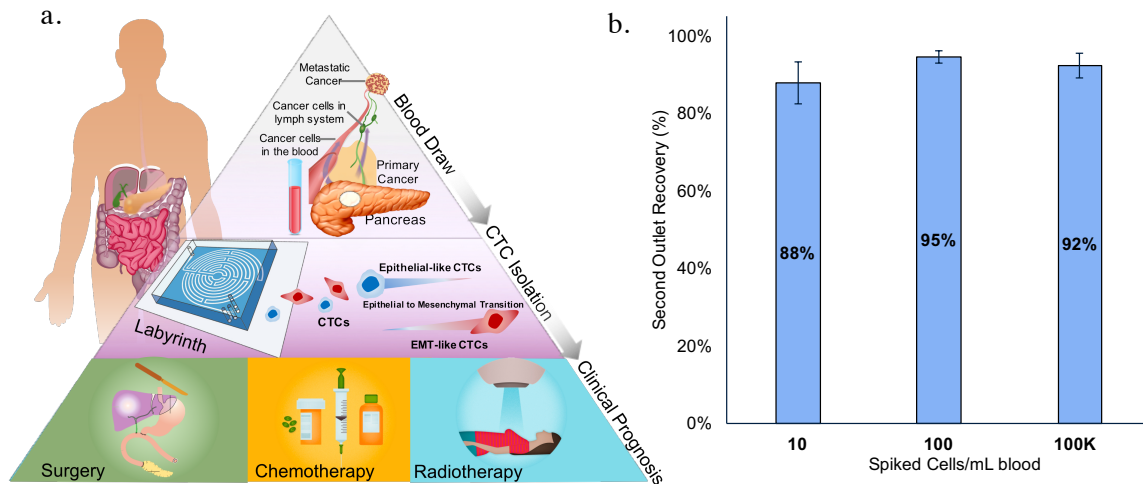
Figure 3.1 CTC isolation in pancreatic cancer patients using Labyrinth a. Experimental outline for this clinical study. b. Cell spike experiments using PANC1 cell line at several concentrations

3.4.2 CTC enumeration for treatment naïve cohort

Treatment naïve pancreatic cancer patients (n = 153) were classified according to their tumor staging: (1) resectable (n = 40), (2) borderline resectable (n = 34), (3) locally advanced (n = 25), and (4) metastatic (n = 54). Patient demographics are listed in Table 3.1. Figure 3.2a shows the total CTC counts per mL and the EMT-like CTC counts per mL of whole blood for all patients, which ranged from 0-117 CTCs/mL and 0-50 EMT-like CTCs/mL, respectively. Box plots were created for statistical analysis of each stage (Figure 3.2b and 3.2c). High variability was observed across all stages. Statistical significance was only observed between resectable and borderline resectable stages (p = 0.03, paired t-test); where borderline resulted in higher CTC counts than resectable. EMT-like CTCs had similar values across all stages. No statistical significance was observed between the stages for EMT-like CTCs. The presence of EMT-like CTCs in the early stages of pancreatic cancer development highlights the aggressiveness of this particular type of cancer. Figure 3.2d shows the overall survival probability for the treatment naïve cohort. By the

60

conclusion of this study, 79 patients (52%) had been declared deceased. The median

survival time of the treatment naïve cohort was 1.33 years (95% CI: 1.18-1.70).

Furthermore, their two-year survival probability was 0.248 (95% CI: 0.165-0.371). Figure

1e shows the survival probability across all stages. A log-rank test yielded significant

results (p < 0.001). The survival probability decreased significantly with stage progression,

with borderline resectable having the highest two-year survival probability (0.505) and

metastatic having the lowest (0). Median times for each category are listed in Appendix B.

Representative images of epithelial-like and EMT-like CTCs from several patients are

shown in Figure 3.3. Despite the size of CTCs being highly variable in these images, CTCs

in general were larger than WBCs. Most patients (83%) tested positive for EMT-like CTCs,

as indicated by cytoplasmic coexpression of panCK and Zeb1.

Table 3.1 Patient demographics for treatment naïve cohort

Variable	Mean	Median	Range
Age	65.3	66.0	34-86
Total CTC	18.04	12.00	0-117
Epithelial CTC	9.445	3.000	0-80
EMT-like CTC	8.863	6.000	0-50
CA19-9	13695	329	2-1393634

Variable	Categories	Count	Percent
Gender	Female	72	47%
	Male	81	53%
Stage	Resectable	40	26%
	Borderline resectable	34	22%
	Locally advanced	25	17%
	Metastatic	54	35%
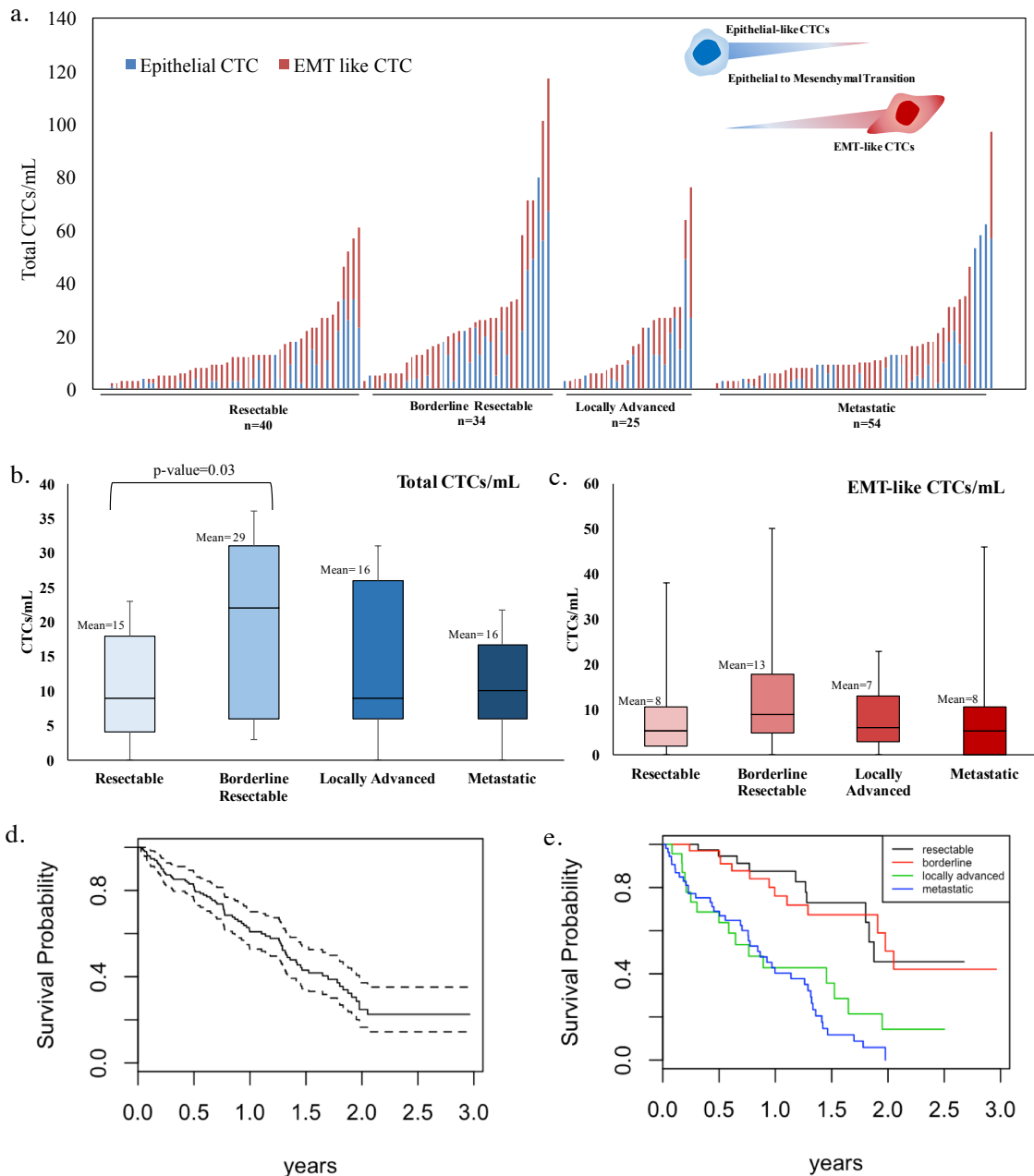
Figure 3.2 CTC enumeration for treatment naïve cohort. a. Enumeration of epithelial and EMT-like CTC for treatment naïve pancreatic cancer patients. b. Box plot for total CTC counts stratified by cancer stage. c. Box plot for EMT-like CTC counts stratified by cancer stage. d. Kaplan Meier curve for overall survival probability in treatment naïve patients e. Kaplan Meier curve for overall survival probability in treatment naïve patients, stratified by cancer stage
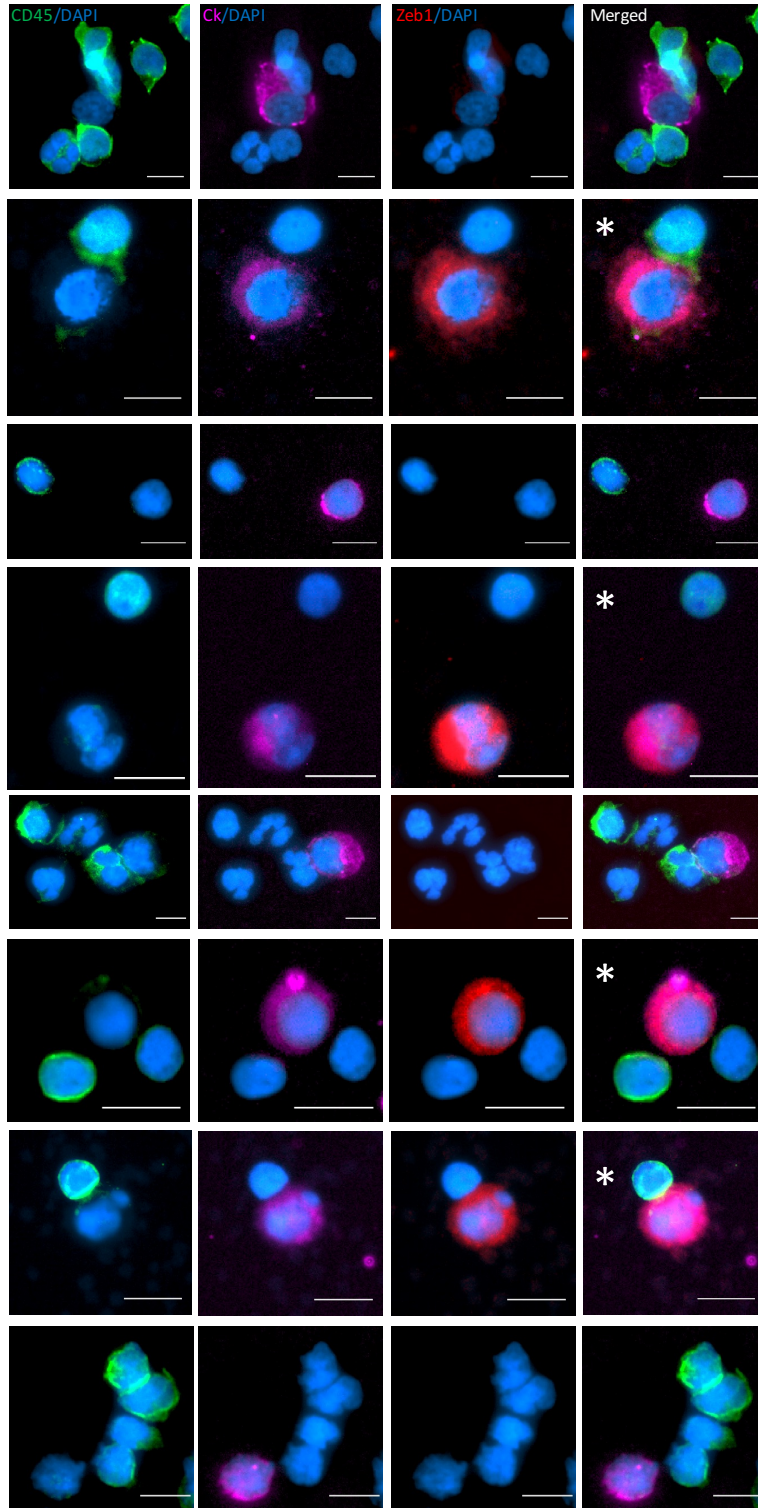
Figure 3.3 CTC image gallery. EMT-like CTCs are marked with an asterisk (*). Scale bar 10μm

3.4.3 CTC enumeration for pre- and post-surgery cohort

Changes in CTC counts were evaluated for pancreatic cancer patients undergoing surgery. Blood samples were collected 22 days (median) prior to surgery and 33 days (median) post-surgery, for a total of 29 patients. Patient demographics for the pre- and post-surgery patient cohort are listed in Table 3.2. A box plot of the data, shown in Figure 4a, revealed a decrease in CTC counts after surgery, which is statistically significant ($p = 0.036$). Figure 3.4b and 3.4c show the overall survival and disease recurrence for this cohort, respectively. Of the 29 patients examined, 10 had recurrence of the disease and 4 were declared deceased. Further analysis was performed by classifying the cohort based on cancer stage. 22 out of 29 patients were classified as resectable, while the remaining 7 were classified as borderline resectable. Figure 3.4d shows a statistically significant difference for the change of CTC for pre- and post-surgery sample between stages ($p = 0.00122$). In both stages, there was a decrease in CTC counts as a result of treatment. In the pre-surgery group, borderline resectable CTC counts were higher than those of resectable. In the post-surgery group, resectable CTC counts were higher than those of borderline resectable. The decrease in CTC counts for the borderline resectable category was greater than that of the resectable category, suggesting an effect of cancer stage on changes in CTC counts. Figure 3.4e and 3.4f show the overall survival and disease recurrence for both cancer stages. The borderline resectable category had a higher survival probability for both overall survival and recurrence than the resectable category. A log-rank test yielded p-values of 0.792 and 0.805 for overall survival and recurrence, respectively.

Table 3.2 Statistical analysis of pre- and post-surgery cohort

Number of patients		29		
Median Age		68		
Range Age		46 to 86		
Gender				
	Male	16	55.2	
	Female	13	44.8	
Median (range) number of days pre-surgery		-22	(0-243)	
Median (range) number of days post-surgery		33	(0-616)	
Total CTCs				
	Median (pre)	13	Mean (pre)	21.83
	Median (post)	6	Mean(post)	11.69
	Median difference b/w pre and post	-1	Mean difference b/w pre and post	-10.14
	Paired Wilcoxon signed-ranked test	0.035*	Paired t-test p-value	0.036*
Epithelial CTCs				
	Median (pre)	3	Mean (pre)	10.28
	Median (post)	0	Mean(post)	4.45
	Median difference b/w pre and post	0	Mean difference b/w pre and post	-5.24
	Paired Wilcoxon signed-ranked test	0.076	Paired t-test p-value	0.10
EMT-like CTCs				
	Median (pre)	6	Mean (pre)	11
	Median (post)	5	Mean(post)	7.28
	Median difference b/w pre and post	0	Mean difference b/w pre and post	-2.8
	Paired Wilcoxon signed-ranked test	0.332	Paired t-test p-value	0.139
Stage				
	Resectable	22		
	Borderline Resectable	7		
	Unresectable	0		
CA19.9				
	Median (pre)	58.50	Mean (pre)	927.00
	Median (post)	29.0	Mean(post)	908.3
	Median difference b/w pre and post	-9.00	Mean difference b/w pre and post	-60.18
	Paired Wilcoxon signed-ranked test.	0.019	Paired t-test p-value	0.097
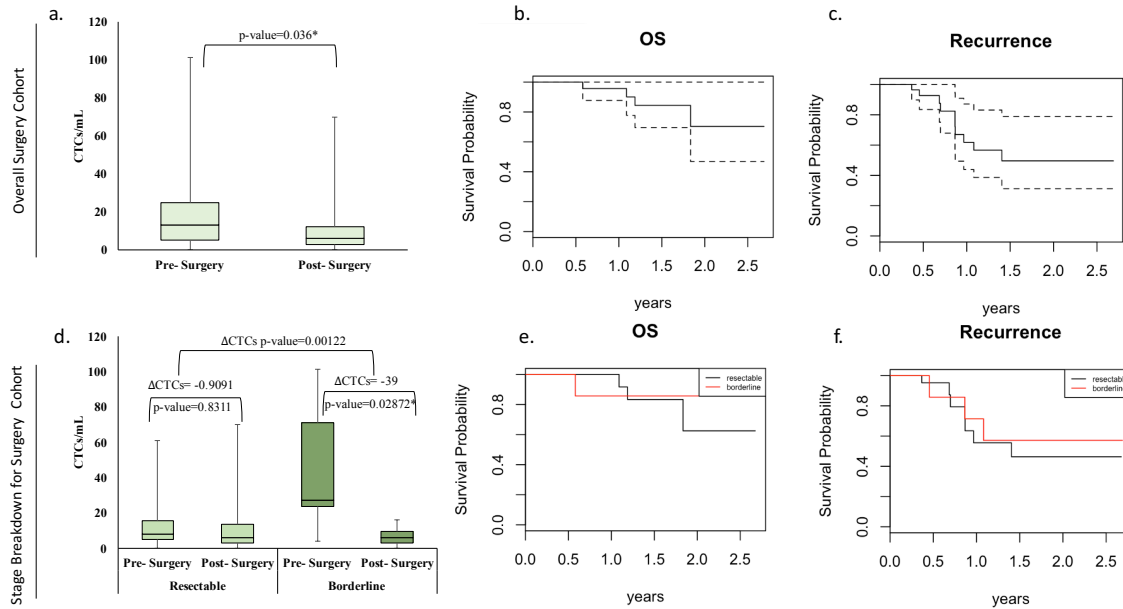
Figure 3.4 CTC enumeration for pre- and post-surgery cohort. a. Box plot for pre- post-surgery total CTC counts b. Kaplan Meier curve for overall survival of surgery cohort. c. Kaplan Meier curve for recurrence free survival of surgery cohort. d. Box plot for pre- post- surgery total CTC counts by stage e. Kaplan Meier curve for overall survival of surgery cohort by stage f. Kaplan Meier curve for recurrence free survival of surgery cohort by stage

3.4.4 CTC usage for treatment monitoring of patients undergoing chemotherapy

The effect of chemotherapy on CTC counts was evaluated during the patients' course of treatment. CTC counts were monitored pre-, on-, and post-chemotherapy. For the pre- and on-chemotherapy cohort, sample collection was performed 20 days (median) prior to treatment and 85 days (median) post-treatment for 35 pancreatic cancer patients. Box plots of the data, shown in Figure 3.5a, also revealed a statistically significant decrease in CTC counts during chemotherapy ($p = 0.046$, paired t-test), with a mean difference of -8. The median survival time of this cohort was 1.48 years. By the conclusion of this study, 13 patients had been declared deceased. For the pre- and post-chemotherapy cohort, sample collection was performed 13 days (median) prior to treatment and 51 days (median) post-treatment for 22 pancreatic cancer patients. Box plots of the data, shown in Figure 3.5c, revealed a statistically significant decrease in CTC counts after

66

chemotherapy (p = 0.002, paired t-test), with a mean difference of -14. From this cohort, 7 patients had been declared deceased by the conclusion of this study (Figure 3.5d). Patient demographics for both cohorts are listed in Table 3.3 and 3.4.

Table 3.3 Statistical analysis of pre- and post-chemotherapy cohort

Number of patients		22			
Median Age		61			
Range Age		46 to 82			
Gender					
	Male	9	40.9		
	Female	13	59.1		
CTC collection pre-CT, median (range), *days*		-13	(1-61)		
CTC collection post-CT, median (range), *days*		51	(12 - 129)		
Total CTCs					
	Median (pre)	23	Mean (pre)	25	
	Median (post)	8	Mean (post)	10	
	Median difference b/w pre and post	-13	Mean difference	-14	
	Paired Wilcoxon signed-ranked test	0.001*	Paired t-test p-value	0.001*	
Epithelial CTCs					
	Median (pre)	9	Mean (pre)	17	
	Median (post)	0	Mean (post)	1	
	Median difference b/w pre and post	-6	Mean difference	-16	
	Paired Wilcoxon signed-ranked test	0.001*	Paired t-test p-value	0.003*	
EMT-like CTCs					
	Median (pre)	8	Mean (pre)	9	
	Median (post)	6	Mean (post)	9	
	Median difference b/w pre and post	1	Mean difference	1	
	Paired Wilcoxon signed-ranked test	0.669	Paired t-test p-value	0.632	
Stage					
	Resectable	3			
	Borderline Resectable	13			
	Unresectable	1			
	Metastatic	5			
CA19.9					
	Median (pre)	472	Mean (pre)	1859	
	Median (post)	136.	Mean (post)	458	
	Median difference b/w pre and post	-425	Mean difference	-1584	
	Paired Wilcoxon signed-ranked test.	0.003*	Paired t-test p-value	0.080	

Table 3.4 Statistical analysis of pre- and on-chemotherapy cohort

Number of patients		35		
Age, median (range), *years*		64	(44-81)	
Gender, N (%)				
	Male	22		
	Female	13		
CTC collection pre-CT, median (range), *days*		20	(0-96)	
CTC collection on-CT, median (range), *days*		85	(10-663)	
Total CTCs				
	Median (pre)	13	Mean (pre)	17
	Median (on)	5	Mean (on)	9
	Median difference b/w pre and on	-6	Mean difference	-8
	Paired Wilcoxon signed-ranked test	0.006*	Paired t-test p-value	0.023*
Epithelial CTCs				
	Median (pre)	3	Mean (pre)	8
	Median (on)	0	Mean (on)	1
	Median difference b/w pre and on	0	Mean difference	-6
	Paired Wilcoxon signed-ranked test	0.002*	Paired t-test p-value	0.006*
EMT-like CTCs				
	Median (pre)	6	Mean (pre)	11
	Median (on)	3	Mean (on)	6
	Median difference b/w pre and on	-3	Mean difference	-5
	Paired Wilcoxon signed-ranked test	0.004*	Paired t-test p-value	0.019*
Stage				
	Resected	2		
	Resectable	4		
	Borderline Resectable	9		
	Unresectable	6		
	Metastatic	14		
CA19.9				
	Median (pre)	267	Mean (pre)	2152
	Median (on)	110	Mean (on)	1171
	Median difference b/w pre and on	-89	Mean difference	-1426
	Paired Wilcoxon signed-ranked test.	0.028*	Paired t-test p-value	0.043*
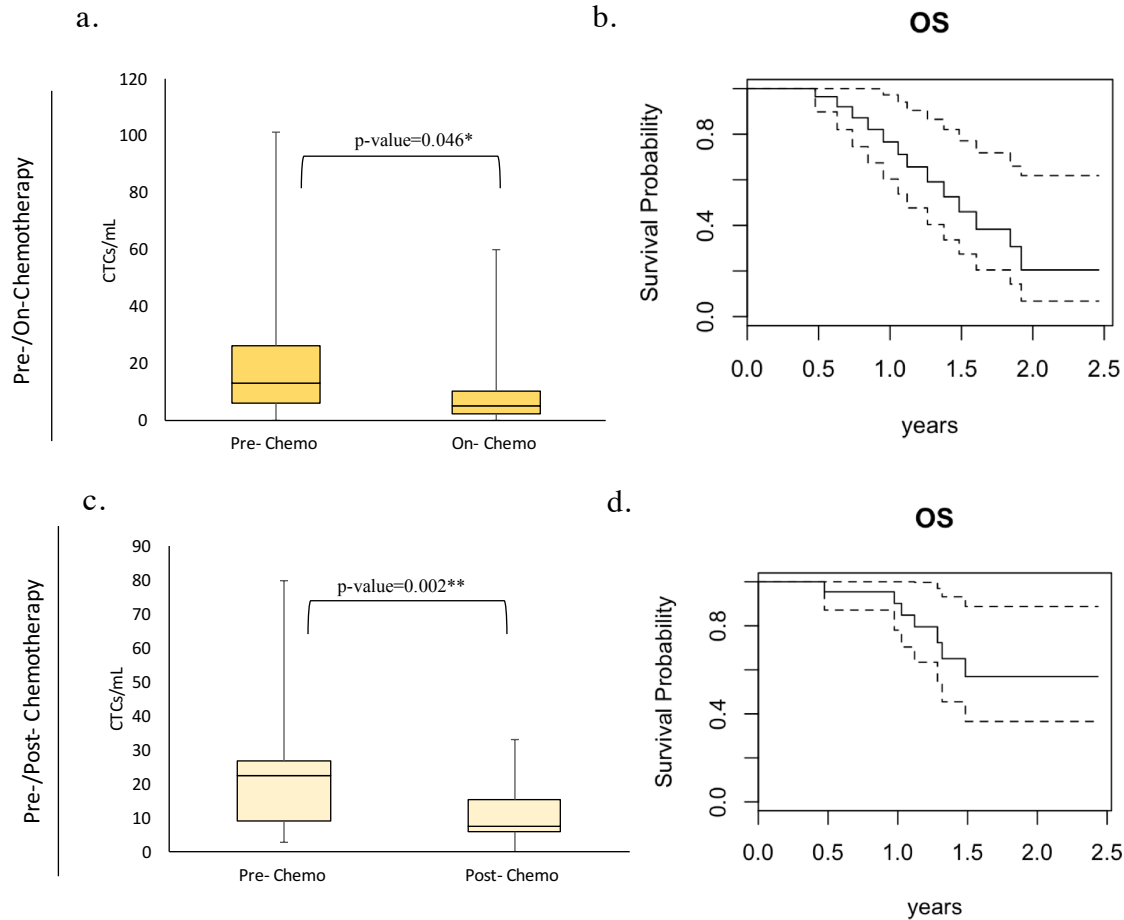
Figure 3.5 CTC enumeration for pre-/post- and pre-/on- chemotherapy cohort. a. Box plot for pre- on- chemotherapy total CTC counts b. Kaplan Meier curve for overall survival of pre- on-chemotherapy cohort. c. Box plot for pre- post- chemotherapy total CTC counts d. Kaplan Meier curve for overall survival of pre- post- chemotherapy cohort.

3.4.5 CTC enumeration for pre- and post-radiotherapy cohort

The effect of radiotherapy on CTC counts was evaluated for 12 patients. Sample collection was performed 135 days (median) prior to treatment and 72 days (median) post-treatment. Patient demographics are listed in Table 3.5. A statistically significant decrease in CTC counts was observed after treatment ($p = 0.023$, paired t-test), with a mean difference of -16, as shown in Figure 3.6a. The Kaplan-Meier curve for overall survival (Figure 3.6b) revealed a mean survival time of 1.79 years. By the conclusion of this study, two patients had been declared deceased.

Table 3.5 Statistical analysis of pre- and post-radiotherapy cohort

Number of patients		12		
Age, median (range), *years*		59		
Gender, *N (%)*				
	Male	2	16.7	
	Female	10	83.3	
CTC collection pre-CT, median (range), *days*		135	(0-282)	
CTC collection post-CT, median (range), *days*		72	(21-280)	
Total CTCs				
	Median (pre)	15	Mean (pre)	23
	Median (post)	6	Mean (post)	8
	Median difference b/w pre and post	-8	Mean difference	-16
	Paired Wilcoxon signed-ranked test	0.017*	Paired t-test p-value	0.023*
Epithelial CTCs				
	Median (pre)	7	Mean (pre)	15
	Median (post)	0	Mean (post)	1
	Median difference b/w pre and post	-4	Mean difference	-13
	Paired Wilcoxon signed-ranked test	0.010*	Paired t-test p-value	0.044*
EMT-like CTCs				
	Median (pre)	8	Mean (pre)	10
	Median (post)	5	Mean (post)	6
	Median difference b/w pre and post	-1	Mean difference	-3
	Paired Wilcoxon signed-ranked test	0.199	Paired t-test p-value	0.180
Stage				
	Resected	1		
	Resectable	1		
	Borderline resectable	8		
	Unresectable	2		
CA19.9				
	Median (pre)	70	Mean (pre)	848
	Median (post)	106	Mean (post)	647
	Median difference b/w pre and post	-30	Mean difference	-223
	Paired Wilcoxon signed-ranked test.	0.180	Paired t-test p-value	0.402
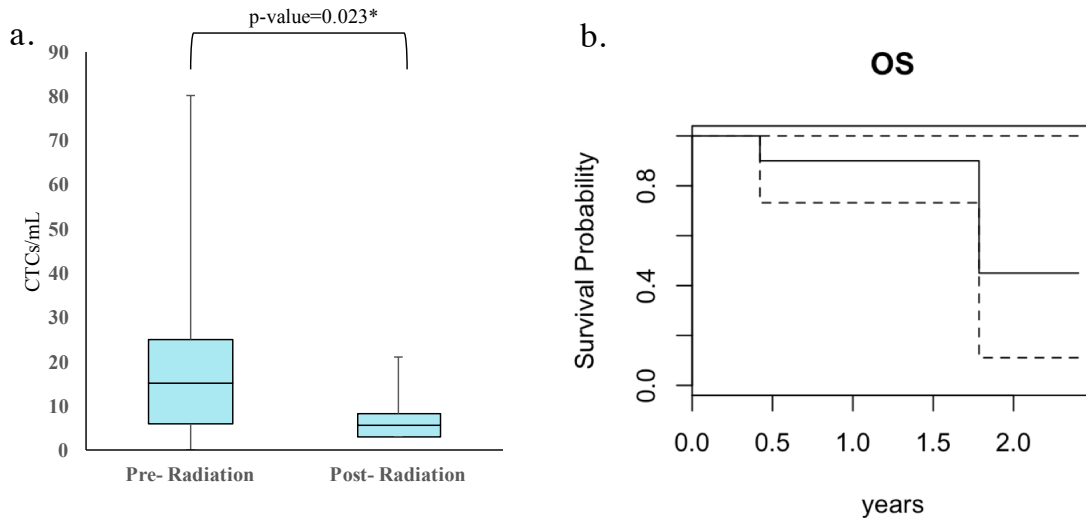
Figure 3.6 CTC enumeration for pre-/post-radiotherapy cohort. a. Box plot for pre-post- radiotherapy total CTC counts b. Kaplan Meier curve for overall survival of pre-post- radiotherapy cohort.

3.4.6   Use of CTCs for predicting clinical prognosis in pancreatic cancer

The correlation of overall survival with the decrease of CTC counts was examined for all treatment options. Figure 3.7a shows the Kaplan-Meier curve for the pre- and post-surgery cohort. Of the 29 patients examined, 17 had a decrease in CTC counts. The log-rank test p-value for these two curves was 0.536. For chemotherapy-treated patients, overall survival for both pre-/on- and pre-/post- categories was calculated. For the pre-/on-chemotherapy patients (Figure 3.7b), 24 of the 35 patients examined had a statistically significant decrease in CTC counts (p = 0.024, log-rank test). Figure 3.7c shows overall survival for the pre-/post- chemotherapy patients. Of the 22 patients examined, 18 had a decrease in CTC counts (p = 0.501, log-rank test). For the radiotherapy-treated patients (Figure 3.7d) 9 of the 12 patients examined had a decrease in CTC counts. A log-rank test for decrease versus non-decrease yielded a p-value of 0.127. In summary, a decrease in CTC counts is correlated with a higher survival chance across all treatment options.
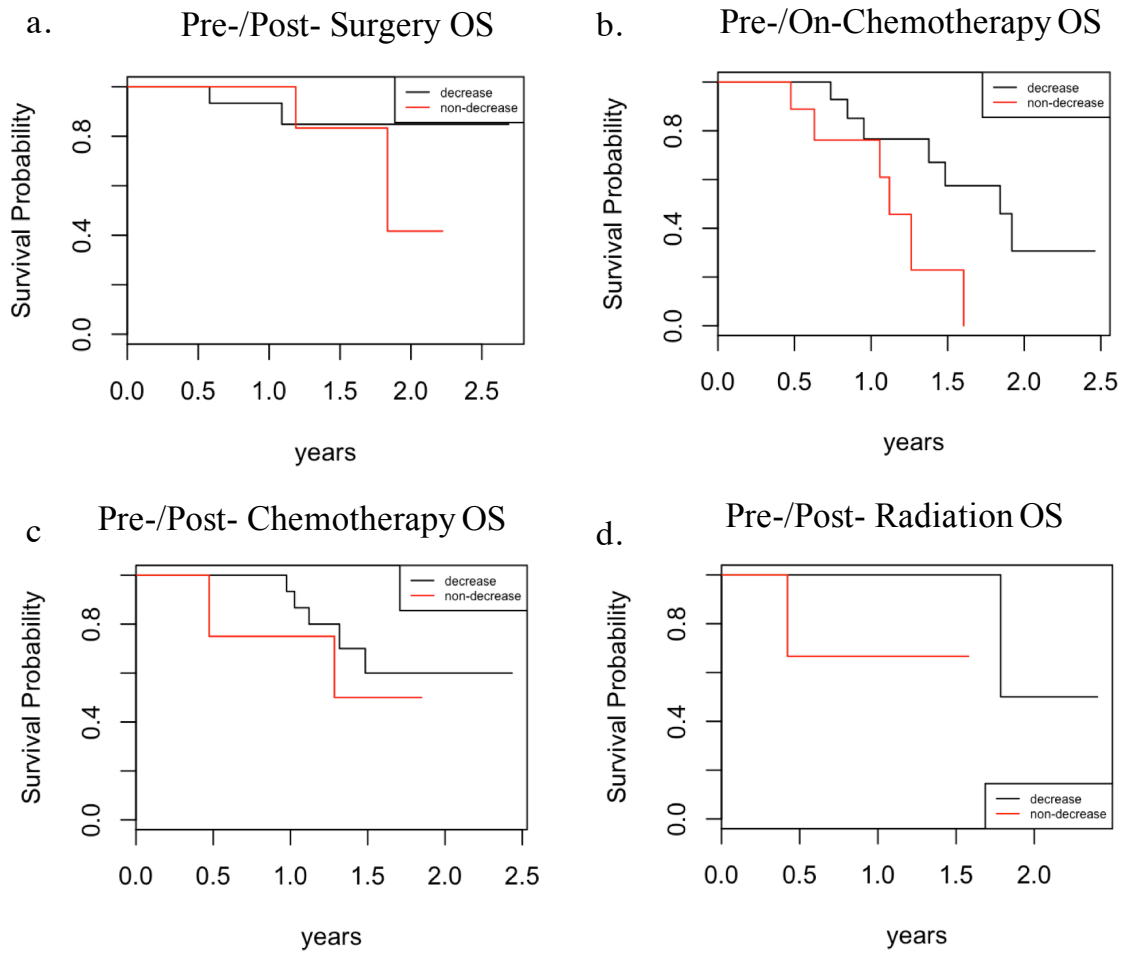
Figure 3.7 Use of CTC for treatment response prediction. Kaplan Meier curve for overall survival in (a) surgery, (b,c) chemotherapy and (d) radiotherapy patient cohorts.

3.5 Discussion

Pancreatic cancer has lowest overall survival rate among all types of cancer. One of the major challenges with pancreatic cancer consists its identification in early stages. The symptoms are vague and non-specific; commonly confused by other types of diseases. Once a patient is diagnosed, their treatment consists of (1) surgery, (2) chemotherapy and (3) radiotherapy. None of these options are curative, as they serve only to slow down the disease progression. Surgery is the first defense line in earlier stages of pancreatic cancer. However, only 15% of the patients qualify for such surgery. Even then, their survival rate only increases to 10-20%. Chemotherapy and radiotherapy are usually administered in advanced cancer stages. The efficacy of these treatments is hampered by the lack of early detection of pancreatic cancer. Even a synergistic approach for such three therapy options still results in poor prognosis for pancreatic cancer. Hence, the need of a biomarker for detecting and monitoring this disease is imperative.

The Labyrinth allows the highly efficient isolation of CTCs in pancreatic cancer (Figure 3.1b). This technology enables the high throughput isolation of the spectrum of CTC subpopulations that are found in pancreatic cancer patients. One subpopulation of interest are the EMT-like CTCs. This subgroup is believed to be highly aggressive and metastatic, having the capability to be highly resistant to therapy. Its use in clinical settings could facilitate the application of CTCs as a biomarker for predicting and monitoring treatment response of such devastating disease (Figure 3.1a).

In order to study the efficacy of CTCs as tumor biomarkers, 153 treatment naïve patient samples were processed and enumerated for Epithelial and EMT-like CTCs. Both populations were observed in most patients, where different morphologies and sizes of

74

CTCs were observed (Figure 3.3). This cohort was further stratified based on their cancer stage: resectable, borderline resectable, locally advanced and metastatic. As observed on the box plots for total CTCs, patients with borderline resectable tumors have a higher CTC count compared to other stages. For EMT-like CTC counts there is a consistent CTC number across all stages. Our results correlate with previously reported studies, where potential for cancer dissemination is observed even on the earlier stages[151]. The treatment naïve patient cohort displays a low 2-year survival rate of 0.248. Its stratification based on stages confirms the increased mortality rate observed in advanced stages.

Currently, the effectiveness of pancreatic cancer treatment is evaluated through CT scans. This method poses many disadvantages including high operating costs and difficulty imaging the tumor location. CTCs could then serve as an improved alternative for monitoring treatment response. For the examination of CTCs' use in surgery treatment, 29 patients were processed for CTC counts at two different time points: pre- and post- surgery. Results showed a significant decrease in total CTC counts in all patients. While considering the stage breakdown of this cohort, a higher decrease change of CTC counts was observed in the more advance stage (borderline resectable). This result could be explained by the fact that tumor size increases with stage. Smaller tumors tend to be more localized, while bigger tumors invade other organs. Hence, more CTCs in the bloodstream are expected as tumor size increases. This trend is also observed in figure 3.2b, with higher CTC counts for borderline resectable stage even before surgery.

Two cohorts were used to evaluate the efficacy of chemotherapy in pancreatic cancer patients: pre-/on- and pre-/post- treatment. In both cohorts, we observed a statistically significant decrease in CTC counts. While both cohorts were studied, pre- on-

chemotherapy results were considered to be clinically relevant. CTC counts for post-chemotherapy were not considered accurate as there were multiple reasons for which the treatment could have stopped. Some of the reasons include: (1) advanced tumor progression, (2) high toxicity, (3) completion of 6mo. treatment and (4) break of treatment. Our results showed that both total CTCs and EMT-like CTCs are highly responsive during chemotherapy and their potential use for treatment monitoring.

The use of CTC counts was also evaluated across twelve patients who have undergone radiotherapy treatment. As shown for the other treatments, there was a significant decrease in CTC counts after radiotherapy was completed. Among the three treatments, this cohort showed the biggest decrease in total CTC counts.

Previous studies on breast and prostate cancer have shown the utility of CTCs as a biomarker for predicting overall survival in cancer patients [120,161,164]. Consistent with these studies, our results showed that patients with a decrease in CTC counts have a higher overall survival than patients with increasing or constant CTC counts. While this trend was observed in all treatment options, a significant p-value was obtained only on the pre-/on-chemotherapy cohort. Because chemotherapy is the most commonly treatment used, our findings highlights the potential of CTCs as a biomarker for predicting overall survival in pancreatic cancer. CTCs can open the opportunity for developing personalized medicine that can be readily monitored to ensure maximum treatment efficacy.

CHAPTER 4. HETEROGENEITY STUDIES FOR THE CHARACTERIZATION OF PANCREATIC CTCs ISOLATED FROM PANCREATIC DUCTAL ADENOCARCINOMA (PDA) PATIENTS

4.1   Abstract

New methods for detection and characterization of circulating tumor cells (CTCs) in the blood are poised to have a significant impact in clinical medicine. An important issue in the monitoring of CTCs is that there may be substantial heterogeneity with several sub-populations denoted by different cell surface marker proteins. Although EpCAM has been used to identify and isolate CTCs from blood, CTCs may transition to a mesenchymal form, which does not have this marker, and these cells may form the majority of the CTCs present. We have thus employed the use of the Labyrinth for CTC isolation, which exploits inertial forces to differentially focus live cells for separation. The CTCs were separated from whole blood from pancreatic cancer patients and were collected on a slide for fluorescence detection. These cells were monitored for circulating cells with markers associated with the cancer stem cell population including CK, CD24 and CD90 and that were CD45-. We found that there were cells that were CK+ which denotes the marker for CTCs that also had CSC markers associated with them in most cases. We also found that there were a substantial number of cells collected that had multiple markers associated with CSCs. Tissue analysis from one of the patients showed cells co-expressing CK and CD90, as well as for CD24 and CD90 combination. This work demonstrates the use of new technology for identifying circulating cells without EpCAM and that have unique

77

combinations of CSC markers that potentially could be used for prognosis and monitoring therapies.

4.2   Introduction

Circulating tumor cells (CTCs) are critical to understanding the biological process of metastasis and could serve as a potential biomarker to noninvasively evaluate tumor progression and response to treatment. It has been extensively shown that CTCs released from the primary tumor travel through the blood to distant anatomic sites leading to lethal metastasis[4]. Therefore, these cells could be a good surrogate biomarker for prognosis, as well as detection and monitoring of the disease[24]. To date, limited data has been collected regarding the numbers of these cells in the bloodstream at different stages of cancer and in different types of cancer, their molecular and biological heterogeneity, and their significance in the natural history of the disease[4]. CTCs hold the potential to serve as a 'liquid biopsy' for cancer patients [7,8]. CTCs can be detected from peripheral blood of patients and hold the promise of being a real-time biomarker for cancer detection and management. The utility of CTCs as a predictive and prognostic marker has been explored in various cancers like pancreatic cancer, breast cancer, prostate cancer, liver cancer and colorectal cancer[19-21].

CTCs have been detected and studied in patients with pancreatic adenocarcinoma[165]. Although evidence showed that the presence of CTCs is associated with poor outcome[3], several studies suggested that relatively low levels of CTCs can be detected in most pancreatic cancer patients compared to other types of malignancies[28]. The inability of current widely used technologies to detect CTCs due to their low sensitivity poses a potential barrier for their use as an effective biomarker.

The detection and characterization of CTCs is a challenging problem for several reasons including the very small numbers of these cells in the bloodstream and their

heterogeneity. CTCs are typically observed at a concentration of 5-20 cells per 7.5 mL whole blood, even in advanced stage cancers, compared to millions of white blood cells and even larger numbers of red blood cells[127,166-168]. A method with high separation capabilities and throughput is needed to collect an isolated population of CTCs in sufficient numbers for further analysis. The second issue is the heterogeneity of CTCs as multiple sub-populations may exist, which have the same genetic basis but a different phenotype due to heterogeneity within the primary tumor. These different sub-populations may have different roles in metastatic progression and thus need to be monitored based on their single cell content. A method which can detect these sub-populations and their relative populations will be essential in determining cancer prognosis and selecting appropriate therapies[169-171].

The standard approach for isolation of CTCs involves methods based on immuno-affinity with antibodies specific for CTC surface proteins that are not present on other blood cells[172]. This strategy has generally employed EpCAM as a surface marker for CTCs. However, many CTCs do not express EpCAM especially after these cells undergo epithelial to mesenchymal transition (EMT) where EpCAM is significantly down-regulated[169]. Alternative approaches have used label free isolation methods based on the physical properties of the cells[24,173,174]. Tumor cells derived from solid tumors are larger compared to most blood cells. Size based filtration techniques have been developed in which cells are separated on filters or through pores in membranes[175]. These methods are subject to problems with clogging and the amount of sample that can be processed without sacrificing yield and purity is limited.

More recently the Nagrath laboratory has developed a method for CTC enrichment using micro-chip technology to separate CTCs from the peripheral blood of cancer patients. This device utilizes inertial forces and is capable of continuous, selective, high-throughput separations without the use of antibodies. The device, termed Labyrinth, structure incorporating a curved path in which cells can be separated from whole blood at a rate of 2.5mL/min through hydrodynamic focusing based on size[91]. The isolated cells remain viable after processing for further analysis. Additionally, this method can separate out CTCs from other cells in the blood regardless of their surface markers. This device facilitates heterogeneity studies to understand the variability of surface marker expression on CTCs.

It has long been appreciated that tumors are composed of heterogeneous populations of cells. To date, limited data has been collected regarding the numbers of these cells in the blood stream at different stages of cancer and in different types of cancer, their molecular and biological heterogeneity, and their significance in the natural history of the disease[4]. EMT and stem cell phenotypes are highly enriched in CTCs[5] and the phenotype of CTCs was established as a stronger predictor of outcome than sole enumeration of CTCs in a defined volume of blood. One of the potential EMT markers for CTCs in pancreatic cancer is CD90, also known as Thy-1. This marker is a heavily glycosylated, glycophosphatidylinositol (GPI)-anchored cell surface protein that has been shown to be a cancer stem cell indicator in different types of cancer[176]. In pancreatic cancer, Zhu et al. reported high levels of CD90 in cancer-associated fibroblast surrounding the tumor cells[177]. In addition, s CD90+ cells were found clustered around CD24+ malignant ducts, indicating that CD90 could play a role in the tumor-stroma interactions and in

cancer-associated fibroblasts that could potentially assist in pancreatic tumorigenesis and development[177].

This work utilized the Labyrinth for the isolation of CTC populations from whole blood of pancreatic cancer patients (n=12). These isolated CTCs will be monitored for markers associated with the cancer stem cell population including CD24, CD90 and that are CD45-. These cells are also known as circulating tumor stem cells(CTSCs)[178]. These combinations are rare in tissues but are shown to be observed in cells circulating in the bloodstream including the markers CD24/CD90. This work demonstrates the use of the Labyrinth for identifying circulating cells without EpCAM and that have unique combinations of CSC markers that potentially could be used for prognosis and monitoring therapies in pancreatic cancer. We also show that there is extensive heterogeneity for CK+ cells for these CSC markers for both intra-patient and interpatient comparisons.

4.3   Methods

4.3.1   Patient Sample Processing

Labyrinth is pre-flowed with 1% Pluronic acid solution (diluted in 1X PBS) at 100 µL/min for 10 minutes to prevent cell clotting on channel walls. RBCs in blood samples were removed using density separation (6% dextran solution, M.W. 250,000) prior to the Labyrinth process. The blood sample with dextran solution was kept still in room temperature for 1 hour to bring down the RBCs driven by density difference. The supernatant, which includes everything in whole blood except RBCs, was carefully taken out using pipets, and was diluted with PBS buffer at a 1:3 ratio. Blood samples were then processed through the device, at a flow rate of 2 mL/min. Patient demographics are found on Appendix C.1.

4.3.2 Preparation of Cytospin slides

Second outlet product is processed using Thermo Scientific™ Cytospin 4 Cytocentrifuge. 300 μL of sample is inserted into each cytospin funnel and cytocentrifuged at a speed of 800 rpm for 10 minutes. Samples are fixes on the cytoslides using 4% PFA and cytocentrifuged at the same conditions described above. Cytoslides are stored at 4° C for further staining.

4.3.3 Immunostaining protocol of cytoslides

Samples were permeabilized by applying 0.05% PBST solution for 15 minutes. Slides were then blocked using 20% donkey serum for 30 min at room temperature (RT). A cocktail of primary antibodies were added and left in a humidified chamber overnight. Next day, cytoslides were washed thrice with 0.05% PBST for 5 minutes. Samples were incubated in dark with secondary antibodies for 45 minutes at RT. Finally, samples were washed thrice with 0.05% PBST for 5 minutes and mounted with Prolong Gold with DAPI. List of antibodies used can be found on Table 4.1.

Table 4.4.1 List of antibodies used in this study

Primary Antibody	Source-Reactivity	Company (Cat No.)	Concentration
CD24	Mouse IgG1-Human	Abcam (ab76514)	1:500
CD90	Rabbit IgG-Human	Abcam (ab9257)	1:500
CD133	Mouse IgG2aκ-Human	Emd Millipore (MAB4399)	1:500
CK-19	Rabbit IgG- Human	Santa Cruz (sc- 25724)	1:500
CK-19	Mouse IgG- Human	Santa Cruz (sc-6278)	1:500
CD45	Rat IgG2b- Human	Santa Cruz (sc-70699)	1:500
PanCK	Mouse IgG1- Human	Biolegend (628602)	1:500

PanCK	Rabbit IgG- Human	Abcam (ab9377)	1:500
SecondaryAntibody	**Source-Reactivity**	**Company (Cat No.)**	**Concentration**
Alexa Fluor® 488	Donkey-Rat IgG	Invitrogen™ (A21208)	1:500
Alexa Fluor® 568	Donkey-Rabbit IgG	Invitrogen™ (A10042)	1:500
Alexa Fluor® 647	Donkey-Mouse IgG	Invitrogen™ (A31571)	1:500
Alexa Fluor® 546	Goat-Mouse IgG2a	Invitrogen™ (A21133)	1:500
Alexa Fluor® 647	Goat-Rabbit IgG	Invitrogen™ (A21244)	1:500
Alexa Fluor® 647	Goat-Mouse IgG1	Invitrogen™ (A-21240)	1:500

4.3.4 Double Fluorescent Immunohistochemistry

The FFPE tissue slides were dewaxed in xylene for 10 min twice and then rehydrated through a series of alcohol solutions (100% ethanol twice, 95% ethanol, 75% ethanol) to water. Antigen retrieval was achieved by boiling the slides in citrate buffer at pH 6.0 (Invitrogen) for 15 min. The slides were incubated with 2% BSA in PBST for 1 hr at room temperature to block non-specific binding. To achieve double fluorescent immunostaining, a mixture of rabbit anti-human CD90 antibody (1:100, Abcam, Cambridge, MA) with mouse anti-human CD24 antibody (1:100, Abcam, Cambridge, MA) or mouse anti-human CK antibodies which included CK19 antibody (1:100, Santa Cruz) and PanCK antibody (1:200, Biolegend) was incubated with the slides, respectively, overnight at 4 ºC. Then DyLight 488 anti-rabbit IgG and DyLight 549 anti-mouse IgG antibodies (Vector laboratories, Burlingame, CA) were diluted (1:150) and incubated with the slides for 1 hr at room temperature. There were three washes of PBST between each step. DAPI (1:8000, Sigma) was then incubated with the slides to visualize nuclei. Finally, the slides were dehydrated in alcohol (75%, 95% and 100% ethanol), cleared in xylene and

then coverslipped using a mounting medium (Sigma). The staining was evaluated under an Olympus BX-51 fluorescent microscope where CD90 staining was shown in green, CD24 or CK in red, and DAPI in blue.

4.4   Results

The Labyrinth is a label free technology that facilitates the study of the phenotypic heterogeneity among CTCs, which remains elusive because platforms that capture CTCs are not comprehensive. EpCAM− CTCs are crucial to understanding cancer metastasis, with the ultimate goal of developing treatments to prolong patient survival[176]. Furthermore, the fraction of CTCs that extravasate and are able to generate distant metastases may have lost EpCAM expression and are believed to have undergone the epithelial-mesenchymal transition (EMT), which results in the downregulation of epithelial cell markers[14,177-179]. In fact, several groups have also reported that CTCs express stem cell and/or EMT-associated markers[179]. This study examines the use of CD90 as an EMT marker and its co expression with epithelial markers CK and CD24, as observed on Figure 4.1.

In order to isolate and analyze protein expression of epithelial and mesenchymal markers in CTCs, 12 blood samples from pancreatic cancer patients were processed through Labyrinth (Figure 4.1). These samples were classified according to their stage: resectable (n=4), unresectable (n=4) and metastatic (n=4). CTC were recovered from the second outlet from each patient. Once isolation was completed, the potential of CTCs as a surrogate for tissue biopsies using immunocytochemistry was studied to analyze protein expression of epithelial and mesenchymal markers.

CTCs were firstly enumerated using the standard definition of a CTC, in which they are identified as DAPI-positive nucleated cells (shown in blue) staining positive for cytokeratin (shown in red) and negative for CD45 (shown in green), as shown on Figure 4.2. Using this criteria, it was observed that all pancreatic cancer patient samples tested positive for CTCs. Results showed an average yield of 10±7 CTCs per mL blood for cancer patients; while healthy controls showed 1±0.6 CTCs per mL blood. Although a more extensive cohort is needed for statistical significant results, there is a higher average CTC number for patients with unresectable tumors than for any other stage.
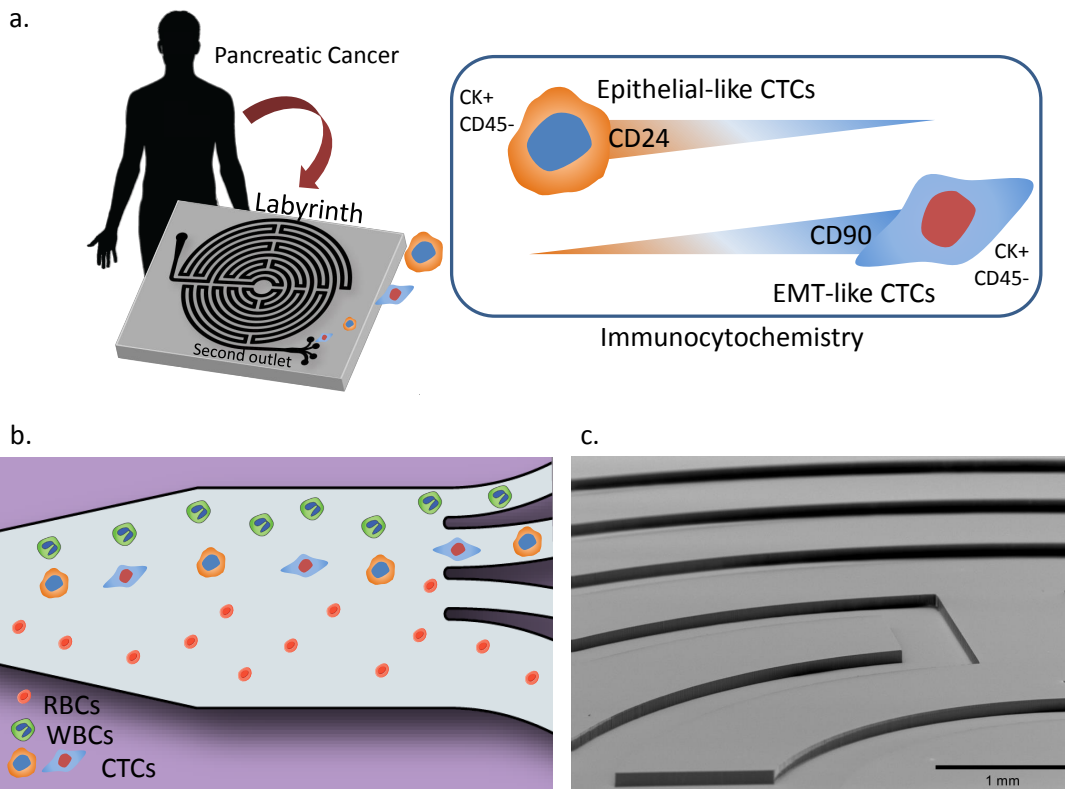
Figure 4.1 Experimental outline for coexpression studies on isolated CTCs a) Schematic showing the experimental procedure for this study. Once CTCs are isolated they are characterized using Epithelial and EMT-like antibodies. b) When patient sample is processed through the device, cell are isolated based on their size. WBCs are discarded from the first outlet, while CTCs are collected on the second outlet. c) SEM image of loops and turns inside the Labyrinth.

Co-expression for CK and CD90 was analyzed for previously mentioned patient samples. Among the isolated CTCs for each patient, Figure 4.3 shows that all analyzed patient samples exhibit CTCs that co-express CK and CD90. Furthermore, more than 50% of CTCs across all patients showed this co-expression pattern, suggesting higher number of EMT-like cells than for the epithelial phenotype (CK+). No significant difference in co-expression patterns was observed across different cancer stages. This could suggest that EMT-like cells are present in early stages of pancreatic cancer, highlighting that this marker could be used for detection at early stages.
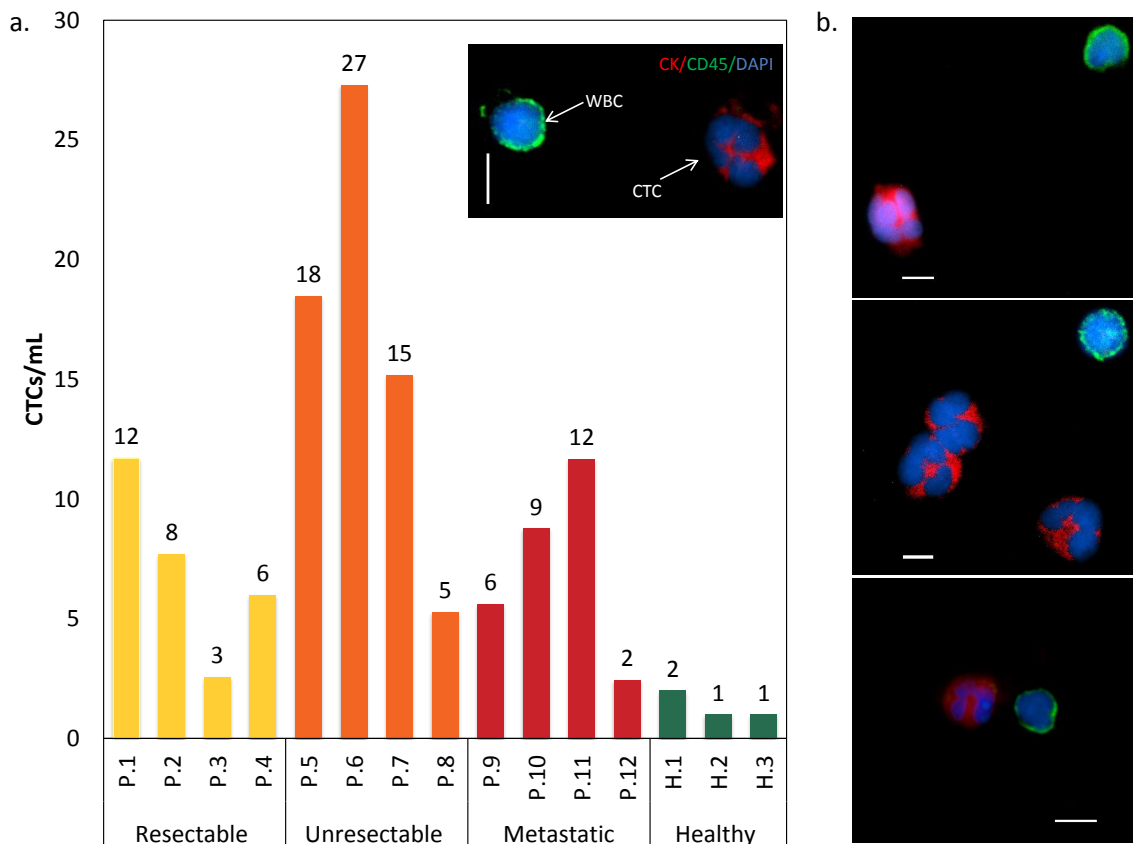
Figure 4.2 CTC counts for pancreatic cancer patient samples. a) Twelve patients from different cancer stages were analyzed for CTC counts. CTCs are defined as CK+ (red), CD45- (green) and DAPI+ (blue) b) Immunofluorescent images of CTCs and WBCs.

To study the potential of other markers as a tool for identifying early stages of cancer we used the markers CD24 and CD90. CD24 was used as a stem-like marker; while CD90 was used as an EMT marker. Figure 4.4 demonstrates the high variability of marker expression CD24+/CD90+ cells across all patients. Most of these patients exhibit a high percentage of CD24+/CD90+ cells through all stages.
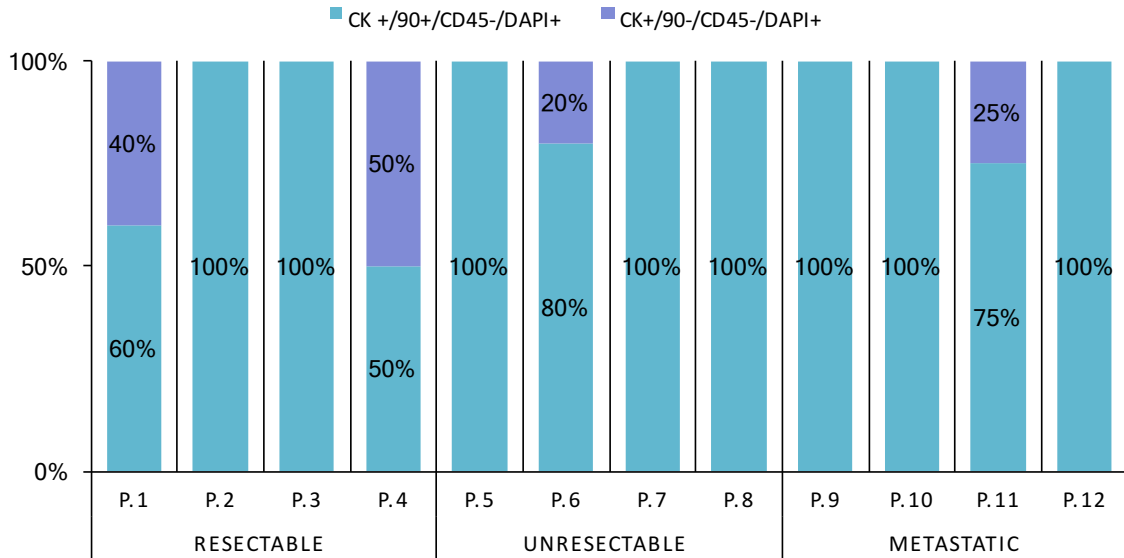
Figure 4.3 Coexpression enumeration for CD90 and CK in CTCs

Double fluorescence IHC staining was performed to investigate the co-expression of CD90 with CD24 or cytokeratin (CK) in pancreatic adenocarcinoma tissue. Figures 4.5 and 6 showed the overlap between CD90 (green) and CK/CD24 (red), respectively, in a patient with PDAC at stage IIA. As shown in Figure 4.5, CK (red) was strongly and abundantly expressed in the cytoplasm and membrane of malignant epithelial cells in PDAC. A small overlap between CD90 and CK (shown as yellow or orange in Figure 4.5) was localized on the cell surface of malignant ductal cells (indicated with arrows in Figure 4.5a) or in the cytoplasm of tumor cells (marked with squares in Figure 4.5b). As shown in Figure 4.6a, the overlap of CD90 and CD24 (indicated by rectangles) was observed in both endothelial cells of vessels (Figure 4.6a) and malignant tumor cells (Figure 4.6b) in PDAC.
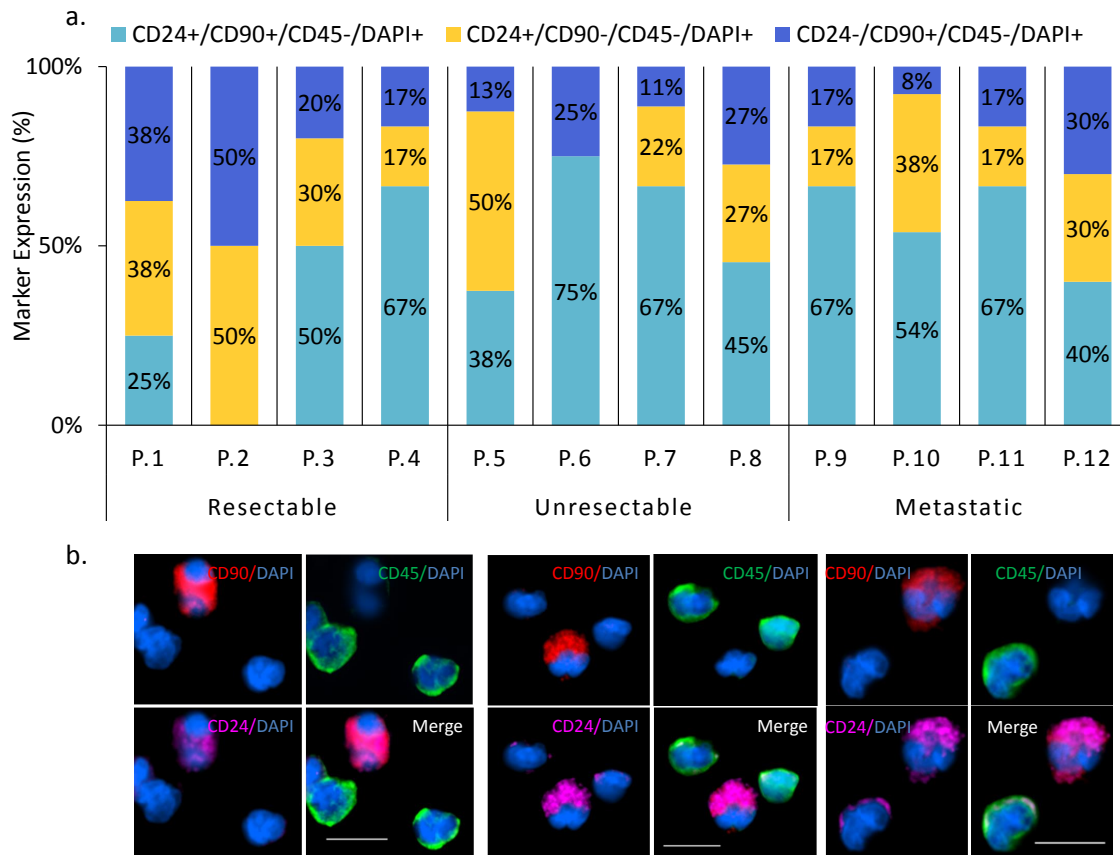
Figure 4.4 Coexpression of CD24 and CD90 on blood cells. a) Quantification of CD24 and Cd90 coexpression b) Immunofluorescent images showing coexpression of CD24 (pink) and CD90 (red) on DAPI+ (blue) cells.
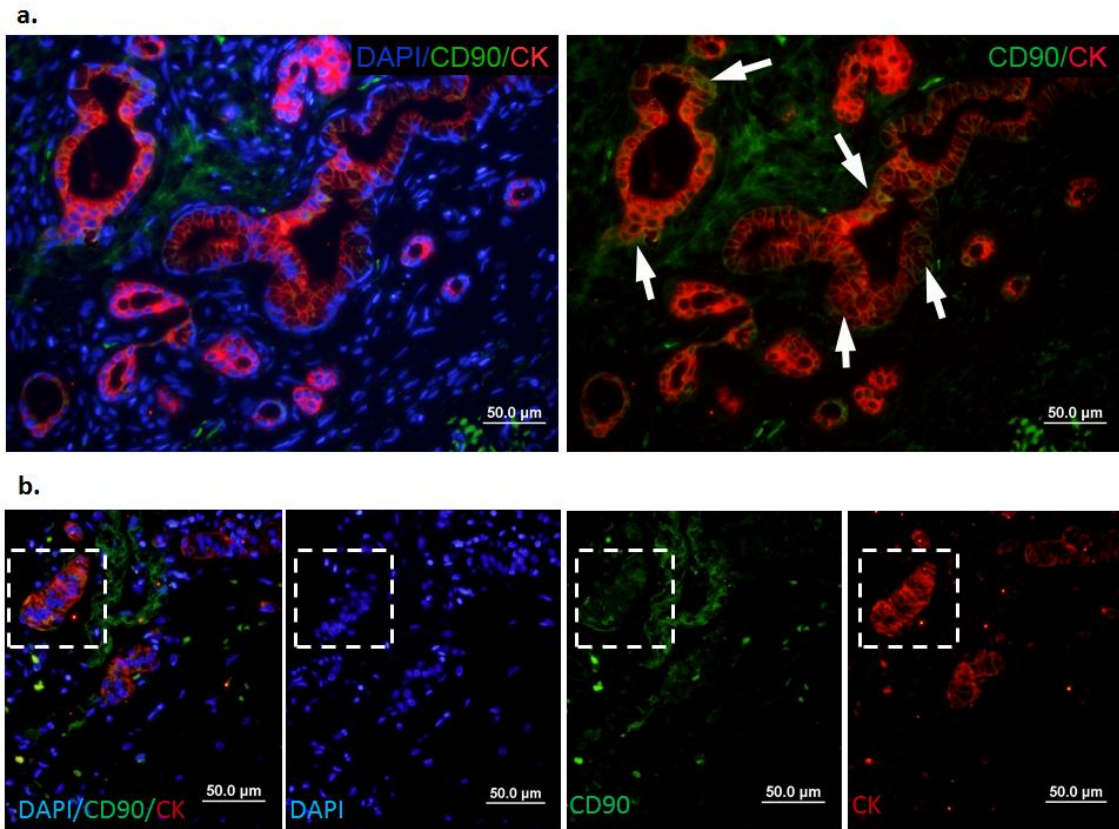
Figure 4.5 Representative images of double fluorescent immunostaining of CD90 (*green*) and CK (*red*) in a patient specimen of PDAC at stage IIA. DAPI counterstaining was used to visualize nuclei (*blue*). The co-expression of CD90 and CK was shown in *yellow* or *orange* in the merged images. a) Overlap of CD90 and CK on the cell surface of malignant ductal cells (indicated with arrows). b) Co-localization of CD90 and CK in the cytoplasm of tumor cells (marked with squares). Scale bars = 50 μm.
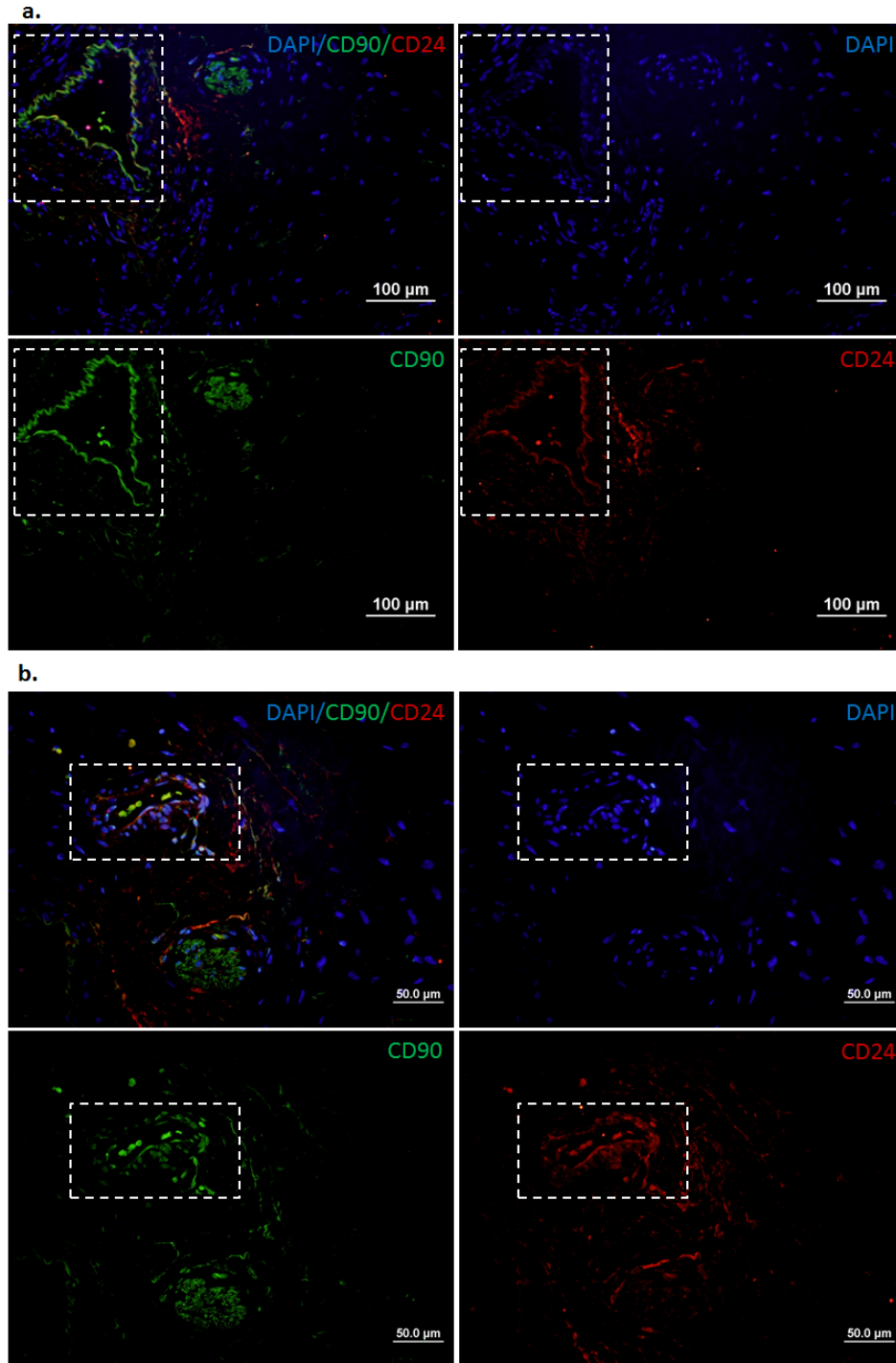
Figure 4.6 Double fluorescent immunostaining of CD90 (green) and CD24 (red) in pancreatic adenocarcinoma. DAPI counterstaining was used to visualize nuclei (blue). The co-expression of CD90 and CD24 was observed in endothelial cells of vessels (Figure 6a, scale bars = 100 μm) and malignant tumor cells (Figure 6b, scale bars = 50 μm) in PDAC.

4.5   Discussion

Consistent with previous studies[178], CD24 exhibited a strong or moderate expression predominantly on the membrane and cytoplasm of malignant ducts and vessels in PDAC, while the overexpression of CD90 was observed in the tumor vasculature of PDAC. In a previous study, Foygel et al. reported that CD90 could serve as a target for PDAC neovasculature imaging due to its significantly increased expression in PDAC vessels[179]. The co-localization of CD90 and CD24 on endothelial cells in tumor vasculature of PDAC indicates that CD90 may play a role in angiogenesis in pancreatic adenocarcinoma and these endothelial CD90+CD24+ cells may escape from primary tumors and invade into the blood circulation as CTCs.

The expression of cells with the CD24+/CD90+ combination of markers is relatively rare in the tissues and is only found in approximately 1% in the tissue examined. In early stage cancers these cells with this combination of markers are rarely if ever observed in pancreatic cancer tissues[178]. The CD24 generally stains in the ducts while CD90 stains outside the ducts on the stellate cells in the stroma. The fact that there are a relatively large percentage of the CTCs, which are circulating with both markers, may be significant. This type of phenomenon has been observed in previous work where CTCs may be arrested in a biphenotypic state[14] where CTCS may still express epithelial markers along with mesenchymal markers during EMT. These cells may be involved in bringing the properties of both types of cells to promote metastasis where tumor stromal signaling in priming cancer cells to metastasize is an essential process.

Another important issue is that these CK+ CTCs have a distribution of CSC markers associated with them. There is a broad heterogeneity of CSC markers even within the same patient where some cells may have one or another or both of the markers associated with

them. This heterogeneity becomes even more apparent when the comparison is made between patients where there are different distributions of these markers. This heterogeneity has only been studied herein for the CD24 and CD90, however the heterogeneity is likely to be even more complex where there are other CSC markers that are not being considered such as CD133 for example. These different markers and their combinations probably represent cells with different functions or properties that may be related to metastasis and the ability to escape the immune system for example.

In summary, we have used a label free method to isolate CTCs from the blood of pancreatic cancer patients where using CK+ as a marker we could typically identify 10-30 CTCs/mL. Moreover, we could identify the presence of the surface markers of CD24 and CD90 on these CK+ cells. The large majority of CK+ cells were also found to be CD90+ where CD90 is a marker of stromal cells in pancreatic cancer and is associated with EMT. We also found a mixed population of CK+ cells in the blood which were CD24+CD90+. A staining of the tissues showed that these CD24+CD90+ cells are very rare making up 1% of the total population whereas in the blood they constitute over 50% of the CTCs in many of the samples. These cells appear to have a mixed epithelial/stromal composition where it is postulated that these cells have enhanced survival properties in the bloodstream and may be important in cancer progression and metastasis. Future work will involve further isolation of these cells for investigation as to their metastatic properties and their transcriptomic and proteomic expression.

CHAPTER 5. EXPANSION AND FUNCTIONAL CHARACTERIZATION OF PANCREATIC CTCs FROM *IN VITRO* AND *IN VIVO* MODELS

5.1 Abstract

Improvement in pancreatic cancer treatment represents an urgent medical goal that has been hampered by the lack of predictive and biomarkers. Circulating Tumor Cells (CTCs) may be able to overcome this issue by allowing the monitoring of therapeutic response and tumor aggressiveness through ex vivo expansion. The successful expansion of CTCs is challenging due to low number in blood and the high contamination of blood cells. Here, we explored the utility of pancreatic CTC cultures as a preclinical model for treatment response. CTCs were isolated from ten locally advanced pancreatic cancer patients disease using the Labyrinth device and expanded three CTC samples in adherent and spheroid cultures. Proliferation and CTC phenotype were evaluated in culture and compared to the original patient specimen. Additionally, we evaluated take rate and metastatic potential in vivo and examined the utility of CTC lines for cytotoxicity assays. Our results demonstrate that CTC cultures are possible and provide a valuable resource for translational pancreatic cancer research while also providing meaningful insight into the development of treatment resistances and distant metastasis.

5.2 Introduction

Pancreatic cancer is the third leading cause of cancer-related death in the United States[180]. In fact, its survival probability has not improved substantially over nearly 40 years[1,180]. While surgical removal of the tumor represents the best treatment option for pancreatic cancer patients, only 20% of patients qualify for surgery[1,181]. Chemotherapy or chemotherapy combined with radiation is typically offered to patients with locally advanced disease[181,182].

A major challenge in the management of these patients is the early assessment of response to therapy that would allow the selection of the appropriate therapy and limit toxicity in treatment-resistant patients. Computed tomography (CT) is routinely used to stage and reassess patients following treatment. However, a number of studies have demonstrated that CT-detected treatment responses are infrequent[183]. Obtaining tissue from pancreatic cancer patients with locally advanced disease for histological diagnosis and acquiring pre- and post-monitoring presents a substantial challenge.

Over the past few years, several studies have studied circulating tumor cells (CTCs) in many epithelial cancers and suggested that CTCs can be used as clinical biomarkers of treatment response and prognosis[3,4,23,120,127,158,161]. CTCs are cancer cells that have shed into the vasculature or lymphatics from a primary tumor and are carried around the body in the circulation. CTCs are believed to have the potential to develop into distant metastases, which are the major cause of cancer related mortality. However, the isolation of viable CTCs is an actively research area with limited success. Hence, the dire need of such technologies hamper culture approaches.

The current gold standard for CTC isolation is the CellSearch system, which uses magnetic beads functionalized with antibodies against the epithelial cellular adhesion molecule (EpCAM)[3,22,30]. Due to the use of antibodies for CTC capture, this system fails to detect cancer cells with reduced EpCAM expression and may thus only enrich a small subpopulation of CTC [20,40,184,185]. Hence, to address the shortcomings of the FDA-approved CellSearch system, the development of new technologies with higher sensitivity is desired. This can be overcome by the use of microfluidic technologies that allow for unprecedented spatio-temporal control of cells [4]. Their application in cancer research is now well established[186] with a number of studies demonstrating successful isolation and characterization of CTCs from clinical samples[133]. Microfluidic CTC isolation technologies are mainly categorized by their exploitation of either CTCs' distinctive (i) biological properties or (ii) physical properties[186]. The former is based on the expression of cell surface markers, while the latter includes size, deformability, density, and electric charge[187]. The use of CTCs' physical properties to develop microfluidic devices allows label-free isolation, which overcomes biased cell selection using the CTCs' biological properties, such as protein expression and molecular markers. Furthermore, isolated cells using label-free technology are not modified, which permits greater flexibility for downstream characterization of CTCs. In summary, advances in label free microfluidic technologies allow the reliable detection and isolation of CTCs from clinically available blood draws. This will in turn allows functional characterization of CTCs to understand the utility of CTCs as predictive and prognostic markers and may serve as a surrogate tumor biopsy. However, previously reported clinical studies have mostly focused on CTC

enumeration in guiding prognosis in metastatic cancer patients, and current research is exploring the pharmacodynamic and predictive biomarker utility of CTCs.

A number of studies have isolated and evaluated CTCs in patients with pancreatic adenocarcinoma[188]. Early studies identified CTCs in pancreatic cancer patients with metastatic disease using several tumor cell markers including CK20, CEA, and c-MET and demonstrated that compared to other types of malignancies, these patients have relatively low numbers of CTCs[189-193]. Recent reports have concentrated on CTCs in patients with locally advanced pancreatic cancer. Ren *et al.* examined CTCs in 31 patients with stage III and nine patients with stage IV pancreatic cancer. Eighty percent of these patients were found to have CTCs prior to chemotherapy, and this number decreased to 29% after treatment[194]. Bidard *et al.* analyzed blood samples of 79 patients with locally advanced pancreatic cancer treated on a clinical trial for CTC detection. This study identified CTCs in only 11% of patients; however, the presence of CTCs was associated with poor outcome[3].

Beyond CTC enumeration, an *ex vivo* expansion and functional characterization of patient-derived CTCs will help to elucidate the clinical application of CTCs in pancreatic cancer. Due to their low frequency in pancreatic cancer patients[188] expanding such cells becomes a dire need of any CTC study. To our knowledge, no CTC cultures in pancreatic cancer have been reported. However, some success has been reported across other types of cancers using affinity based approaches. In breast cancer, CTC cultures were reported by Yu *et al.* using the CTC-iChip[115]. Cultures were done under hypoxic and nonadherent non-adherent culture conditions, achieving success for 6/36 breast samples. In colon cancer, Cayrefourcq *et al.* was also able to expand CTCs from 2/71 colon cancer patients[116]. Our

own research group reported CTC culture in lung cancer using a microfluidic co-culture device, where 14 out of 19 samples were expanded[64]. While these technologies have shown the ability to expand CTCs, the inherent biased CTC selection of immunoaffinity based technologies limits the *ex vivo* functionality study of all distinct subpopulations of CTCs.

In order to further validate the utility of expanded CTCs, researchers have started developing CTC-derived xenografts (CDX) models. Such models serve as a method to examine expanded CTCs' *in vivo* properties including tumorigenicity and drug susceptibility. For example, Cayrefourcq *et al.* showed the generation of colon tumors from a CTC-derived cell line in immunodefficient mice[116]. In breast cancer, Yu *et al.* successfully established five CTC cell lines, where three were tumorigenic in mice[115]. In small-cell lung cancer, Hodgkinson *et al.* demonstrated that CTCs from patients with either chemosensitive or chemorefractory tumors are tumorigenic in immune-compromised mice. Furthermore, their findings mirrored the donor patient's response to platinum and etoposide chemotherapy[114]. In order to successfully perform these *in vivo* CTCs studies, a high initial concentration of CTCs was required ($>10^6$ cells) for all studies, making CTC expansion essential.

Recently, we developed and optimized a microfluidic device, the "Labyrinth", for the high throughput label free isolation of CTCs, which takes a hydrodynamic approach for the size based isolation of CTCs (Chapter 2). The Labyrinth is an inertial microfluidics based separation technology that demonstrated greater than 90% recovery when tested with various cell lines including pancreatic cancer cell lines, while achieving an 89% WBC removal. In our approach, since no positive or negative selection of cells is needed, the Labyrinth enables the study of CTC heterogeneity and allows the identification of multiple

CTC subpopulations through further downstream biological and functional studies. Our previous study showed the presence of CTCs that have undergone the epithelial-to-mesenchymal transition (EMT) across all pancreatic cancer patients. The use of our label free Labyrinth device enables the study on viable EMT-like CTCs, which are believed to be the most aggressive subtype of CTCs[151,195,196]. Building upon our previous expansion work on lung cancer, this study uses the Labyrinth to expand CTCs using a monoculture approach to maintain the simplicity of the Labyrinth by eliminating the need of CTC purification from other cell lines.

In the present study we explore the utility of pancreatic CTC cultures as a preclinical model for treatment response. CTCs were isolated from the blood of pancreatic cancer patients with locally advanced disease using the Labyrinth and expanded *in vitro*. CTC cultures were then characterized in both 2D (adherent) and 3D (spheroid) conditions. Such characterization was performed through the examination for epithelial and EMT features and compared to the original patient specimen. Furthermore, we evaluated tumorigenicity *in vivo* by injecting cultured CTCs into a NOD/SCID mice, thus creating a pancreatic CDX model. To our knowledge, these are the first ever pancreatic CTC cultures developed from pancreatic patient samples. The isolation and expansion of CTCs can provide meaningful information to elucidate the process of pancreatic tumorigenesis and dissemination to preempt its fatal result.

5.3 Methods

5.3.1 Patients

10 ml of whole blood for CTC extraction was obtained from ten patients with locally advanced pancreatic cancer as part of an Institutional Review Board approved

99

protocol (HUM00085016). Informed consent was obtained from all participating patients. Patient Demographics are shown on appendix table D.1.

5.3.2 CTC isolation using Double Labyrinth

For patient samples, red blood cells were removed from the samples using density separation (6% dextran solution, M.W. 250,000) prior to the labyrinth. The sample-dextran solution was kept still in room temperature (RT) for 1h to sediment the red blood cells. The supernatant was removed and diluted with PBS buffer at a 1:3 ratio. Samples were then processed through the pre-flowed labyrinth, at a flow rate of 2.5mL/min. To achieve higher purity all the second outlet product for all samples were diluted 1:2 samples and run through another labyrinth. The purified CTCs were used for characterization by immunofluorescence and culture.

5.3.3 CTC culture

The second outlet was processed using a RBC lysis buffer at a 2:1 (buffer:sample) and incubated on ice for 3min. Samples were then spun down and the pellet resuspended in culture medium (RPMI1640) supplemented with 10% FBS and 1% antibiotics. For adhered cultures, the cell suspension was plated into fibronectin coated 24 well plates. For spheroid cultures, CTCs were seeded on hanging drop array plates with 10cells/drop using serum supplemented RPMI. Confocal microscopy for live/dead staining using calcein and ethidium homodimer at Day 14, indicate high viability within CTC spheroids.

For growth curve analysis, CTC cultures were seeded in 96 well dishes at 1000 cells per well. Cell proliferation was evaluated using Alamar blue per the manufacture's guidelines for 6 days. Absorption was measured using the Biotek-Synergy Neo-Plate reader.

5.3.4 Immunofluorescence staining

CTCs were processed using Thermo Scientific™ Cytospin 4 Cytocentrifuge according to the manufactures guidelines. Cytoslides were fixed using 4% PFA and stored at 4°C until staining.

For immunostainings, samples were permeabilized with 0.05% PBST solution for 15min and blocked using 20% donkey serum for 30min at RT. A cocktail of primary antibodies was added and incubated at 4°C in a humidified chamber overnight. Samples were incubated in dark with secondary antibodies for 45min at RT and mounted with Prolong Gold () with DAPI. CTCs were classified PanCK and DAPI positive and CD45 negative. White blood cells (WBC) were considered to be CD45 and DAPI positive.

Slides with spheroid sections were deparaffinized and rehydrated by dipping three times in xylene, two times in 100% ethanol and once each in 95% and 70% ethanol. Antigen retrieval was performed by boiling slides in citrate buffer (pH=6.0) for 10min. Chamber slides with cultured cells were fixed with 4% Paraformaldehyde (Electron Microscopy Sciences) for 10min and then washed with PBS. Samples were then permeabilized with ice-cold 1:1 Methanol:Acetone for 1min and washed with PBS. Blocking buffer consisting of 5% goat serum (Sigma Aldrich) diluted in PBS was applied at room temperature for 30min to prevent non-specific adhesion. Monoclonal anti-vimentin (5µg/ml, Thermo Fisher: MA1-10459) was diluted in blocking buffer and applied to samples overnight at 4°C. Samples were washed 3 times for 5minwith PBS. Goat anti-mouse IgM CF770 (4µg/ml, Biotium: 20385), anti-Pan-Keratin Alexa Fluor 555 (0.64µg/ml Cell Signaling Technology: 3478S), anti-EpCAM APC (0.24µg/ml BD Biosciences: 347200), anti-CD44 BV510 (1µg/ml, BioLegend: 103043), and anti-CD45

FITC (1μg/ml, BioLegend: 304005) were diluted in blocking buffer and applied to samples overnight in a refrigerator at 4°C. Samples were again washed 3 times for 5min with PBS. DAPI (1μg/ml, Thermo Fisher) diluted in PBS was applied for 10min at room temperature to label nuclei. A drop of Prolong® Diamond Antifade Mountant (Thermo Fisher) was then added and coverslips were mounted onto the slides for imaging.

5.3.5 Flow cytometry

Cells were trypsinized, washed with ice-cold PBS, and fixed at a concentration of 2×106 cells/ml in ice-cold 70% ethanol. For γH2AX analysis, samples were incubated with a mouse anti–γH2AX-specific antibody (clone JBW301; Millipore) overnight at 4°C followed by incubation with a fluorescein isothiocyanate–conjugated secondary antibody (Sigma) as previously described [33]. For quantification of γH2AX positivity, a gate was arbitrarily set on the control, untreated sample to define a region of positive staining for γH2AX of approximately 5%. This gate was then overlaid on the treated samples. Samples were stained with propidium iodide to measure total DNA content and analyzed on a FACScan flow cytometer (Becton Dickinson) with FlowJo software (Tree Star).

5.3.6 Immunohistochemistry

Xenograft tumors were excised, fixed and paraffin embedded. Paraffin tissue sections were cut, dried and dewaxed. Endogenous peroxidase was blocked in 3% hydrogen peroxide for 10 min. Microwave antigen retrieval was carried out under pressure at 120C for 10 min in 10 mM Citrate buffer, pH 6.0 using a T/T Mega microwave oven. Endogenous biotin was blocked in Vector's biotin blocking kit, and then slides were labeled with primary antibodies to cytokeratin (DAKO, Glostrup, Denmark, AE1/AE3, 1:200) and Smad4 overnight. Biotinylated anti-mouse IgG incubations were carried out

followed by streptavidin biotin detection system (Signet Pathology System, Deham, MA, USA) for 30min each Immunoreactivities were revealed by incubation in Nova Red substrate (Vector Lab, Burlingame, CA, USA) for 5min and counterstained in Mayer's haematoxylin.

5.3.7 Cell Proliferation Assay

Cultured cells were seeded at a concentration of 500 cells/well in 100μL of RPMI media into 96 well plates. Cells were incubated from 1-6 days at 37ºC and 5% CO_2. 10μL/well Cell Proliferation Reagent WST-1 (Roche) was added and incubated for 1h and. Plate shaken for 1min on a shaker. The absorbance was measured at an emission wavelength of 450nm, using a BioTek-Synergy Neo multi-purpose plate reader.

5.3.8 Treatments

Cultured cells were seeded at a concentration of 1000 cells/well in 100 μL of RPMI media into 96 well plates. Cells were incubated for 24h at 37ºC and 5% CO_2. Media was exchanged for Gemcitabine (0, 0.05 0.1, 0.5, 1, 5 uM) or 5-FU (0, 1, 5, 10, 50, 100 uM) diluted on RPMI media. Cells were incubated for 24h, the media was replaced and cells cultured for 48h. 10μL/well Cell Proliferation Reagent WST-1 (Roche) was added and incubated for 1h. Plate was then shake for 1min on a shaker. The absorbance was measured at an emission wavelength of 450nm, using a BioTek-Synergy Neo multi-purpose plate reader.

For radiation treatments, cells were treated with a single dose of 4Gy at 60% confluency and fixed for flow cytometry 16h after treatment. For gemcitabine treatments, cells were treated with 100nM gemcitabine for 2h and fixed for flow cytometry 22h after treatment.

5.3.9 Xenografts

Animal experiments were carried out using protocols approved by the University Animal Care Committee (PRO00006457) under the guidelines of the Association for Assessment and Accreditation of Laboratory Animal Care.

For CTC xenografts, 10^6 cells were injected subcutaneously into the flank of 4-5 week old NOD/SCID mice. Tumors were grown until the humane endpoint of ~1cm in diameter or distress due to ascites or metastasis. Tumor size was evaluated twice a week using calipers.

5.3.10 STR Fingerprinting

The UM DNA Sequencing Core performed cell identity verification using the Applied Biosystems IdentifilerPlus kit to assess CODIS markers. DNA testing was performed according to manufacturer's recommended protocols. Resulting fragments were assessed on an ABI 3730XL Genetic Analyzer. Analysis of resulting electropherograms were performed using ABI GeneMapper V5.0 software, as per manufacturer's recommended protocols.

5.4 Results

5.4.1 Patients

9-10 ml of whole blood for CTC extraction was obtained from 10 patients with locally advanced pancreatic cancer as part of an Institutional Review Board approved protocol (HUM00085016).

The patients displayed an age range common for pancreatic cancer patients (53 -74 years of age) and were evenly distributed between males and females (Table 1). All patients presented with locally advanced pancreatic cancer (T4N0M0) at the beginning of the study.

Blood samples were taken as part of a routine visit prior to the start of the treatment. A second blood sample was taken from three of the patients (patient 1, 2, 4) at the end of the first cycle of chemotherapy.

5.4.2 Isolation of patient-derived pancreatic circulating tumor cells

9-10 ml of whole blood were obtained from 10 patients with locally advanced pancreatic cancer prior to the start of therapy and CTCs were isolated based on size using the continuous high throughput label free Labyrinth device (Fig 1A). The isolated CTCs were divided in order to: (1) enumerate CTCs (~15% of isolated CTCs) and (2) set up a CTC culture (~85% of isolated CTCs).Similar to previous studies[188], we observed a wide range of CTC numbers from different patients. CTC numbers ranged from 8 cells/ml in patient 4 to 83 cells/ml in patient 2 (Fig 1B, Table 1).

Since the EMT is believed to be essential for the generation of metastatic cells, we examined the presence of EMT-like and epithelial cells in enriched CTC samples. (Fig 1C, Table 1). The majority of patients (6/10) show both EMT- like and epithelial cells in the purified CTC samples. Nevertheless, EMT-like cells represent the majority of CTCs. Only EMT-like cells were observed in the remaining 4 patients.

We were able to obtain a second blood sample from three of the patients (patient 1, 2, 4). This sample was taken after the first round of chemotherapy. The epithelial CTC fraction was lost in all three patients in response to chemotherapy, suggesting that CTCs can be used to monitor treatment response (Fig 1D, Table 2).
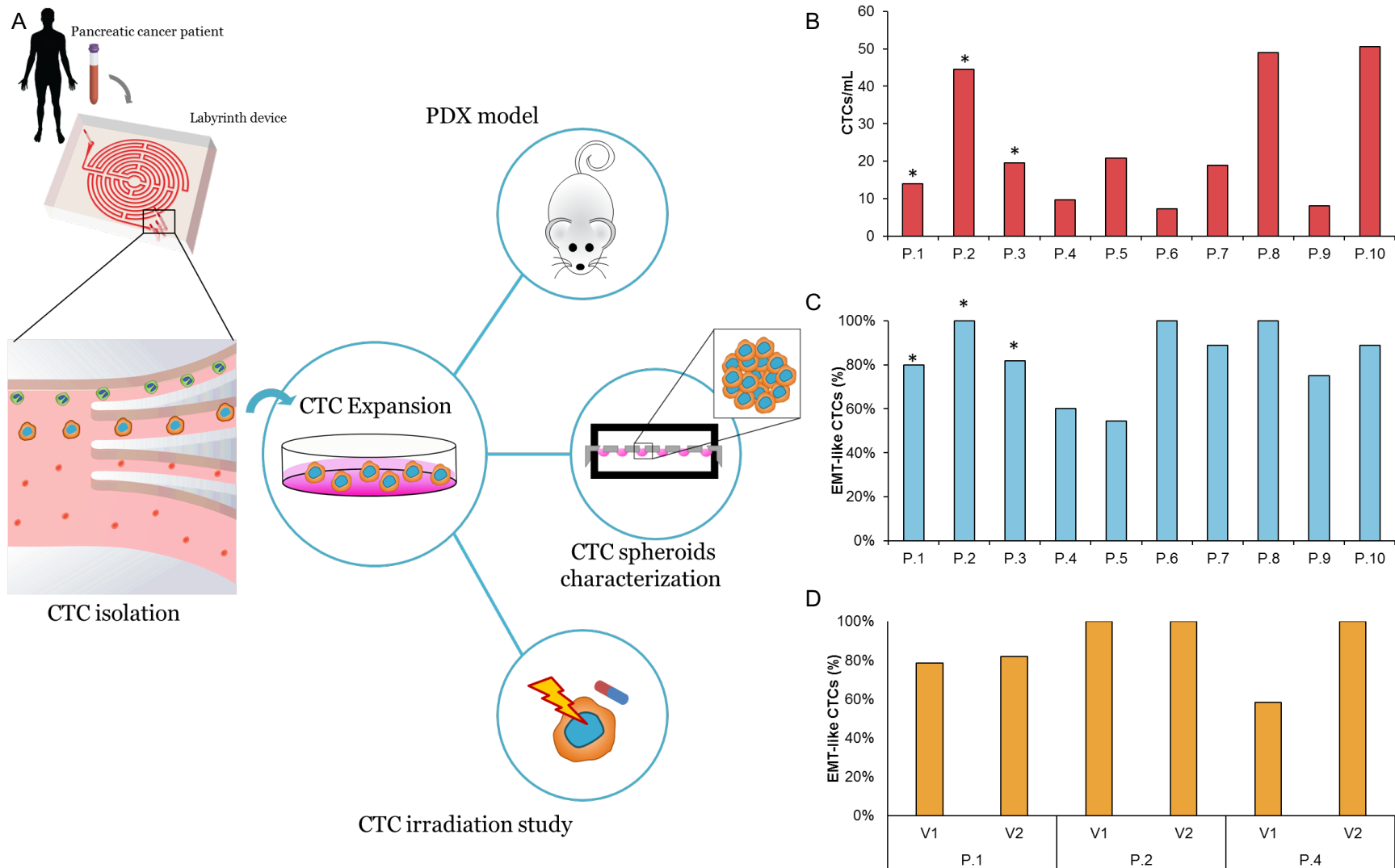
Figure 5.1 Characterizing patient-derived pancreatic CTC's (A) Workflow of CTC extraction, culture and subsequent analysis. (B) CTC/mL enumeration for 10 PDAC patients. Asterisk marks the samples that were successfully expanded. (C) Co-expression percentage of cytokeratin and vimentin of CTCs isolated from 10 PDAC patients and (D) two consecutive visits of 3 patients prior to treatment and after the first course of chemotherapy.

5.4.3 Circulating tumor cell culture

Purified CTCs of all 10 patients were seeded onto fibronectin coated 24 well plates in order to generate CTC-derived cell lines. We were able to generate CTC-derived cell line from 3 individual patients (patient 1, 2 and 3). The majority of samples did not grow into stable CTC-derived cell lines. We observed an outgrowth of WBCs in one of the patients, while the remaining samples showed no growth or lost proliferation potential after the first passage. We did not find any correlation between stage (Table 1), CTC number (Fig 1B) or prior treatment with CTC growth in culture.

The three CTC-derived cell lines display distinctly different morphologies in culture that are consistent with the morphology observed in pancreatic cancer cell lines (Fig 2A). We observed differences in growth rate that remain stable over a number of passages (Fig 2B). Similar to what we observed in the original CTC specimen, the cultures display a mixture of EMT-like and epithelial cells, which can be observed through differences in morphologies within cells of the same patient as well as staining for the respective markers (Fig 2A, C, Table 3). Patient 3 showed no presence of epithelial cells in the original CTC specimen. The CTC-derived cell line from this patient, however, shows both epithelial and EMT-like cells (Fig 1C, Fig 2C). This may be attributed to either a sampling related error due to low frequency in the original specimen or to a morphological drift that is related to the culture conditions.

Established CTC-derived cell lines were seeded on hanging drop array plates with 10cells/drop in order to evaluate their ability to form spheroids (Fig 3A). All cell lines formed spheroids within 14 days, although we observed difference in growth rates across the three sample, which was similar to that of observed in the adherent cultures (Fig 2B).

107

H&E section of the spheroids show a patient-specific morphology that is consistent with the range of morphologies observed in pancreatic cancer (Fig 3B). Staining for the EMT maker vimentin and the epithelial marker cytokeratin show a mix of both populations that is similar to what we observed in the adherent cell lines (Fig 3C, Table 3).

In order to verify the identity of the CTC-derived cell lines, we used STR fingerprinting to compare WBC and with the corresponding CTC-derived cell line. Additionally, we also included WBC cell line that came up during a CTC culture attempt in one of the patients. The WBC cell line showed a perfect match (15/15 markers) when compared to WBC extracted from the buffy coats of the patients archived blood sample. The CTC-derived cell lines, however, show very little match with their corresponding WBCs (patient 1: 2/15, patient 2: 1/15, patient 3: 1/15). We do observe high similarities between CTC cell lines of different patients (8-13/15 markers), suggesting a selection towards a similar phenotype.
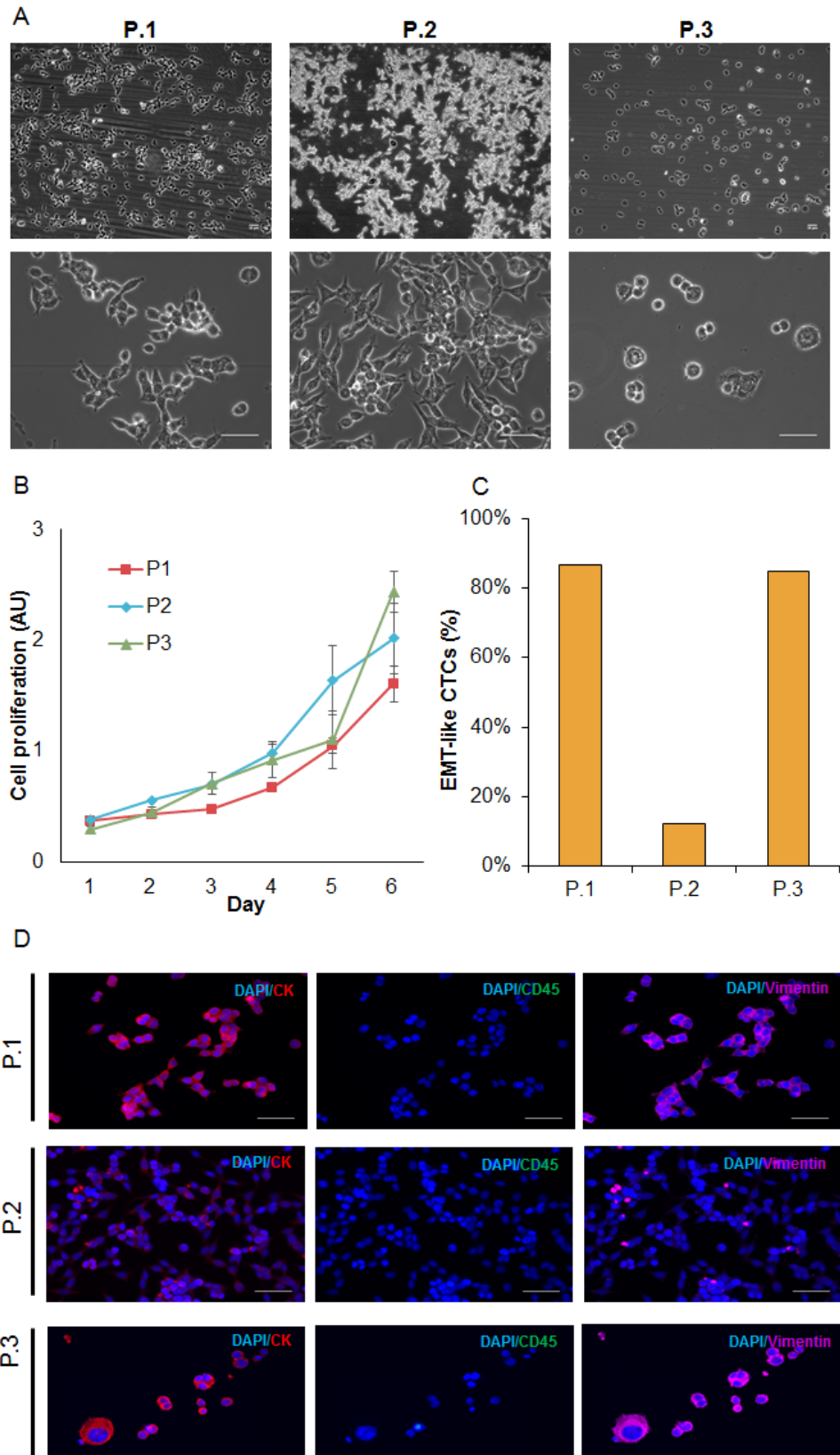
Figure 5.2 Characterizing CTC-derived cell lines (A) Brightfield images (10x and 40x) of expanded CTC cultures. (B) Growth curve analysis of adherent CTC cultures (n=3). (C) Percentage of EMT-like CTC in adherent cultures. (D) Representative images of immunofluorescence staining using
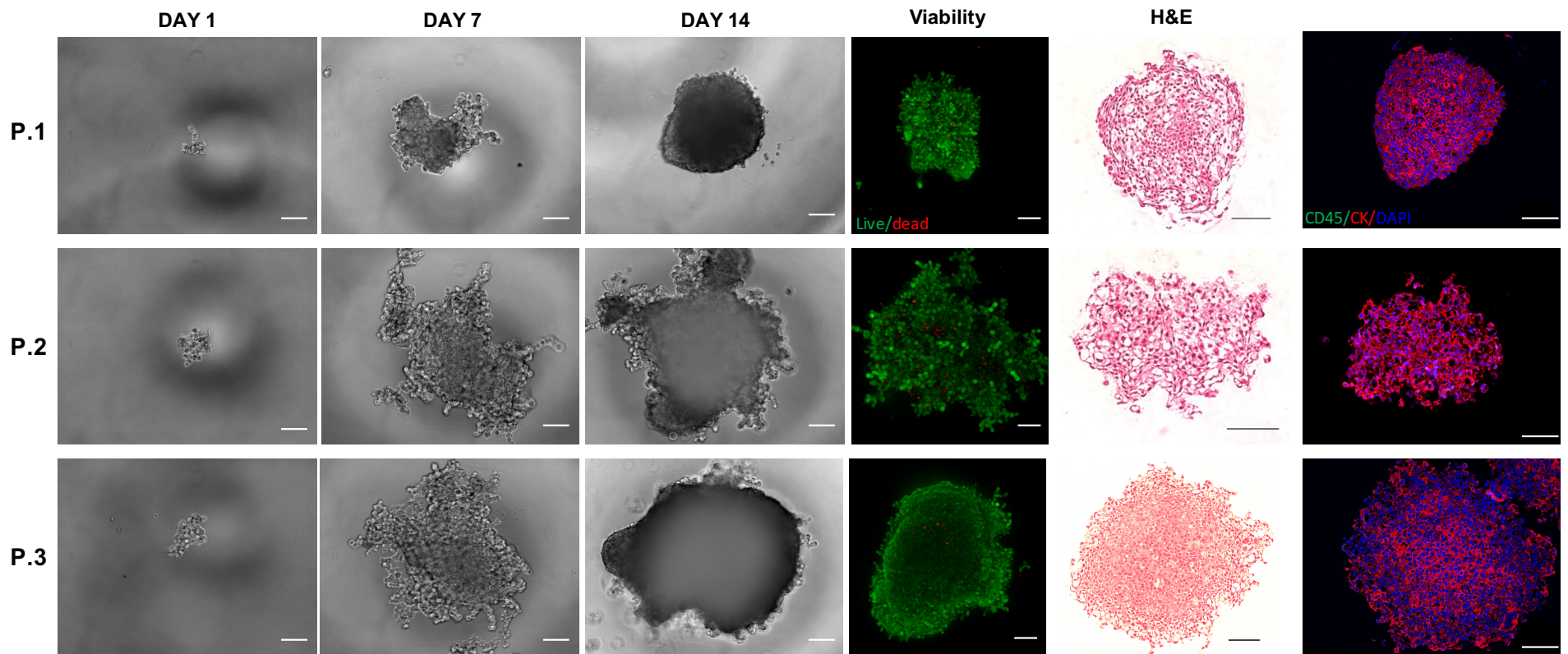
Figure 5.3 Characterizing CTC-derived spheroid cultures (A) Pancreatic CTCs were seeded on hanging drop array plates with 10 cells/drop. Alamarblue fluorescence was used to monitor viability/proliferation (expressed as a fold increase at Day 7 and Day 14, compared to Day 1). (B) Representative images of live/dead staining using calcein and ethidium homodimer at Day 14, indicate high viability within pancreatic CTC spheroids. (C) Representative images H&E of spheroids. (D) Immunoflourescence staining for cytokeratin (red), CD45 (green) and DAPI (blue) on spheroids. (Scale bar = 100μm)

5.4.4 Molecular Characterization of CTC PDX

In order to investigate the whether the CTC cell lines maintain the ability to form tumor in vivo that maintain the morphological characteristics of pancreatic tumors, the CTC cell line derived from patient 3 was injected into the flanks of 4-5 week old NOD/SCID mice.

We observed the appearance of tumors in all injected mice 3-4 weeks after injection of 10^6 cells (Fig 4A). Tumors were harvested when the tumor size reached the humane end point. At that time, we observed wide spread metastasis from the subcutaneous injection side to a number of organs, including liver, peritoneum and pancreas, as well as the development of ascites (Fig 4A, B). Immunohistochemistry shows cytokeratin positive subcutaneous tumors of pancreatic morphology that display large areas of tumor-associated stroma and invasion into the peritoneum (Fig 4C).

We observed the formation of macro (Fig 4B) and micro (Fig 4D) metastasis in the liver. While larger tumor masses were mostly observed on the surface of liver, a high number of micro metastases were observed throughout the entire liver and were located near blood vessels.

Pancreatic tumor masses were observed in 75% of the injected animals. Although some pancreatic tissue remains, the majority of the pancreas has been overtaken by tumors (Fig 4E). These tumors display large areas of tumor-associated stroma that are characteristic for the desmoplastic reaction typically observed in pancreatic cancer. Smad 4 staining is observed throughout the subcutaneous tumors (Fig 4F). We do however observe a reduction in staining intensity in areas of pleural invasion. While Smad4 staining

111

is lost in macro and micro metastases of the liver (Fig 4G), the expression is preserved in the pancreatic masses (Fig 4H). Similar to the subcutaneous tumors, staining intensity is reduced in areas of tissue invasion when compared to the tumor bulk.
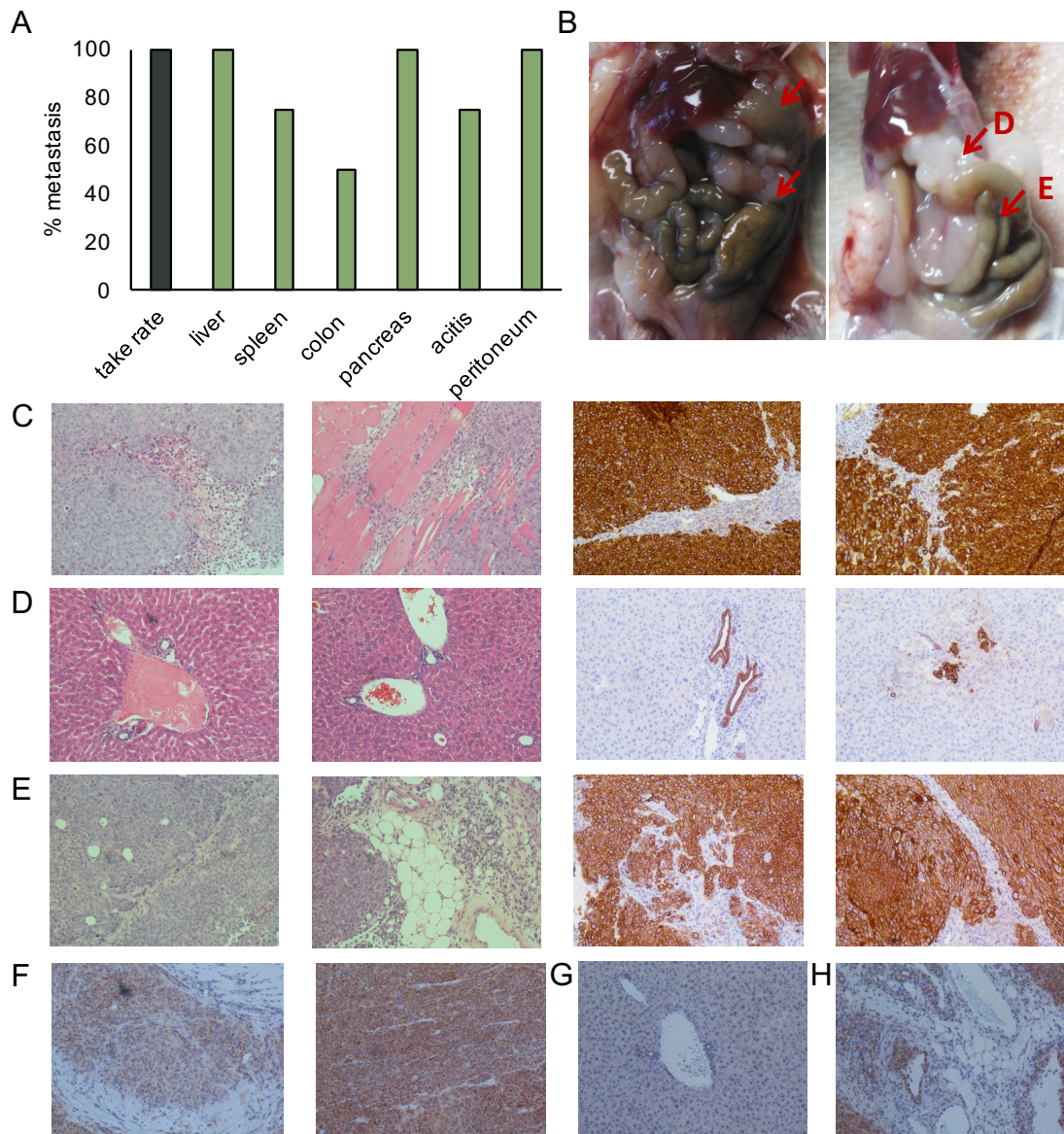
Figure 5.4 Characterization of the CTC PDX. (A) Injection of the CTC cell line derived from patient 3 into the flanks of NOD/SCID mice resulted in the development of subcutaneous tumors in all injected mice. Additionally, we observed wide spread metastases and the development of ascites. (B) Representative images of mice showing metastases in the liver, peritoneum, colon and pancreas. Representative images of sections stained for cytokeratin and H&E of (C) subcutaneous tumors, (D) liver metastases and (E) pancreatic metastases. Representative images of sections stained for Smad4 of (F) subcutaneous tumors, (G) liver metastases and (H) pancreatic metastases.

5.4.5 CTC cultures as a surrogate for treatment response

The failure to predict treatment responses based on serum markers or biopsies is a major obstacle in the treatment of patients with pancreatic cancer. While the CTC numbers extracted from clinically available blood samples are too low to allow a direct analysis (Fig 1B), a high number of cells for the analysis of treatment responses can be obtained from low passage cultures.

The CTC cultures can be used for WST assays accessing proliferation in response to treatment as demonstrated by treatment with gemcitabine and 5FU (Fig 5A) as well as Flow cytometry based assays evaluating changes in cell cycle progression and accumulation of DNA damage in response to treatment with ionizing radiation (IR) or gemcitabine (Fig 5B). CTC cultures derived from patient 1 and 3 show significant differences in 5FU and gemcitabine sensitivity that are consistent with a previously untreated pancreatic cancer cell. Treatment with gemcitabine resulted in the expected accumulation of CTCs in s-phase, while treatment with 4Gy led to arrest in G2.
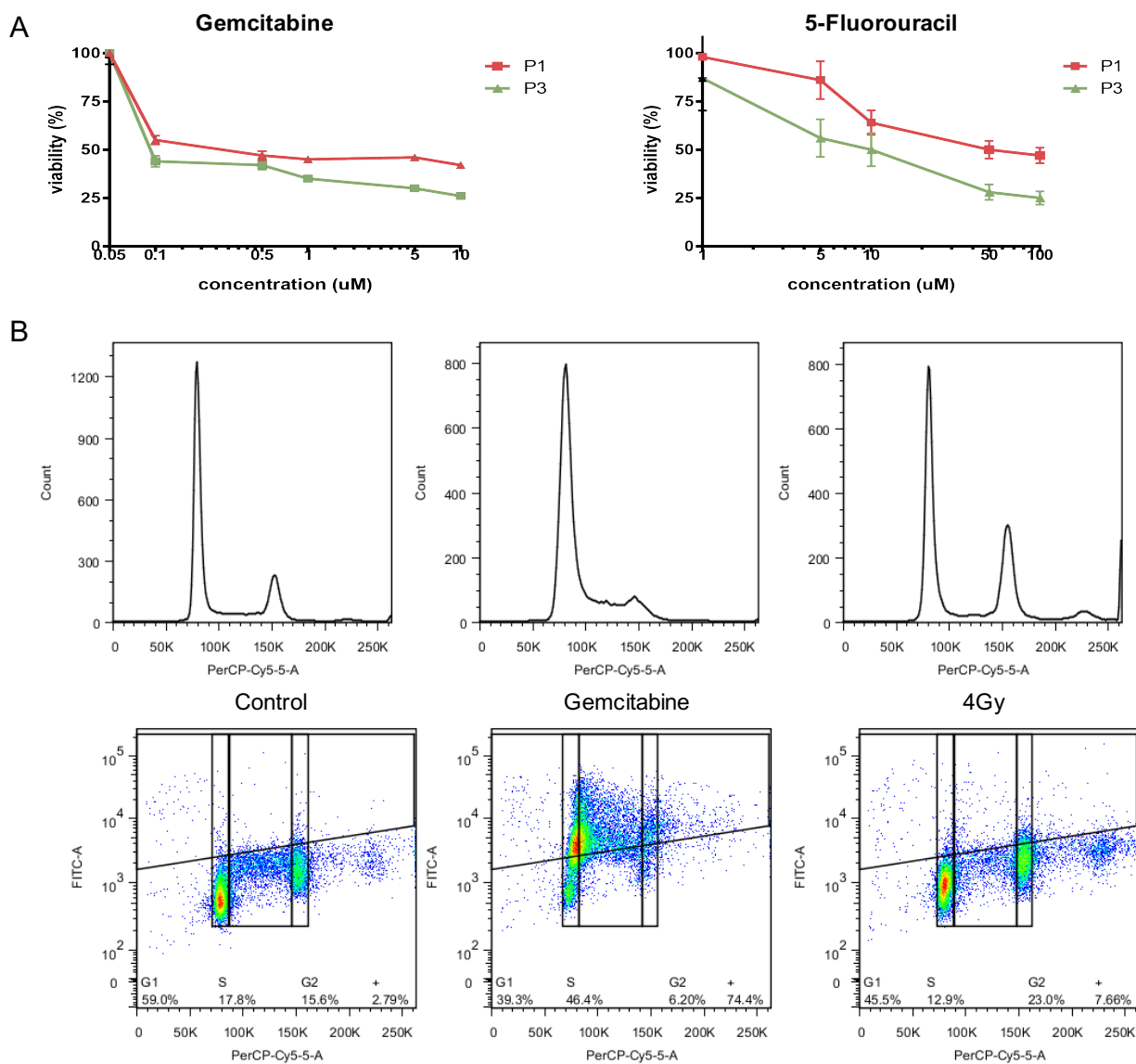
Figure 5.5 Treatment response of CTC cultures to chemotherapy. Response to treatment with (A) gemcitabine, 5FU and (B) IR was evaluated using WST assays and flow cytometry, respectively.

115

5.5   Discussion

Despite decades of extensive preclinical and clinical research, survival rates of patients with advanced pancreatic cancer have not improved significantly. The development of novel treatment approaches has been mostly hampered by the lack of available biomarkers, which can be used to access aggressiveness and metastatic potential and predictive/pharmacological markers of treatment response. Obtaining serial tissue biopsies to evaluate treatment response is not feasible in pancreatic cancer patients due to the invasive nature and risks associated with a biopsy. This can be overcome with CTCs, which can be safely obtained at any time point over the course of the treatment as part of routine blood draws.

Systematic evaluation of CTC prior and during treatment will broaden our understanding of the biology of tumor aggression and metastasis, and ultimately improve treatment outcomes for pancreatic cancer patients. Beyond CTC enumeration, an ex vivo expansion and functional studies with in addition to the ability of screening drugs and evaluating patient specific therapeutic targets, patient-derived CTCs will also help to elucidate the presence and functional differences of small CTC subpopulations within the CTC pool. This can address one the critical challenges in treating pancreatic cancer; that is the ineffectiveness of drugs to treat the aggressive pancreatic cancer to eradicate cancer totally. Expanded CTCs will enable designing tailor-made treatments targeting all of the sub clones instead of basing decisions solely on the predominant clone. Due to low CTC frequency in pancreatic cancer patients, especially in early stages, expanding such cells becomes a dire need of any CTC functional study[151]. While CTC cultures have been reported in literature, including breast[115], colon[116] and lung[64],success rates are low. So far,

116

no CTC cultures have been reported in pancreatic cancer. We have previously reported culture of lung cancer-derived CTCs using a microfluidic co-culture device, where 14 out of 19 samples were expanded[64]. However, this approach limits the use of the cultured CTC for downstream applications due to non-CTC cell contaminations. To overcome these limitations, the study presented here used a monoculture approach of patient-derived pancreatic CTC isolated through the label free approach Labyrinth.

Using the Labyrinth technology, we were able to isolate CTCs from 10 patients with locally advanced pancreatic cancer. The majority of the recovered cells were used to establish CTC cultures *in vitro,* while a small amount was used to evaluate and characterize the presence of epithelial- and EMT-like CTC sub populations.

We were able to isolate and evaluate CTC from all patients enrolled in this study; however, we were only able to establish CTC lines from 3 of the patients. We observed the presence of both epithelial- and EMT-like populations in two patient samples, and found that EMT-like cells were significantly more abundant, pointing to the aggressive nature of pancreatic cancer. Similar ratios of EMT to epithelial cells were also observed in the 2D and 3D cultures, suggesting that our culture conditions maintained the heterogeneity of the patient CTC population. We are, however cognizant of the fact that extended *in vitro* culture will result in the enrichment of single clones. Hence, for our experimental studies using CTC cultures, we restricted the usage to CTCs expanded within a maximum of 10 passages, which allowed us to perform several functional studies. However, it is important to note that we are able to grow these cells with repeated thaws and freezes beyond 10 passages. In our expanded CTCs, we observed distinct morphological differences associated with different phenotypes, ranging from epithelial to mesenchymal types as well

as significant differences in growth rate. Interestingly, we observed that CTC cell morphology was not predictive of molecular phenotype. For example, patient 2 exhibits mesenchymal-like cells with spindle like morphology (2D) and loosely packed spheroids (3D). However, the vimentin expression for this culture was substantially low compared to the other two CTC cultures. This highlights the importance of several functional studies to achieve a better understanding of CTCs rather than just few biomarkers by themselves. In an effort to verify the identity of the three CTC-derived cell lines though STR fingerprinting, we observed a high similarity between CTC lines. Indeed, the similarity between cell lines was higher that between matched pairs of CTCs and WBCs. We hypothesize that the adaptation for survival in the blood stream enriches for cells with similar pheno- and genotypes. While this observation is certainly very interesting, due to the low sample number we are at this time unable to draw any conclusion with respect to the significance of this observation.

Previously, there are limited studies in other cancer for testing the tumor initiating ability of CTCs in-vivo[114-116] but none in pancreatic cancer. For the first time, we were able to not only expand CTCs in pancreatic cancer, but also were able to demonstrate the tumor initiating ability of the expanded CTCs in a mouse model. Recently, a number of studies provided evidence for the role of CTCs in the formation of distant metastasis[8,66]. While treatment of the primary tumor is a major concern in pancreatic cancer patients that do not qualify for surgery, most patients succumb to the disease because of the formation of metastasis in liver, lung, spleen and bowel. Consistent with the clinical phenotype of pancreatic cancer patients, the CTC-derived cell lines display rapid tumor growth *in vivo*. We observed wide spread metastasis in mice injected with CTC-derived cell lines that

118

match the metastatic sides that are commonly found in patients, such as liver and bowel, as well as the formation of ascites. These results further support the importance of CTC models in enhancing our understanding of the metastatic process in pancreatic cancer. Treatment options are very limited for pancreatic cancer patients and they typically receive treatment based on their tumor stage rather than using precision medicine approaches due to the lack of predictive markers of treatment response. We believe that CTC cultures may be able to fill this gap by allowing for preclinical testing of newly developed compounds or personalized treatment approaches in a clinical setting. We have evaluated the utility of two of the most commonly used methods for in vitro drug toxicity testing. Our CTC lines performed well in MTT cell toxicity assays and flow cytometry analysis of DNA damage and cell cycle progression, suggesting that these cultures can be used in range of cytotoxicity assays. These assays may be adapted to high throughput assays and used in personalized medicine approaches. Future studies will be necessary to evaluate the robustness of this system in a larger number of patient-derived CTC lines and evaluate the genetic and phenotypical stability of the cultures.

Two consecutive samples from 3 patients were collected. These samples were collected prior to the start of the therapy and after the first course of chemotherapy. While we were not able to establish CTC lines from consecutive visits, these samples enabled us to evaluate changes in the CTC phenotype in response to chemotherapy. Although both samples contained epithelial- and EMT-like populations of CTC, we observed a trend towards increased numbers of EMT-like cells in response to treatment with gemcitabine. The small patient population enrolled in this study was not sufficient to further address this observation or make conclusions on the general population. Future studies in a larger

cohort will aim to collect multiple samples throughout the patients treatment cycle are currently in the planning/enrollment stage and will allow us to follow changes in the CTC phenotype in response to different treatment regimen. Once completed, these studies will shed further light on the importance of pancreatic CTCs in tumor metastasis and the impact of anti-cancer therapy on CTC populations.

CHAPTER 6. CONCLUSIONS

6.1   Summary of Research Findings

6.1.1   High-throughput Labyrinth for CTC isolation in pancreatic cancer

A label-free microfludic device, named "Labyrinth" (Chapter 2), was developed. This technology is a high-throughput, continuous, and true biomarker-independent (without positive or negative selection) device that isolates CTCs from whole blood. The device facilitates the study of CTC heterogeneity by using inertial forces that lead to a size-based isolation approach. This, in turn, enables the study of EMT-like CTCs, which are believed to be the most aggressive type of CTC that leads to metastasis. For applications in pancreatic cancer, the device was optimized at a flow rate of 2.5 mL/min, yielding both high CTC recovery (92%) and WBC removal (89%). Similar recoveries were achieved at different cell concentrations in whole blood, ranging from 10-100K cells/mL. Isolated CTCs were highly viable and preserved their morphology despite the high flow rate that the cells experienced traversing through the device. A preliminary clinical study was performed with 20 PDA patient samples, where CTCs were detected in all patients. CTCs isolated from these patients were found to contain subpopulations of CTCs expressing markers of both epithelial and mesenchymal-like cells. Based on these studies, the Labyrinth was determined to have a strong clinical application in the field of CTCs.

6.1.2 Clinical utility of isolated CTCs using Labyrinth

The use of CTCs for treatment monitoring was described in Chapter 3. More than 150 patients diagnosed with pancreatic cancer were processed using the Labyrinth for CTC isolation and enumeration. Among this cohort, pre- and post-treatment CTC counts were collected from three treatment groups: (1) surgery, (2) chemotherapy, and (3) radiotherapy. Results showed a decrease in CTC counts for all treatment options, with statistically significant decreases for both chemotherapy- and radiotherapy-treated patients. The use of CTCs for survival predictability of pancreatic cancer patients was also studied. Results showed that a decrease in CTC counts correlates with higher survival probability for all treatment options. However, only pre-/on- chemotherapy patients had a statistically significant correlation. This study exhibited the potential clinical application of CTCs for monitoring treatment in pancreatic cancer patients.

6.1.3 Heterogeneity among isolated CTCs

This study utilized the Labyrinth to assess heterogeneity among pancreatic CTCs (Chapter 4). Patient samples were processed for CTC isolation and monitored for markers associated with the EMT-like and stem-cell population, including CK, CD24, and CD90. It was found that CK+ CTCs had CSC markers associated with them in most cases. A substantial number of cells collected also had multiple markers associated with CSCs. Lastly, tissue analysis from one patient revealed cells co-expressing CK and CD90, as well as CD24 and CD90. Such cells appeared to have a mixed epithelial/stromal composition. It is postulated that these cells have enhanced survival properties in the bloodstream and that they may be important for cancer progression and metastasis. This study identified CTCs without the use of EpCAM and revealed unique combinations of CSC markers in

CTCs that could potentially be used for prognosis of and monitoring therapies for pancreatic cancer.

6.1.4 *In vitro and in vivo* studies of CTC cultures

In this functional study, the use of pancreatic CTC cultures as a preclinical model for treatment response was explored (Chapter 5). CTCs were isolated in 10 patients with locally advanced pancreatic cancer using the Labyrinth and expanded *in vitro* for at least 30 days using fibronectin coated plates. CTC expansion was successfully achieved in 3 of the samples (30% success rate). These CTC cultures were then characterized in 2D (adherent) and 3D (spheroid) conditions *in vitro*. Proliferation and epithelial/EMT features in both conditions were investigated and compared to the original patient specimens. Differences between CTC cultures for commonly used chemotherapy agents for pancreatic cancer therapy were also investigated. Interestingly, different patterns of drug susceptibility between the patient-derived CTC cultures were found. Lastly, an *in vivo* pilot study was conducted by injecting cultured CTCs into a NOD SCID mouse ($n = 4$), creating a pancreatic CDX model. To our knowledge, these are the first pancreatic CTC cultures developed from pancreatic patient samples. Both the expansion of CTCs and the heterogeneous population of cells that promote metastasis can provide meaningful information that can be used to elucidate the process of pancreatic tumorigenesis and preempt its often fatal outcome.

6.2 Limitations and Future Directions

6.2.1 Automation of Labyrinth in clinical setting

The Labyrinth has been proven to have high clinical utility for CTC isolation in pancreatic cancer patients. Running the device is a relatively simple procedure and does

not require advanced technical skills. However, the Labyrinth could benefit from a streamlined process where sample processing is completely automated. Such a system could consist of a blood injection into an apparatus that would automatically perform all of the pre- and post-processing steps, including CTC counts. Clinical staff would just have to load the blood to receive automated CTC counts within a few hours. To make this process possible, an automatic staining and scanning procedure must be developed and optimized. Roche© currently offers a system called the Discovery Ultra[197]. This automated IHC/ISH research slide staining system could be optimized for the use of ICC staining for isolated CTCs. The combination of this technology along with an automated CTC counter could streamline and automate the process of using the Labyrinth as a reliable CTC scanning procedure performed in a clinical setting.

6.2.2 CTCs as an early detection tool in high risk pancreatic cancer patients

Despite the utility of CTCs being strongly focused towards PDA patients, the Labyrinth could also be used for early screening of pancreatic cancer. By looking into high-risk groups, the early stages of metastasis could be identified and an appropriate treatment course, in turn, could be developed to circumvent the disease. Preliminary studies performed with the Labyrinth suggest that such groups test positive for CTCs (Figure 6.1). Furthermore, these groups show greater CTC counts than healthy controls (HC) and lower CTC counts than PDA patients, for both epithelial and EMT-like phenotypes. These results indicate the potential for CTCs to be used in early screening. Future studies should focus on understanding the reason for this pattern as well as identifying correlations between CTC counts and various clinical parameters, such as disease progression, CA19-9 numbers, and treatment response. Furthermore, parameters within the categories classified as high-

risk, such as pancreatic cysts, family history, and chronic pancreatitis, should also be investigated.

The potential of CTCs as a biomarker for early assessment of treatment response for pancreatic cancer should be evaluated as a result of this study. Molecular analysis using PCR from the extracted genetic material of CTCs could be used to look for mutations in pancreatic cancer related genes, such as KRAS and p53. Such approach could assist in further stratification of high risk patients, including intervention and watchful waiting. This could also lay the groundwork for treatment decisions for targeted therapies. Future work could include longitudinal studies that allow disease progression monitoring during a course of chemotherapy and radiation therapy and then correlating the findings with patient outcome.
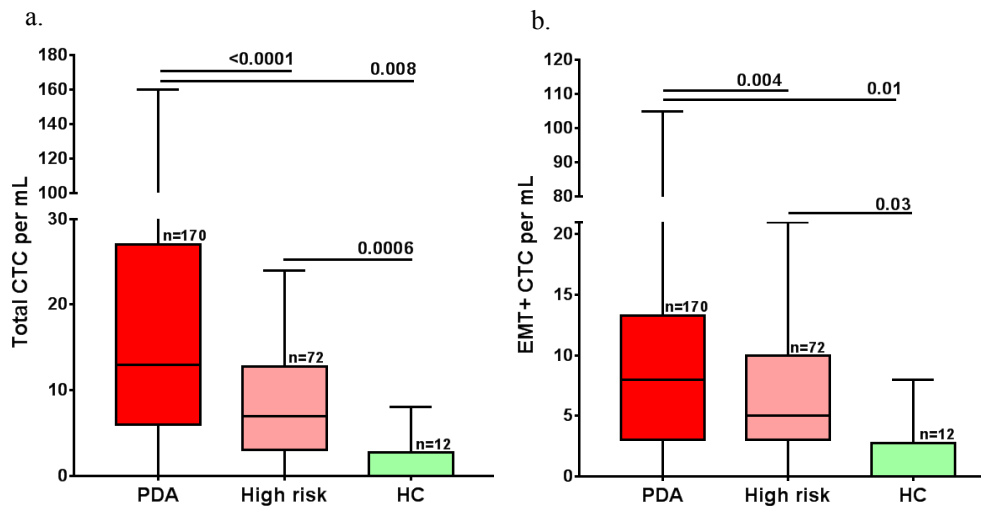
Figure 6.1 Preliminary Results for CTC counts in high risk patients a. total CTCs/mL vs b. EMT-like CTCs

6.2.3   CTC expansion

Although 3 CTC cultures were able to be successfully expanded, the 30% success rate could be significantly improved. Its relatively low success rate is due to due to the lack of cell-to-cell interaction inherent to monoculture systems. Ideally, a protocol should be

established to achieve a 100% success rate on CTC culture expansion. Alternative approaches to improve upon the discussed work could focus on identifying additional extracellular proteins that could provide a more nurturing microenvironment for the cells. For example, the Lahann laboratory has developed a synthetic polymer coating (PMEDSAH) that permits an undifferentiated stem cell to expand in fully defined xeno-free conditions over the long term (> 25 passages)[198]. This approach would ensure that CTCs under culture would not change from their original isolation phenotype. Such an approach would provide greater confidence when looking to answer clinical questions that arise from the study of CTCs.

Another future study would be further classification of the current CTC cultures into smaller CTC subpopulations. Within such subpopulations, functional studies could be performed to provide insight about each subgroup and their unique characteristics. For example, exploring what makes some CTC subpopulations more aggressive than others. Single-cell studies would also be a great tool to explore this question.

6.2.4 Use of miRNA for molecular studies on expanded CTCs

Once CTCs are successfully expanded, a plethora of functional studies could be performed to elucidate CTCs' critical role in metastasis. For example, an interesting topic is the use of miRNAs to investigate heterogeneity among pancreatic CTCs[196]. Recently, miRNAs have been identified as key regulators of gene expression. miRNAs are involved in crucial biological processes encompassing development, differentiation, apoptosis, and proliferation through imperfect pairing with target messenger RNAs of protein-coding genes and the transcriptional or posttranscriptional regulation of their expression[199,200]. Furthermore, it was shown that the miR-200 family plays a critical role in regulating EMT

by directly targeting the mRNA encoding genes Zeb1 and Zeb2, which are E-cadherin repressors[201]. Moreover, recent studies showed that members of the miR-200 family can regulate pancreatic cancer cell sensitivity to gemcitabine, which is accomplished through EMT induction[202].

As a proof of concept, miRNA 200 was upregulated in the established CTC cultures (Chapter 5) to observe phenotypic and genotypic changes related to EMT. Preliminary results have shown that miRNA200a can be successfully administered and transfected in CTC cultures. Future work involves the quantification of such miRNA200a uptake at both bulk and single-cell levels. For bulk studies, cultures will be examined for changes of epithelial and mesenchymal markers using immunofluorescence staining. Their invasion and migratory capability will also be studied. For single-cell level studies, CTCs will be microinjected with miRNA200a to show that its upregulation leads to a more epithelial phenotype. This study will help elucidate the clinical utility of miRNAs in understanding CTCs and their involvement in biological process leading to metastasis.

6.2.5   The use of expanded CTCs for personalized therapy and drug therapies

Failure to predict treatment responses based on serum markers or biopsies is a major obstacle in treating patients with pancreatic cancer. While the CTC counts extracted from clinically available blood samples are too low to allow for a direct analysis of treatment responses, a high number of cells can be obtained from low passage cultures. Therefore, it is hoped that expanded CTCs will serve as a potential avenue for the personalized treatment of pancreatic cancer. This goal could be facilitated by analyzing drug susceptibility on patient-derived CTCs. Several drug combinations could be tested on cultures and used as a guide before delivering treatment to the patient. It is hoped that, in the future, CTC

cultures could help identify ideal drug doses for individual patients, thus leading to more personalized therapies.

6.2.6   CTCs for *in vivo* studies

This study showed the potential of developing CDX models for the *in vivo* study of CTCs and their role in metastasis. While we were able to use one mice as a proof-of-concept, future work will involve developing mouse models for the remaining two expanded cultures. Additionally, many functional studies could be performed to understand the similarities and differences between the *in vitro* and *in vivo* expanded CTCs. One potential aim could be the pre-selection of EMT-like CTCs to observe if they are more likely to metastasize faster than other CTC subgroups. Another study could focus on the development of CDX from high-risk patients, with the hope to investigate the early stages of cancer.

APPENDICES

A. Development and optimization of Labyrinth for pancreatic cancer

Physics of the labyrinth

The inertial migration based particle separation relies on the equilibrium between inertial lift forces and Dean flow that results in the migration of particles during laminar flow in microfluidic devices with curved channels. Particles in a straight channel experience stresses that act over the entire channel surface, including shear stress that yields drag forces and normal stress that yields lift forces perpendicular to the direction of flow. The migration of particles due to lift forces was first observed by Segré and Silberberg in the 1960s [137,138]. Di Carlo reported that particles would be maintained at specific positions due to the combination of inertial lift forces where shear gradient lift pushes the particles toward the wall and the wall lift effect pushes the particles toward the center (Fig. S1a). These forces will confine the particles in a straight channel to several equilibrium positions, where the number of equilibrium positions is related to the geometry of the channel (Fig. S1c). A relation describing the magnitude of lift force (F_z) was reported by Asmolov [140]:

$$F_z = \frac{\mu^2}{\rho} Re_p{}^2 f_c(\text{Re}_c, x_c) \tag{1}$$

where Re_p is the particle Reynolds number, Re_c is the channel Reynolds number, and x_c is the position of the particle within the channel. The Dean flow, on the other hand, occurs

in the flow of curved channels. Dean flow is the secondary flow due to the centrifugal effects that will affect the particle equilibrium positions. Dean flow is characterized by counter-rotating vortices where the flow at the midline of the channel is directed outward around a curve, while the flow at top and bottom of the channel is directed inward (Fig. S1b). The drag force due to Dean flow is correlated with the particle size and curvature of the channel, and this drag force will also affect the equilibrium position of the particles. Therefore, the equilibrium between inertial lift forces and drag force from Dean flow can be utilized for size-based sorting. The lift forces stabilize particles at positions located along the centerline of a channel cross section, while Dean flow drag forces cause particles to circulate in the cross section (Fig. S1d). A new equilibrium position can be estimated from the ratio of F_z to F_D[203]:

$$\frac{F_z}{F_D} = \frac{1}{\delta}\left(\frac{a}{D_h}\right)^3 \text{Re}_c{}^n, \ (n < 0) \tag{3}$$

δ is the curvature ratio, $\delta = \frac{D_h}{2r}$.

CTCs can be isolated from other blood cells in curved microfluidic devices by specifying an appropriate flow rate and radius of curvature. The inertial force can be considered as the driving force that focuses the particles, while the drag force from Dean flow is the force that migrates the particles away from the center of the channel, leading to size-based separation. For the situation where F_D dominates, either particles might not be focused due to the insufficiency of F_z, or all the particles with different sizes could be pushed to the same focusing position due to the strong migration force (F_D). For the case when F_z dominates, particles with different sizes remain at the same equilibrium positions

as that in a straight channel due to the dearth of migration force. A proper control of flow rate and good design of microfluidic structure would lead to an adequate ratio of F_z to F_D that will cause cells to be well separated by size.

Hypothesis for sharp corners in Labyrinth
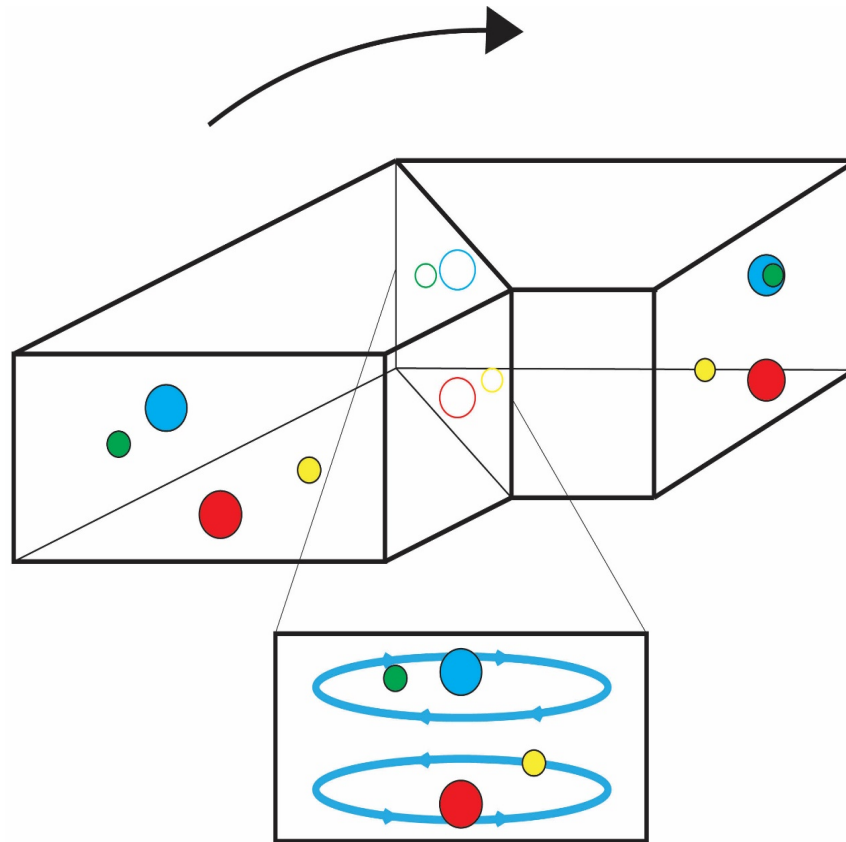
Figure A. 1 Hypothesis for sharp corners in Labyrinth. Strong Dean vortices at corners would help the focusing of small particles. Inertial lift forces acting on smaller particles are much weaker compared to that on larger particles (F_Z is proportional to the 4th power of particle size). Therefore, smaller particles (e.g. RBCs, WBCs) are generally difficult to focus. For instance, the large particles (red and blue) are easily focused thus they are already at the focusing position while passing through the sharp corners. The smaller particles (green and yellow), on the other hand, are not focused yet at the corner. The focusing of the green particle is enhanced by the strong Dean vortex at the corner and thus the green particle gets closer to its focusing position after passing through the corner. The focusing of yellow particle will be enhanced by the other corners in opposite direction.

Table A. 1 Ratio between Inertial force and Dean force

r (m)	Fz/Fd (WBCs)	Fz/Fd (Cancer Cells)
0.00225	0.405	0.81
0.00375	0.675	1.35
0.00525	0.945	1.89
0.00675	1.215	2.43
0.00825	1.485	2.97
0.00975	1.755	3.51
0.01125	2.025	4.05
0.01275	2.295	4.59
0.01425	2.565	5.13
0.01575	2.835	5.67
0.01725*	**3.105**	**6.21**
0.01875	3.375	6.75

*Currently used curvature for optimized design

Optimization of Labyrinth configuration

The optimization of the configuration in Labyrinth was based on both calculations and observations from experiments. As shown in following Table S1, the ratio between the inertial force (Fz) and Dean force (Fd), which dominates the equilibrium position of sized particles, were calculated in each loop for both WBCs and CTCs. Dean force is dominant in the inner loops (smaller r and Fz/Fd ratio), causing particles/cells focused in inner wall or unfocused. Lift forces are dominant in the outer loops (larger r and Fz/Fd ratio), resulting in the same focusing positions for both small and large particles as the condition is similar to straight channel. The purpose of this calculation was to find a loop which has the best curvature to separate CTCs from WBCs while maintaining their focusing. We also

observed that it takes 47 corners and 480 mm in length for WBCs to be focused, and therefore the design must incorporate more than this amount of corners. Combining experimental observations (Figure 2.1f), theoretical calculations, and numerous revisions in device design, we were able to fine tune and optimize the configuration of Labyrinth.
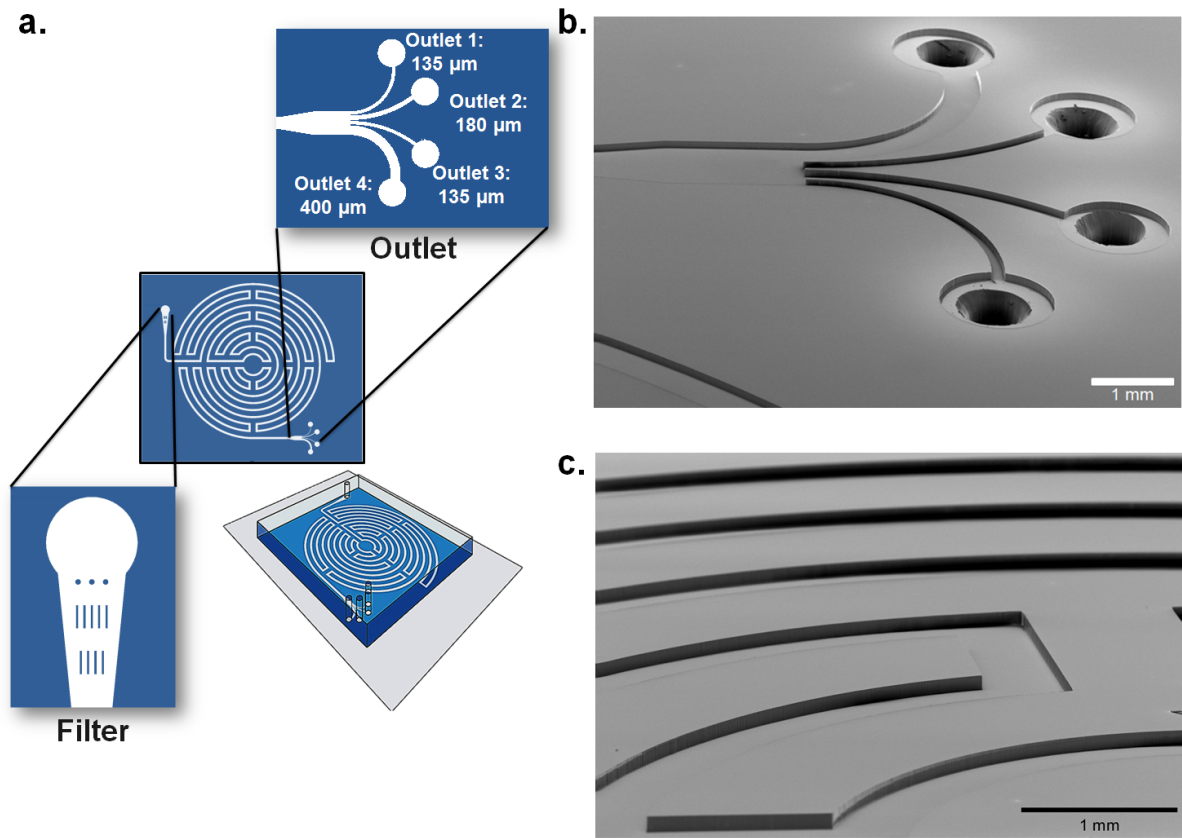
Figure A. 2 Optimized design of Labyrinth b, SEM image of Labyrinth's outlet   c, SEM image of corners and turns in Labyrinth Scale bar 1mm

CTC enrichment as a function of Labyrinth Height

Optimization of Labyrinth and flow rate was conducted using pre-labeled MCF-7 cell line (GFP) and WBCs (DAPI). Labyrinth with different height of microfluidic channels (range: 90-110 µm) were tested with spiked buffer sample at various sample flow rate (range: 500-3000 µL/min). In all models of Labyrinth, no streamline focusing or cell separation was observed at low flow rate (500-1000 µL/min), and cell focusing occurred at flow rate above 1500 µL/min.

Labyrinth with 95 µm channel height was selected as the finalized model due to its widest separation distance among all models. The separation is optimized at 2500 µL/min, where the two streamlines of cells are apart for 238 µm with a minimum gap distance of 150 µm (as shown in Figure A.4)
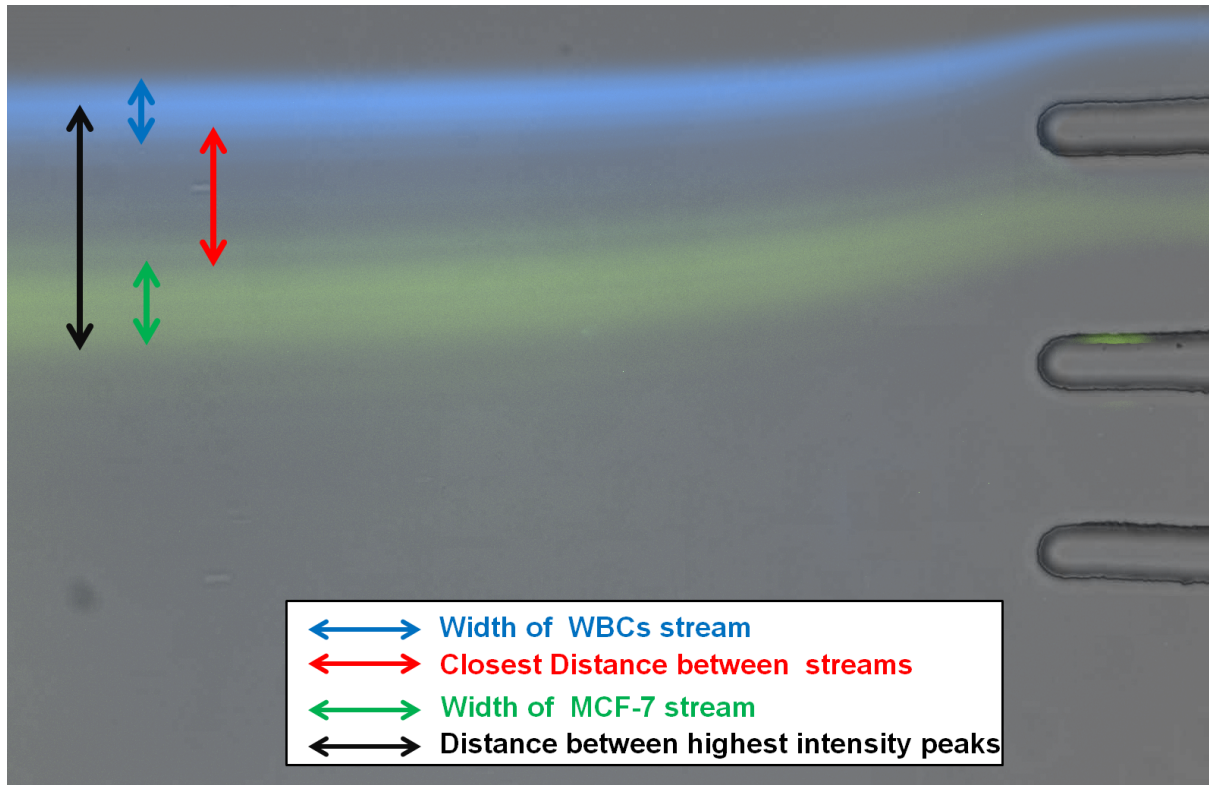
Figure A. 3 Legend for recorded values regarding Labyrinth height optimization

Table A. 2 Streamline measurements for the Labyrinth of height 90 µm

Labyrinth Height (90 µm)				
Flow rate (mL/min)	FITC W (µm)	DAPI W (µm)	Peak to peak Dist. (µm)	Closest Dist. (µm)
0.5	-	-	-	-
1.0	-	-	-	-
1.5	-	64	-	-
2.0	109	45	214	90
2.5	73	66	252	125
3.0	102	142	185	52

Table A. 3 Streamline measurements for the Labyrinth of height 95 µm

Labyrinth Height (95 µm)				
Flow rate (mL/min)	FITC W (µm)	DAPI W (µm)	Peak to peak Dist. (µm)	Closest Dist. (µm)
0.5	-	-	-	-
1.0	-	-	-	-
1.5	118	54	130	57
2.0	140	90	159	33
2.5	126	40	238	150
3.0	114	142	190	73

Table A. 4 Streamline measurements for the Labyrinth of height 100 µm

Labyrinth Height (100 µm)				
Flow rate (mL/min)	FITC W (µm)	DAPI W (µm)	Peak to peak Dist. (µm)	Closest Dist. (µm)
0.5	-	-	-	-
1.0	-	-	-	-
1.5	168	60	219	16
2.0	74	73	206	111
2.5	116	47	230	118
3.0	140	45	240	128

Table A. 5 Streamline measurements for the Labyrinth of height 110 μm

Labyrinth Height (110 μm)				
Flow rate (mL/min)	FITC W (μm)	DAPI W (μm)	Peak to peak Dist. (μm)	Closest Dist. (μm)
0.5	-	-	-	-
1.0	-	-	-	-
1.5	170	180	135	26
2.0	116	49	164	73
2.5	118	67	195	60
3.0	95	61	197	61
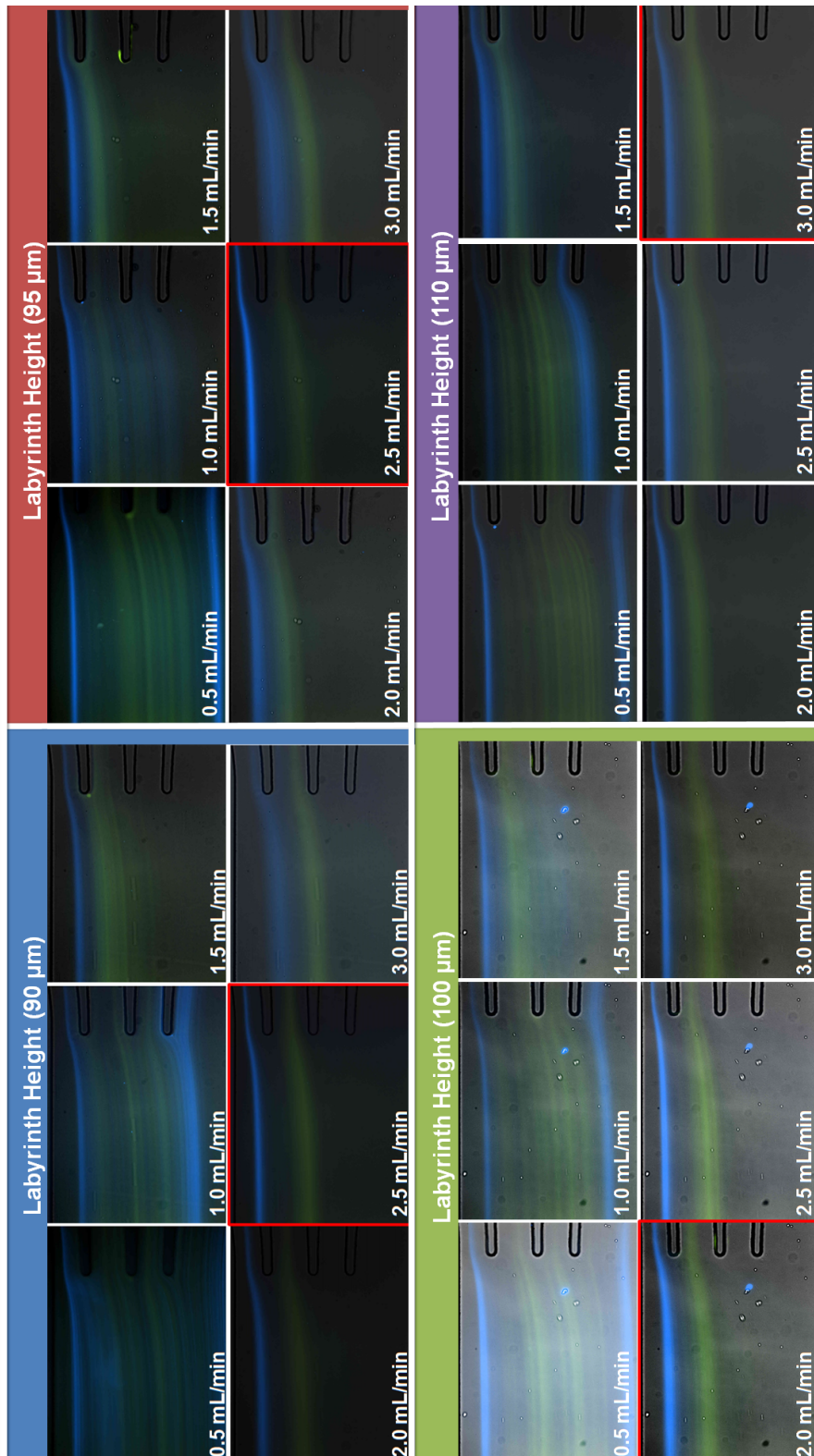
Figure A. 4 Determination of optimal flow rate for Labyrinth. Higher separation between MCF-7 and WBCs streamlines projects in higher recovery of MCF-7 as well as higher purity.

Determining flow stabilization time for optimal sample recovery

In order to determine the appropriate time for flow stabilization and sample collection, the recovery of samples was measured over time. Using pre-labeled MCF-7 cell line (GFP) and WBCs (DAPI), samples were processed through the Labyrinth. For each of the four outlets, samples were collected in individual tubes every 30-second time frame for 90 seconds. Figure S6 shows that optimal performance is achieved within the 60-90 second time frame, having 93% recovery of MCF-7 and >88% WBC removal. In concordance to these results, our patient sample recollection analysis was only assessed for the recollected sample only after 1 minute.
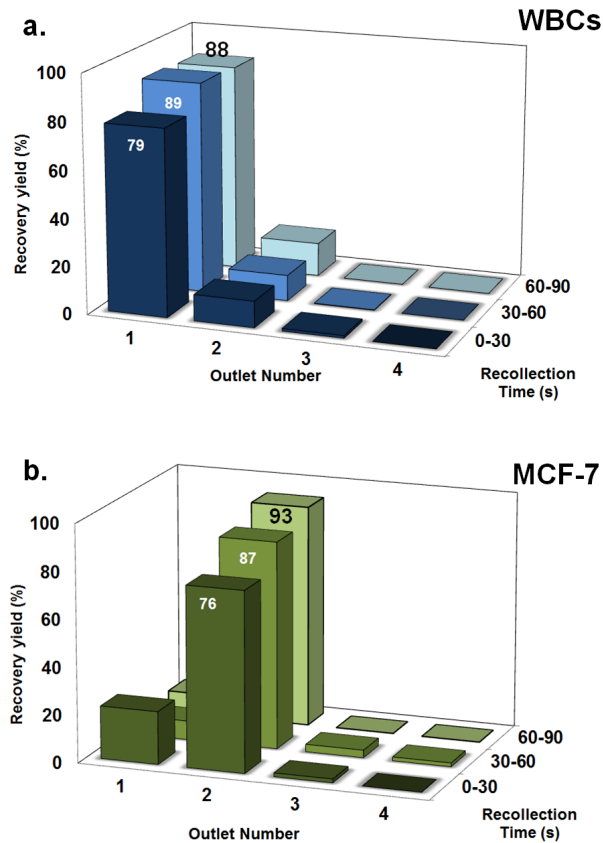
Figure A. 5 Flow stabilization measurements. a, MCF-7 breast cancer cell line and b, WBCs

Table A. 6 Comparison of microfluidic technologies with the Labyrinth

Technology	Approach	Flow rate	Recovery cell lines	Purity WBCs/mL	Patient samples	Whole blood	Live cells	Genomic analysis	Biomarker Independent?
Immuno-affinity Based Separation Methods									
Cell Search	EpCAM coated magnetic beads	NA	>80%	Very Low	< 50% in breast [30] 32% in lung cancer, 5CTCs/7.5ml [160]	N	N	N	N
Epic Sciences	No enrichment, RBCs lysed blood deposited on slides	NA	NA	None	73% in lung cancer[204], 55% in melanoma[205]	N	N	Y, single cell for copy number	N
Mag Sweeper	Flow through immunomagnetic capture		62% ± 7%		100% in metastatic breast cancer, 12CEpCs/9 mL[206]	Y, need dilution	Y	Y	N
FACS Sorting	Surface marker based selection	Very Low	NA	Very Low	<10% [207]	Y	Y	Y	N
RosetteSep kit	Depletion of WBCs	NA	NA	NA	NA[61,114,116]	multiple steps	Y	Y	N
CTC chip	Positive selection	1 mL/hr	>95%	NA	72% in lung cancer[24]	Y	Y	Y	N
GO Chip	Nano pillars with Graphene Oxide	1-3 mL/hr	> 95% 2-5 CTCs	<1000	> 95% sensitivity, 10CTCs/mL[44]	Y	Y	Y	N
Size Based Separation Methods									
CTC iChip	Size based separation +ve or –ve selection with mag beads	9.6 mL/hr	> 95% for –ve 78%-98% for +ve	>10,000 for –ve <10,000 for +ve	90% from multiple types of metastatic cancers[56]	Y, not a single step	Y	Y, single cell RNA expression	N
ISET	Size based filtration	NA	One CTC per 1ml of blood	NA	80% in lung cancer [10,19,208]	N	N	Y, FISH	Y
Inertial Spiral Devices	Inertial size based separation	6-20 mL/hr (~500μL/min)	>80%	>100,000/mL	NA[93,98,135]	N	Y	N	Y
tilted-angle standing surface acoustic waves	Acoustic waves	20 μL/min	>83% with MCF-7, HeLa, UACC903M-GFP, LNCaP	≈90% removal rate of WBCs	Tested with 3 metastatic breast cancer patients[75,76]	N (RBC lysis and centrifugation)	Y	N	Y
p-MOFF	Hydrodynamic	0.6 mL/min	93.75% with MCF-7 91.60% with MDA-MB-231	NA	Tested with 24 breast cancer patient samples[100]	N (RBC lysis)	NA	N	Y
Deterministic lateral displacement (DLD)	Hydrodynamic	2 mL/min 12 mL/hr (whole blood)	99% for MCF-7 80% for MDAMB231	47%	No patient samples reported [134]	Y, need 10X dilution	NA	N	Y
Microfluidic Labyrinth	**Inertial microfluidics size based separation**	**2.5 mL/min >30 mL/hr (whole blood)**	**> 95%**	**<200**	**> 95% sensitivity, 10CTCs/mL in breast and 50CTC/mL in pancreatic cancer**	Y	Y	**Y, single cell RNA expression**	Y

Fabrication of SU-8 mold for Labyrinth

The mold for the polydimethylsiloxane (PDMS) device is formed from a negative photoresist SU-8 100 patterned using soft lithography. Using a spin-coater, the negative photoresist layer, SU-8 100, is deposited onto silicon wafer rotating at 2450 rpm for 1 minute. The wafer is then soft-baked for 10 minutes at 65 °C and 70 minutes at 95°C. The mask is aligned to the wafer and is exposed to UV light for 20 seconds. Post-exposure-baking is applied for 3 minutes at 65 °C and 10 minutes at 95°C. Then, the wafer is developed by soaking in developer for 6 minutes and in IPA for 1 minute to remove the inactivated photoresist. It is hard baked for 4 minutes at 150-180 °C. The height of the mold built on silicon wafer is 100 μm, and the width of the channel is 500 μm.

Fabrication of PDMS device

The flow chamber for labyrinth is made from PDMS. 30 mL Sylgard polymer base and 3 mL curing agent are well-mixed and poured onto a silicon mold. The mixture is put in a desiccator for 2 hours to remove bubbles from the mixture. It is then heated at 65 °C overnight to harden the polymer. The polymer is cut into the desired shape, and punched with needle for tubing. The PDMS device is then bonded to standard sized glass slides via plasma surface activation of oxygen. The bonded device is tubed with 0.66 mm diameter tubes.

Processing of samples using the Double Labyrinth

Processing samples through LL involves collecting samples from second outlet and processing it again through a second Labyrinth device. In cell line experiments, MCF-7 was pre-labelled with cell tracker and spiked into blood (200/mL) from healthy donors. 10 mL of spiked blood samples was diluted to 25 mL with PBS buffer solution. The diluted

samples were processed through first Labyrinth at 2500 μL/min and product from second outlet was collected (6 mL). The collected product from first Labyrinth was processed through second Labyrinth at the same flow rate (2500 μL/min) and product from second outlet was collected as final product.

Measuring cell viability for Labyrinth-processed cell line

Cell viability was assessed using the MTT ((3-(4,5-Dimethylthiazol-2-yl)-2,5-diphenyltetrazolium bromide) colorimetric assay. In principle, MTT is taken up into cells by endocytosis or a protein-facilitated mechanism and is reduced by mitochondrial enzymes to yield a purple formazan product. The ability of cells to reduce MTT provides an indication of the mitochondrial integrity and activity, which, in turn, may be interpreted as a measure of cell viability [209]. After labyrinth processing, PANC-1 cells were seeded in a 96 well plate for 6 days and compared with unprocessed cells (control). Data points were taken every 24 hours by adding 8 μL of a 5mg/mL solution of MTT powder in PBS to the desired well. Once violet crystals were formed, media was aspirated and 150 μL of isopropanol/0.1% 4mM HCL solvent was added to each well. Absorbance was measured at 520 nm using a Microplate reader (Bio-Tek, Winooski, VT). As shown in figure S7 cells started proliferating just 24 hours after being incubated, increasing their population by 50% within just three days. This preliminary result demonstrates that the shear stress that cells experience in labyrinth does not have a significant effect on their viability or their proliferation rates.
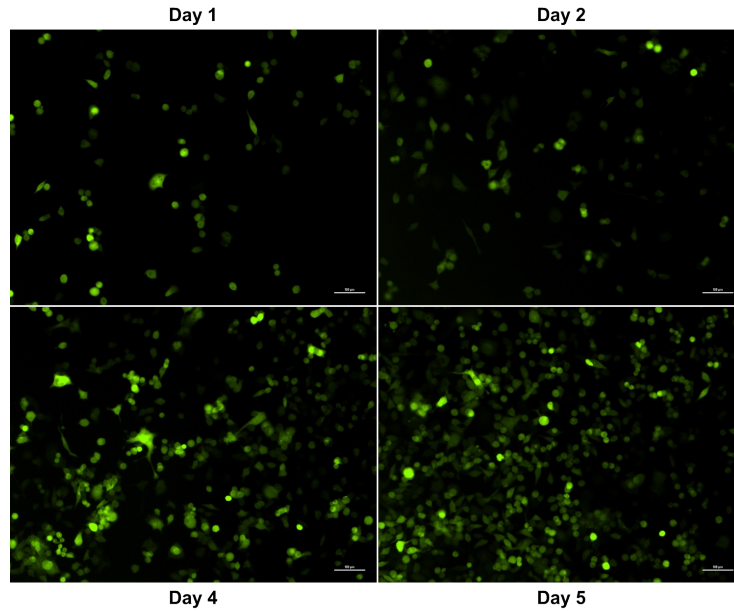
Figure A. 6 Fluorescence images of PANC-1 after Labyrinth processing

Preparation of Cytospin slides

Second outlet product was processed using Thermo Scientific™ Cytospin 4 Cytocentrifuge. 300 µL of sample is added into each cytospin funnel and cytocentrifuged at a speed of 800 rpm for 10 minutes. Samples are fixed on the cytoslides using 4% PFA and cytocentrifuged at the same conditions described above. Cytoslides are stored at 4° C until further staining.

Calculation of Log Depletion

The log depletion for single Labyrinth is calculated based on the initial number of WBCs spiked into the samples. After single Labyrinth, an average of 96.6% (n = 9) of WBCs were depleted into outlet 1, hence resulting in an average of 1.78 log depletion (range 1.49-2.23). The log depletion for double Labyrinth is based on the initial number of WBCs per mL (~0.7×10^7). The average of 350 WBCs/mL (n = 5) results in a log depletion of 4.3 in average (range 3.9-4.5).
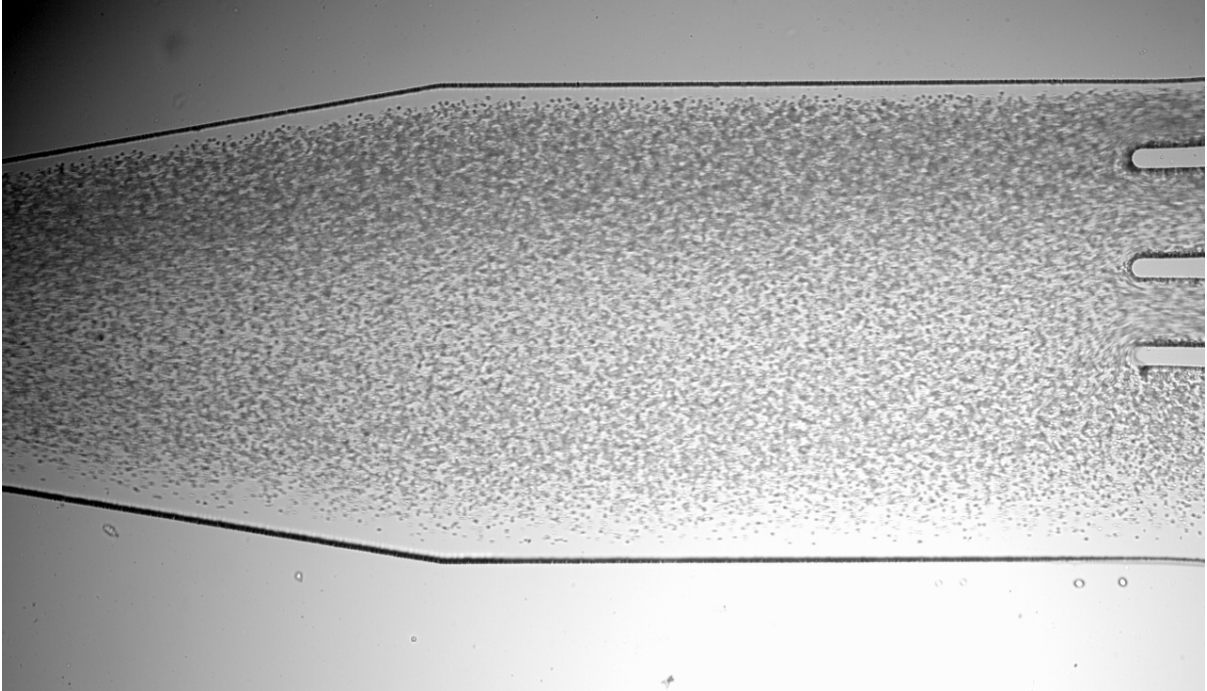
Figure A. 7 RBC distribution across four outlets in Labyrinth
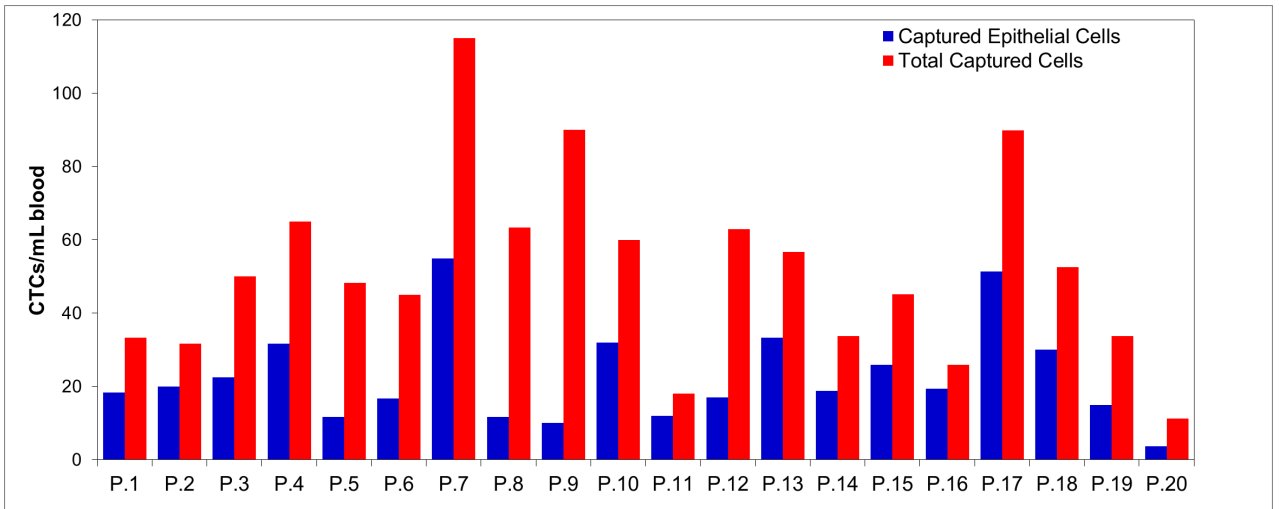
Figure A. 8 Comparison between total number of CTCs/mL in pancreatic cancer. Total number of CTCs/mL in pancreatic cancer patients stained positive for CK19 vs total number of CTCs/mL in whole blood that stained positive for either epithelial (CK19) or for any of the two EMT markers used (ZEB1 and ATDC)

Table A. 7 Quantification of CTCs from pancreatic cancer patients

Sample number	Cancer type	Staining	CTC/mL	Stage
P.1	Pancreatic Cancer	CK-19	18	Unknown
		ATDC	2	
		ZEB1	5	
P.2	Pancreatic Cancer	CK-19	20	Unknown
		ATDC	0	
		ZEB1	5	
P.3	Pancreatic Cancer	CK-19	23	Metastatic
		ATDC	0	
		ZEB1	20	
P.4	Pancreatic Cancer	CK-19	32	Locally advanced/borderline resectable
		ATDC	0	
		ZEB1	0	
P.5	Pancreatic Cancer	CK-19	12	Borderline resectable
		ATDC	0	
		ZEB1	25	
P.6	Pancreatic Cancer	CK-19	17	Metastatic
		ATDC	2	
		ZEB1	0	
P.7	Pancreatic Cancer	CK-19	55	Borderline resectable/metastatic
		ATDC	12	
		ZEB1	30	
P.8	Pancreatic Cancer	CK-19	12	Borderline resectable/metastatic
		ATDC	7	
		ZEB1	32	
P.9	Pancreatic Cancer	CK-19	10	Metastatic
		ATDC	0	
		ZEB1	63	
P.10	Pancreatic Cancer	CK-19	32	Metastatic
		ATDC	0	
		ZEB1	10	
P.11	Pancreatic Cancer	CK-19	12	Metastatic
		ATDC	4	
		ZEB1	2	
P.12	Pancreatic Cancer	CK-19	17	Borderline resectable/metastatic
		ATDC	10	
		ZEB1	19	
P.13	Pancreatic Cancer	CK-19	33	Metastatic
		ZEB1	23	
P.14	Pancreatic Cancer	CK-19	19	Locally advanced
		ZEB1	15	
P.15		CK-19	26	

	Pancreatic Cancer	ZEB1	19	Borderline resectable
P.16	Pancreatic Cancer	CK-19	19	Metastatic
		ZEB1	6	
P.17	Pancreatic Cancer	CK-19	51	Unknown
		ZEB1	39	
P.18	Pancreatic Cancer	CK-19	30	Metastatic
		ZEB1	23	
P.19	Pancreatic Cancer	CK-19	15	Metastatic
		ZEB1	19	
P.20	Pancreatic Cancer	CK-19	4	Locally advanced
		ZEB1	8	

DNA isolation and mutational analysis

DNA was extracted from five patient samples using the Acturus PicoPure DNA Extraction Kit. Manufacturer's protocols were adapted for microfluidic extraction. Extracted DNA was concentrated using the Cleanup Protocol of the QiAmp DNA Micro Kit (Qiagen). All DNA samples were amplified using the REPLI-g UltraFast Mini Kit (Qiagen) for whole genome amplification. DNA quality and quantity were measured using TapeStation Genomic Tape (DNA Sequencing Core, University of Michigan). Mutations were detected by the ABI 7900HT (384-well Fast Block) in the 384-well format (96x4) of the qBiomarker Somatic Mutation PCR Array: Human Pancreatic Cancer (Qiagen/SABiosciences). The average Ct method was used for analysis of mutations as per manufacturer recommended template.

Table A. 8 Somatic mutations in pancreatic cancer patients

Gene/Sample	C.1	C.2	C.3	C.4	C.5	HC	NTC

APC	WT	WT	WT	WT	WT	WT	WT
BRAF	WT	WT	WT	WT	WT	WT	WT
CDKN2A	WT	WT	**Mutant**	WT	WT	WT	WT
CTNNB1	**Mutant**	WT	**Mutant**	WT	**Mutant**	WT	WT
KRAS	**Mutant**	**Mutant**	**Mutant**	**Mutant**	**Mutant**	WT	WT
NRAS	WT	WT	WT	WT	WT	WT	WT
PIK3CA	WT	WT	WT	WT	WT	WT	WT
SMAD4	WT	**Mutant**	WT	WT	WT	WT	WT
TP53	WT	**Mutant**	WT	**Mutant**	**Mutant**	WT	WT

Table A. 9 Patient demographics for mutational analysis

Patient No.	Age	Sex	Diagnosis	Stage	Ep CTCs/mL	EMT CTCs/mL	Total CTCs/mL
C.1	**71**	**M**	**PDA**	**Metastatic**	**0**	**0**	**0**
C.2	**50**	**M**	**PDA**	**Metastatic**	**0**	**11**	**11**
C.3	**64**	**M**	**PDA**	**Borderline Resectable**	**3**	**0**	**3**
C.4	**72**	**M**	**PDA**	**Borderline resectable**	**0**	**0**	**0**
C.5	**61**	**M**	**PDA**	**Metastatic**	**0**	**3**	**3**

Table A. 10 Comparison of CTC counts among several microfluidic technologies

Name of Device	Cancer Type (Patient Sample)	No. of samples	Average CTC/mL	Range (CTCs/mL)
p-MOFF	Breast	24	N/A	0-21
Portable Filter	Breast	11	3.3	0.33-8

Ultra-high-throughput spiral	Breast	5	47.4	20-67
Vortex Chip	Breast	4	N/A	3.3-6.8
CTC-iChip	Breast	12	0.93	0-3.7
Cell Search	Breast	422	11.2	0-3267
GO-Chip	Breast	10	5.6	0-16
CTC-iChip	Pancreas	6	0.59	0-1.4
CTC-chip	Pancreas	15	196±227	9-831
Cell Search	Pancreas	8	2.7±4	0-11
NanoVelcroCTC chip	Pancreas	72		0-12
GEDI chip	Pancreas	11	14.1±18.1	0-59
SELEX aptamer	Pancreas	14	25.7	0-126
ISET	Pancreas	60	7	1-54
Labyrinth	**Breast**	**56**	**9.1**	**2-31**
Labyrinth	**Pancreas**	**20**	**51.6**	**11-115**

CTC subpopulations found on Patient Sample P.1

Wang et al. have identified ATDC as a protein highly expressed in the majority of human pancreatic adenocarcinomas and pancreatic cancer precursor lesions. They have also demonstrated that expression of ATDC in pancreatic cancer cells promotes cellular proliferation and enhanced tumor growth and metastasis. ATDC has been studied as a novel EMT trigger proven to be highly expressed in the majority of human PDAC. Moreover, our technology have been able to isolate ATDC expressing cells on P.1, in which colocalization with ZEB1 is observed in figure A.9. As a commonly accepted EMT marker, ZEB1 expression suggests that this subpopulation is of mesenchymal phenotype.
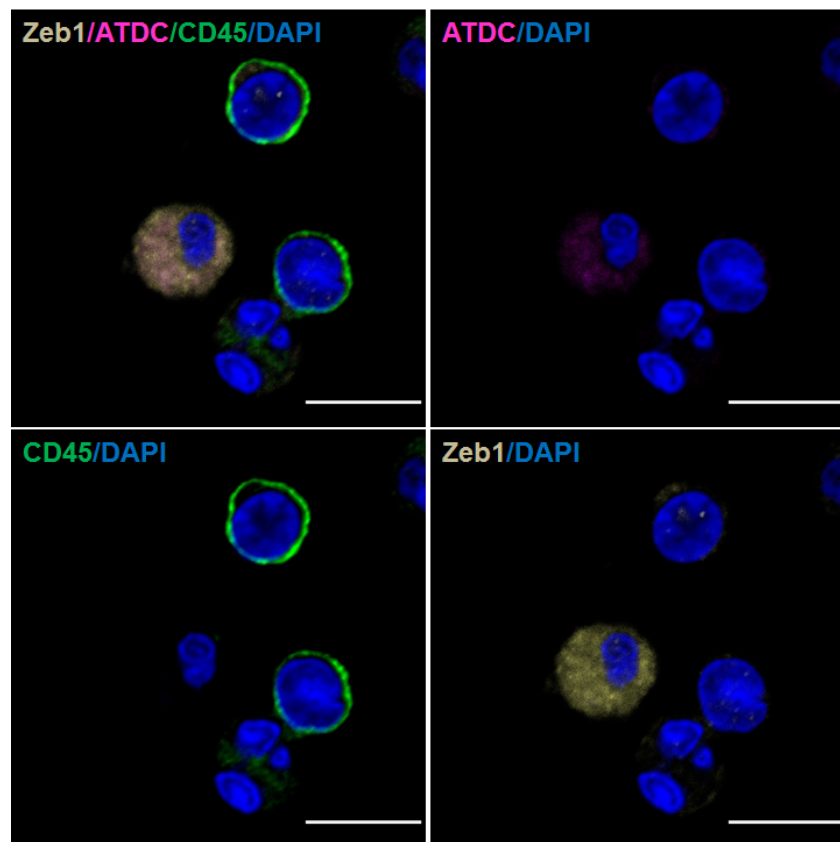
Figure A. 9 CTC showing staining colocalization of ATDC and ZEB1 on P.1.
Scale bar 10 μm.
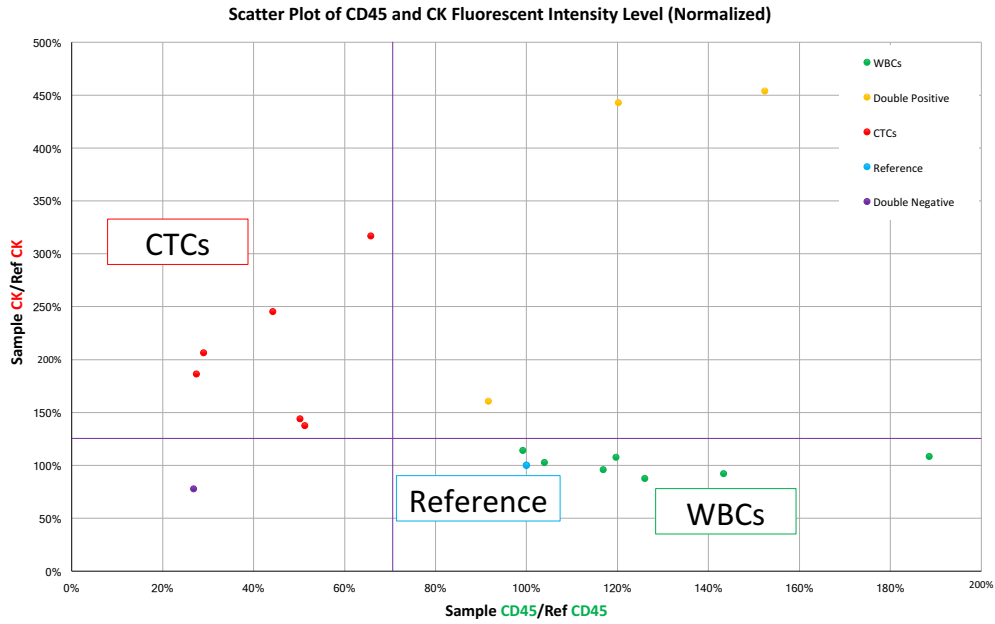
Figure A. 10 Scatter plot of CK and CD45 fluorescent intensity.

After a patient sample was processed through Labyrinth and fluorescently stained with DAPI, CD45 and CK, a typical WBC from the slide was selected as reference for its CD45 and CK fluorescent intensity levels. A cell could be recognized as a WBC by having similar CD45 and CK expressions comparing to the reference cell. A cell could be recognized as a CTC by having at least 50% lower CD45 and 50% higher CK expressions comparing to the reference cell. Cells with both CD45 and CK significant expressions with respect to the reference cell would be considered as double positive cells. Cells with DAPI positive but much lower expressions in CD45 and CK when compared to the reference cell would be considered as double negative cells.

B. Enumeration of CTCs isolated from pancreatic patient samples: a clinical study

Table B. 1 Median time and survival probability for treatment naive patients

Categories	Median time	2 yr survival probability	Logrank test
Resectable	1.875 (1.802, NA)	0.456 (0.253, 0.823)	<0.001
Borderline	2.051 (1.908, NA)	0.505 (0.312, 0.817)	
Locally Advanced	0.764 (0.498, 1.95)	0.143 (0.041, 0.493)	
Metastatic	0.865 (0.704, 1.31)	0	

C. Heterogeneity studies for the characterization of pancreatic CTCs

Table C. 1 Patient Demographics

	Stage	Age	Sex
P.1	resectable T3N0M0	63	M
P.2	resectable T3N1Mx	78	F
P.3	resectable T3N0M0	58	F
P.4	borderline resectable	70	M
P.5	unresectable	62	M
P.6	locally advanced unresectable	68	F
P.7	locally advanced unresectable	81	M
P.8	unresectable	52	M
P.9	metastatic	75	M
P.10	metastatic	66	F
P.11	metastatic	X	X
P.12	metastatic	X	X
H.1	Healthy	25	M
H.2	Healthy	26	F
H.3	Healthy	26	F

Table C. 2 Cell counts for CD24 and CD133 co-expression (per mL of whole blood)

	CD24+/CD133+/CD45-/DAPI+	CD24-/CD133+/CD45-/DAPI+	CD24+/CD133-/CD45-/DAPI+
P.1	9	0	2
P.2	8	5	0
P.3	5	0	0
P.4	5	3	5
P.5	0	5	3
P.6	16	0	0
P.7	6	0	0
P.8	11	8	0
P.9	8	0	3
P.10	3	9	0
P.11	9	3	0
P.12	2	4	1

Table C. 3 Cell counts for CD90 and CD133 co-expression (per mL of whole blood)

	CD90+/CD133+/CD45-/DAPI+	CD90-/CD133+/CD45-/DAPI+	CD90+/CD133-/CD45-/DAPI+
P.1	14	7	0
P.2	10	0	0
P.3	10	0	0
P.4	13	5	0
P.5	16	3	0
P.6	8	3	0
P.7	21	6	0
P.8	8	3	5
P.9	11	0	3
P.10	9	9	0
P.11	15	0	0
P.12	6	5	1

D. Expansion and functional characterization of pancreatic CTCs

Table D. 1 Patient Demographics

Patient	Sex	Age	Diagnosis	Stage	CTC number/ml	EMT-like CTC/ml	Epithelial-like CTC/ml
P.1*	m[#]	53	PDAC[$]	T4N0M0[**]	14	11	3
P.2*	f[##]	74	PDAC	T4N0M0	44	44	0
P.3*	f	54	PDAC	T4N0M0	20	16	4
P.4	m	64	PDAC	T4N0M0	10	6	4
P.5*	m	53	PDAC	T4N0M0	21	11	9
P.6	f	73	PDAC	T4N0M0	7	7	0
P.7	f	60	PDAC	T3N0M0	19	17	2
P.8	f	69	PDAC	T4N0M0	49	49	0
P.9	m	61	PDAC	T4N0M0	8	6	2
P.10	f	50	PDAC	T4N0M0	51	45	6

* CTC cell lines were established for these patients, [#] male, [##] female, [$] pancreatic ductal adenocarcinoma, **TNM classification of tumors of the exocrine pancreas: T4, tumor extends directly into any of the following: stomach, spleen, colon, adjacent large vessels; N0, no regional lymph node metastasis; M0, no distant metastasis

Table D. 2 CTC number and characteristics change in response to treatment

Patient	Visit	Treatment	CTC number/ml	EMT-like CTC/ml	Epithelial-like CTC/ml
P.1	V1*	untreated	14	11	3
	V2	Gemcitabine, AZD1778	11	9	2
P.2	V1*	untreated	44	44	0
	V2	Gemcitabine, AZD1778	3	3	0
P.4	V1	untreated	10	6	4
	V2	Gemcitabine, AZD1778	2	2	0

* CTC cell lines were established for these visit

Table D. 3 CTC characteristics in CTC cultures

Patient	Adherent culture		Spheroid culture	
	EMT-like CTC (%)	Epithelial-like CTC (%)	EMT-like CTC (%)	Epithelial-like CTC (%)
P.1	87%	13%	57%	43%
P.2	12%	88%	37%	63%
P.3	85%	15%	66%	34%
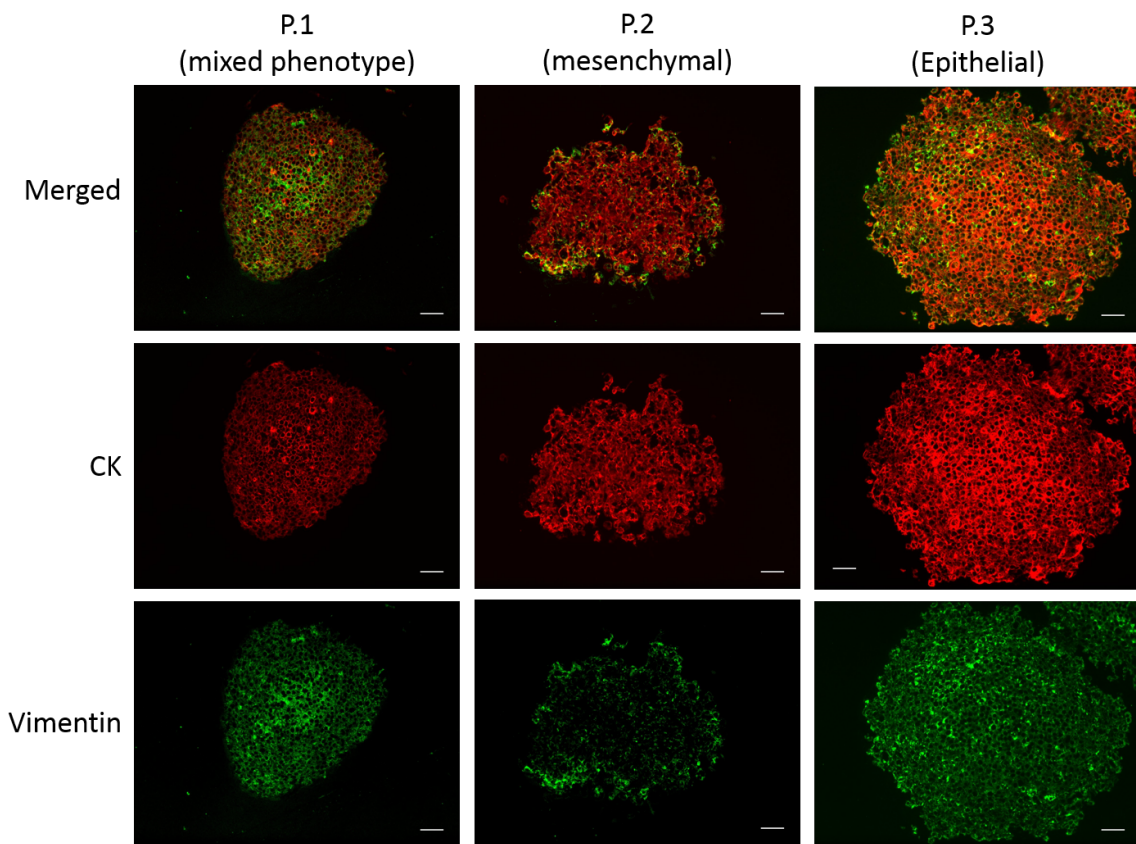
Figure D. 1 Immunoflourescence staining of CTC culture spheroids
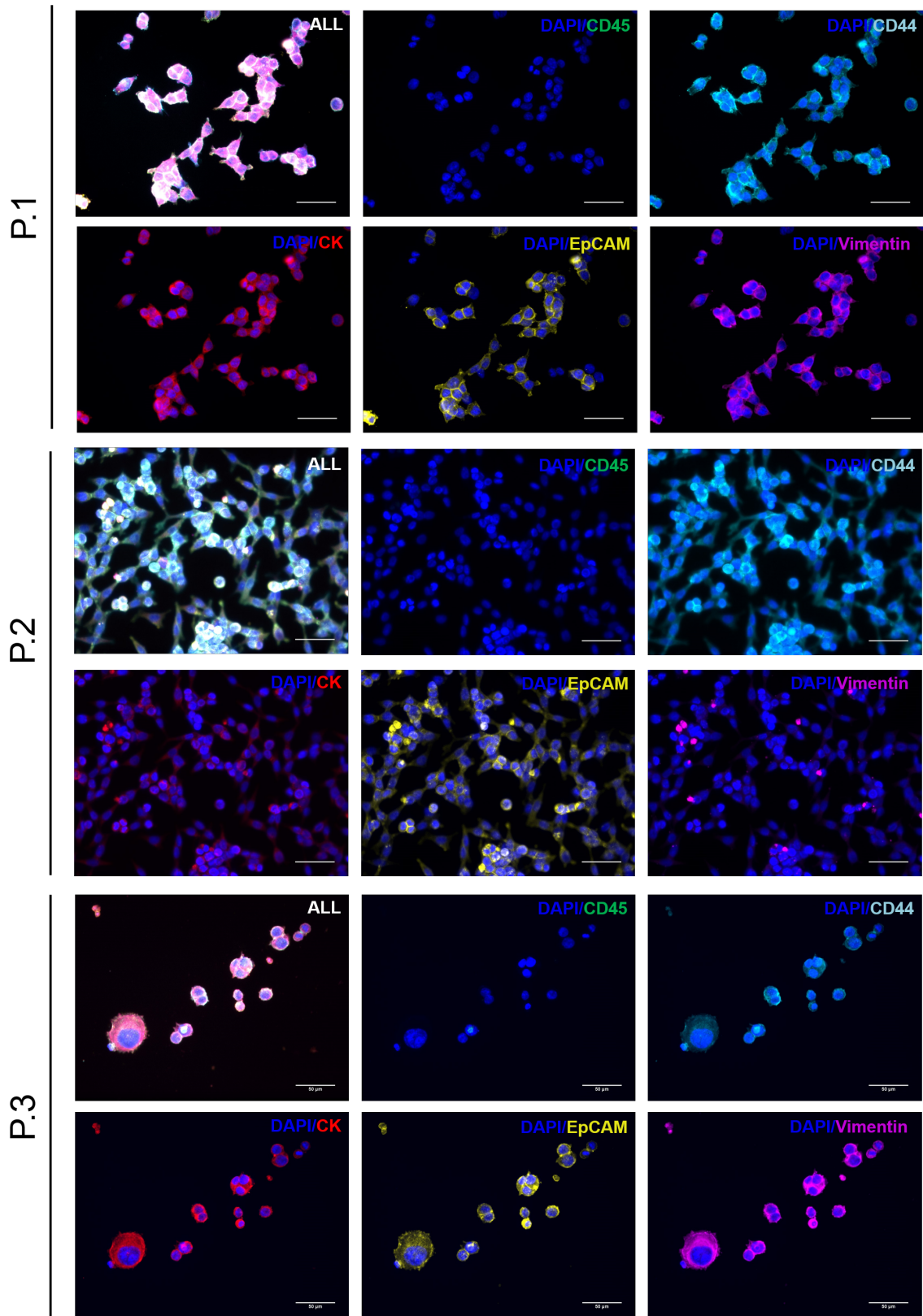
Figure D. 2 Six channel staining of CTC cultures
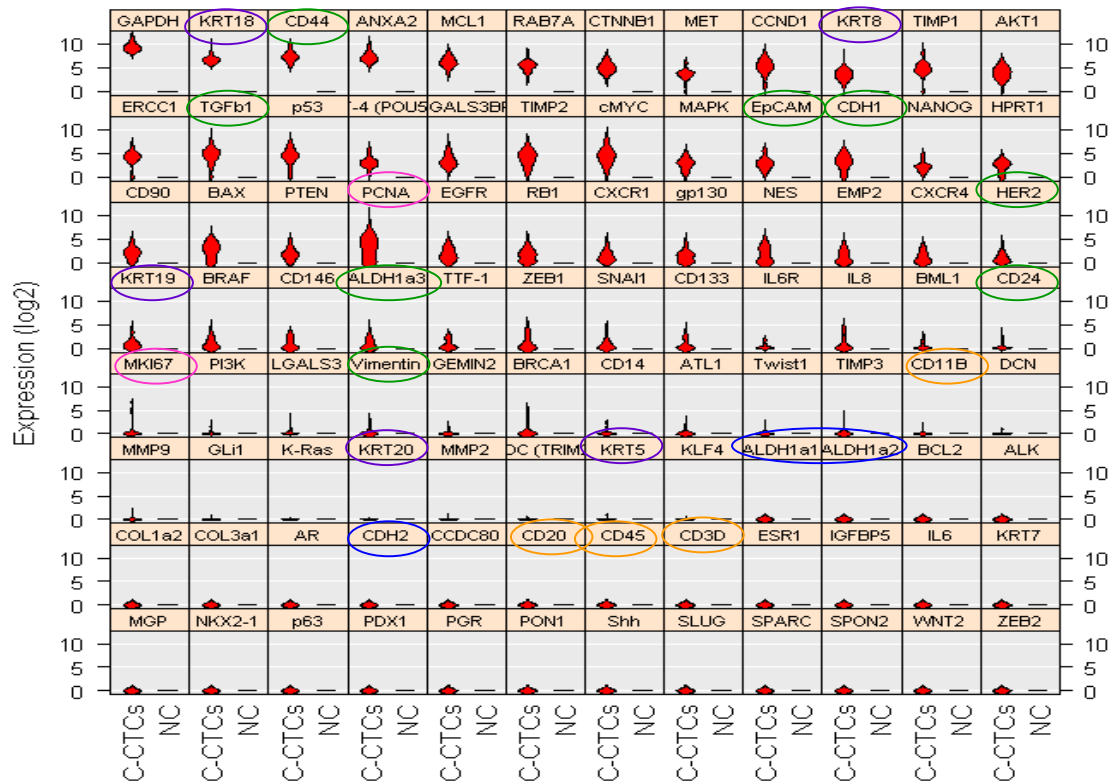
Figure D. 3 Single cell analysis of CTCs from patient 3. Results from patient 3 (C-CTCs) compared to no cell (NC), shows the cultured cells are CTCs with EpCAM+/ALDH1A3+/CD44+/CD24low expression and negative for WBCs markers (CD20, Cd45 and CD3D).

REFERENCES

1   American Cancer, S. Cancer Facts & Figures 2014. (2014).

2   Hidalgo, M. Pancreatic cancer. *New England Journal of Medicine* **362**, 1605-1617 (2010).

3   Bidard, F. C. *et al.* Circulating tumor cells in locally advanced pancreatic adenocarcinoma: the ancillary CirCe 07 study to the LAP 07 trial. *Annals of Oncology : Official Journal of the European Society for Medical Oncology / ESMO* **24**, 2057-2061, doi:10.1093/annonc/mdt176 [doi] (2013).

4   Yu, M., Stott, S., Toner, M., Maheswaran, S. & Haber, D. A. Circulating tumor cells: approaches to isolation and characterization. *The Journal of cell biology* **192**, 373-382, doi:10.1083/jcb.201010021 [doi] (2011).

5   Yu, M. *et al.* RNA sequencing of pancreatic circulating tumour cells implicates WNT signalling in metastasis. *Nature* **487**, 510-513, doi:10.1038/nature11217 (2012).

6   Marrinucci, D. *et al.* Fluid biopsy in patients with metastatic prostate, pancreatic and breast cancers. *Physical biology* **9**, 016003, doi:10.1088/1478-3975/9/1/016003 (2012).

7   Pantel, K. & Alix-Panabieres, C. Real-time liquid biopsy in cancer patients: fact or fiction? *Cancer research* **73**, 6384-6388, doi:10.1158/0008-5472.CAN-13-2030 [doi] (2013).

8   Maheswaran, S. & Haber, D. A. Circulating tumor cells: a window into cancer biology and metastasis. *Current opinion in genetics & development* **20**, 96-99 (2010).

9   Wu, L. & Qu, X. Cancer biomarker detection: recent achievements and challenges. *Chem Soc Rev* **44**, 2963-2997, doi:10.1039/c4cs00370e (2015).

10   Khoja, L. *et al.* A pilot study to explore circulating tumour cells in pancreatic cancer as a novel biomarker. *Br J Cancer* **106**, 508-516, doi:10.1038/bjc.2011.545 (2012).

11   Riethdorf, S. *et al.* Detection and HER2 expression of circulating tumor cells: prospective monitoring in breast cancer patients treated in the neoadjuvant GeparQuattro trial. *Clin Cancer Res* **16**, 2634-2645, doi:10.1158/1078-0432.CCR-09-2042 (2010).

12   Azim, H. A., Jr. *et al.* Circulating tumor cells and response to neoadjuvant paclitaxel and HER2-targeted therapy: a sub-study from the NeoALTTO phase III trial. *Breast* **22**, 1060-1065, doi:10.1016/j.breast.2013.08.014 (2013).

13   Alix-Panabieres, C. & Pantel, K. Circulating tumor cells: liquid biopsy of cancer. *Clin Chem* **59**, 110-118, doi:10.1373/clinchem.2012.194258 (2013).

14   Ting, D. T. *et al.* Single-cell RNA sequencing identifies extracellular matrix gene expression by pancreatic circulating tumor cells. *Cell Rep* **8**, 1905-1918, doi:10.1016/j.celrep.2014.08.029 (2014).

15   Yu, M. *et al.* Circulating breast tumor cells exhibit dynamic changes in epithelial and mesenchymal composition. *Science* **339**, 580-584, doi:10.1126/science.1228522 (2013).

16   Aceto, N. *et al.* Circulating tumor cell clusters are oligoclonal precursors of breast cancer metastasis. *Cell* **158**, 1110-1122, doi:10.1016/j.cell.2014.07.013 (2014).

17   Mohamadi, R. M. *et al.* Nanoparticle-mediated binning and profiling of heterogeneous circulating tumor cell subpopulations. *Angewandte Chemie* **54**, 139-143, doi:10.1002/anie.201409376 (2015).

18   Haber, D. A. & Velculescu, V. E. Blood-based analyses of cancer: circulating tumor cells and circulating tumor DNA. *Cancer Discov* **4**, 650-661, doi:10.1158/2159-8290.CD-13-1014 (2014).

19   Vona, G. *et al.* Impact of cytomorphological detection of circulating tumor cells in patients with liver cancer. *Hepatology* **39**, 792-797, doi:10.1002/hep.20091 (2004).

20   Armstrong, A. J. *et al.* Circulating tumor cells from patients with advanced prostate and breast cancer display both epithelial and mesenchymal markers. *Molecular cancer research : MCR* **9**, 997-1007, doi:10.1158/1541-7786.MCR-10-0490 [doi] (2011).

21   Cristofanilli, M. *et al.* Circulating tumor cells, disease progression, and survival in metastatic breast cancer. *N Engl J Med* **351**, 781-791, doi:10.1056/NEJMoa040766 (2004).

22   Miller, M. C., Doyle, G. V. & Terstappen, L. W. Significance of Circulating Tumor Cells Detected by the CellSearch System in Patients with Metastatic Breast Colorectal and Prostate Cancer. *Journal of oncology* **2010**, 617421, doi:10.1155/2010/617421 [doi] (2010).

23   Hayes, D. F. *et al.* Circulating tumor cells at each follow-up time point during therapy of metastatic breast cancer patients predict progression-free and overall survival. *Clinical cancer research : an official journal of the American Association for Cancer Research* **12**, 4218-4224, doi:12/14/4218 [pii] (2006).

24   Nagrath, S. *et al.* Isolation of rare circulating tumour cells in cancer patients by microchip technology. *Nature* **450**, 1235-1239, doi:10.1038/nature06385 (2007).

25   Kurkuri, M. D. *et al.* Plasma functionalized PDMS microfluidic chips: towards point-of-care capture of circulating tumor cells. *Journal of Materials Chemistry* **21**, 8841, doi:10.1039/c1jm10317b (2011).

26   Maheswaran, S. *et al.* Detection of mutations in EGFR in circulating lung-cancer cells. *N Engl J Med* **359**, 366-377, doi:10.1056/NEJMoa0800668 (2008).

27   Wu, L., Wang, J., Ren, J. & Qu, X. Ultrasensitive Telomerase Activity Detection in Circulating Tumor Cells Based on DNA Metallization and Sharp Solid-State Electrochemical Techniques. *Advanced Functional Materials* **24**, 2727-2733, doi:10.1002/adfm.201303818 (2014).

28   Allard, W. J. *et al.* Tumor cells circulate in the peripheral blood of all major carcinomas but not in healthy subjects or patients with nonmalignant diseases. *Clinical Cancer Research* **10**, 6897-6904 (2004).

29   Punnoose, E. A. *et al.* Molecular biomarker analyses using circulating tumor cells. *PLoS One* **5**, e12517, doi:10.1371/journal.pone.0012517 (2010).

30   Riethdorf, S. *et al.* Detection of circulating tumor cells in peripheral blood of patients with metastatic breast cancer: a validation study of the CellSearch system. *Clinical cancer research : an official journal of the American Association for Cancer Research* **13**, 920-928, doi:13/3/920 [pii] (2007).

31   Miyamoto, D. T. *et al.* Androgen receptor signaling in circulating tumor cells as a marker of hormonally responsive prostate cancer. *Cancer Discov* **2**, 995-1003, doi:10.1158/2159-8290.CD-12-0222 (2012).

32   Dong, Y. *et al.* Microfluidics and circulating tumor cells. *The Journal of molecular diagnostics : JMD* **15**, 149-157, doi:10.1016/j.jmoldx.2012.09.004 (2013).

33   den Toonder, J. Circulating tumor cells: the Grand Challenge. *Lab Chip* **11**, 375-377, doi:10.1039/c0lc90100h (2011).

34   Zhang, Z. & Nagrath, S. Microfluidics and cancer: are we there yet? *Biomedical Microdevices*, 1-15 (2013).

35   Bhagat, A. A., Hou, H. W., Li, L. D., Lim, C. T. & Han, J. Pinched flow coupled shear-modulated inertial microfluidics for high-throughput rare blood cell separation. *Lab Chip* **11**, 1870-1878, doi:10.1039/c0lc00633e (2011).

36   Stott, S. L. *et al.* Isolation of circulating tumor cells using a microvortex-generating herringbone-chip. *Proceedings of the National Academy of Sciences of the United States of America* **107**, 18392-18397, doi:10.1073/pnas.1012539107 [doi] (2010).

37   Sun, Y. F. *et al.* Circulating tumor cells: advances in detection methods, biological issues, and clinical relevance. *Journal of cancer research and clinical oncology* **137**, 1151-1173, doi:10.1007/s00432-011-0988-y (2011).

38   Alix-Panabieres, C. & Pantel, K. Technologies for detection of circulating tumor cells: facts and vision. *Lab Chip* **14**, 57-62, doi:10.1039/c3lc50644d (2014).

39   Mittal, S., Wong, I. Y., Deen, W. M. & Toner, M. Antibody-functionalized fluid-permeable surfaces for rolling cell capture at high flow rates. *Biophysical journal* **102**, 721-730, doi:10.1016/j.bpj.2011.12.044 (2012).

40   Mikolajczyk, S. D. *et al.* Detection of EpCAM-Negative and Cytokeratin-Negative Circulating Tumor Cells in Peripheral Blood. *J Oncol* **2011**, 252361, doi:10.1155/2011/252361 (2011).

41   Pecot, C. V. *et al.* A novel platform for detection of CK+ and CK- CTCs. *Cancer discovery* **1**, 580-586, doi:10.1158/2159-8290.CD-11-0215 [doi] (2011).

42   Adams, A. A. *et al.* Highly efficient circulating tumor cell isolation from whole blood and label-free enumeration using polymer-based microfluidics with an integrated conductivity sensor. *J Am Chem Soc* **130**, 8633-8641, doi:10.1021/ja8015022 (2008).

43   Nora Dickson, M. *et al.* Efficient capture of circulating tumor cells with a novel immunocytochemical microfluidic device. *Biomicrofluidics* **5**, 34119-3411915, doi:10.1063/1.3623748 (2011).

44   Yoon, H. J. *et al.* Sensitive capture of circulating tumour cells by functionalized graphene oxide nanosheets. *Nat Nanotechnol* **8**, 735-741, doi:10.1038/nnano.2013.194 (2013).

45   Lu, Y. T. *et al.* NanoVelcro Chip for CTC enumeration in prostate cancer patients. *Methods* **64**, 144-152, doi:10.1016/j.ymeth.2013.06.019 (2013).

46   Hou, S. *et al.* Polymer nanofiber-embedded microchips for detection, isolation, and molecular analysis of single circulating melanoma cells. *Angewandte Chemie* **52**, 3379-3383, doi:10.1002/anie.201208452 (2013).

47   Fachin, F., Chen, G. D., Toner, M. & Wardle, B. L. Integration of Bulk Nanoporous Elements in Microfluidic Devices With Application to Biomedical Diagnostics. *Journal of Microelectromechanical Systems* **20**, 1428-1438, doi:10.1109/jmems.2011.2167669 (2011).

48   Yoon, H. J., Kozminsky, M. & Nagrath, S. Emerging role of nanomaterials in circulating tumor cell isolation and analysis. *ACS Nano* **8**, 1995-2017, doi:10.1021/nn5004277 (2014).

49   Zhang, N. *et al.* Electrospun TiO2 nanofiber-based cell capture assay for detecting circulating tumor cells from colorectal and gastric cancer patients. *Adv Mater* **24**, 2756-2760, doi:10.1002/adma.201200155 (2012).

50   Gleghorn, J. P. *et al.* Capture of circulating tumor cells from whole blood of prostate cancer patients using geometrically enhanced differential immunocapture (GEDI) and a prostate-specific antibody. *Lab Chip* **10**, 27-29, doi:10.1039/b917959c (2010).

51   Galletti, G. *et al.* Isolation of breast cancer and gastric cancer circulating tumor cells by use of an anti HER2-based microfluidic device. *Lab Chip* **14**, 147-156, doi:10.1039/c3lc51039e (2014).

52   Sheng, W. *et al.* Aptamer-enabled efficient isolation of cancer cells from whole blood using a microfluidic device. *Anal Chem* **84**, 4199-4206, doi:10.1021/ac3005633 (2012).

53   Wong, L., Bateman, W., Morris, A. & Fraser, I. Detection of circulating tumour cells with the magnetic activated cell sorter. *British journal of surgery* **82**, 1333-1337 (1995).

54   Hoshino, K. *et al.* Microchip-based immunomagnetic detection of circulating tumor cells. *Lab Chip* **11**, 3449-3457, doi:10.1039/c1lc20270g (2011).

55   Casavant, B. P. *et al.* A negative selection methodology using a microfluidic platform for the isolation and enumeration of circulating tumor cells. *Methods* **64**, 137-143, doi:10.1016/j.ymeth.2013.05.027 (2013).

56   Ozkumur, E. *et al.* Inertial Focusing for Tumor Antigen–Dependent and–Independent Sorting of Rare Circulating Tumor Cells. *Science translational medicine* **5**, 179ra147-179ra147 (2013).

57   Wu, Y. *et al.* Isolation and analysis of rare cells in the blood of cancer patients using a negative depletion methodology. *Methods* **64**, 169-182, doi:10.1016/j.ymeth.2013.09.006 (2013).

58   Liu, Z. *et al.* High throughput capture of circulating tumor cells using an integrated microfluidic system. *Biosensors & bioelectronics* **47**, 113-119, doi:10.1016/j.bios.2013.03.017 (2013).

59   Murlidhar, V. *et al.* A radial flow microfluidic device for ultra-high-throughput affinity-based isolation of circulating tumor cells. *Small* **10**, 4895-4904, doi:10.1002/smll.201400719 (2014).

60   Saucedo-Zeni, N. *et al.* A novel method for the in vivo isolation of circulating tumor cells from peripheral blood of cancer patients using a functionalized and structured medical wire. *International journal of oncology* **41**, 1241-1250, doi:10.3892/ijo.2012.1557 (2012).

61   Baccelli, I. *et al.* Identification of a population of blood circulating tumor cells from breast cancer patients that initiates metastasis in a xenograft assay. *Nat Biotechnol* **31**, 539-544, doi:10.1038/nbt.2576 (2013).

62   Carvalho, F. L. *et al.* Tumorigenic potential of circulating prostate tumor cells. *Oncotarget* **4**, 413-421, doi:10.18632/oncotarget.895 (2013).

63   Hou, H. W. *et al.* Isolation and retrieval of circulating tumor cells using centrifugal forces. *Sci Rep* **3**, 1259, doi:10.1038/srep01259 (2013).

64   Zhang, Z. *et al.* Expansion of CTCs from early stage lung cancer patients using a microfluidic co-culture model. *Oncotarget* **5**, 12383-12397, doi:10.18632/oncotarget.2592 (2014).

65   Thege, F. I. *et al.* Microfluidic immunocapture of circulating pancreatic cells using parallel EpCAM and MUC1 capture: characterization, optimization and downstream analysis. *Lab Chip* **14**, 1775-1784, doi:10.1039/c4lc00041b (2014).

66   Aceto, N., Toner, M., Maheswaran, S. & Haber, D. A. En Route to Metastasis: Circulating Tumor Cell Clusters and Epithelial-to-Mesenchymal Transition. *Trends in Cancer* **1**, 44-52, doi:10.1016/j.trecan.2015.07.006 (2015).

67   Sarioglu, A. F. *et al.* A microfluidic device for label-free, physical capture of circulating tumor cell clusters. *Nat Methods* **12**, 685-691, doi:10.1038/nmeth.3404 (2015).

68   Sethi, N. & Kang, Y. Unravelling the complexity of metastasis - molecular understanding and targeted therapies. *Nature reviews. Cancer* **11**, 735-748, doi:10.1038/nrc3125 (2011).

69   Gay, L. J. & Felding-Habermann, B. Contribution of platelets to tumour metastasis. *Nature reviews. Cancer* **11**, 123-134, doi:10.1038/nrc3004 (2011).

70   Labelle, M., Begum, S. & Hynes, R. O. Direct signaling between platelets and cancer cells induces an epithelial-mesenchymal-like transition and promotes metastasis. *Cancer Cell* **20**, 576-590, doi:10.1016/j.ccr.2011.09.009 (2011).

71   Wicha, M. S. & Hayes, D. F. Circulating tumor cells: not all detected cells are bad and not all bad cells are detected. *Journal of clinical oncology : official journal of the American Society of Clinical Oncology* **29**, 1508-1511, doi:10.1200/JCO.2010.34.0026 (2011).

72   Shah, A. M. *et al.* Biopolymer system for cell recovery from microfluidic cell capture devices. *Anal Chem* **84**, 3682-3688, doi:10.1021/ac300190j (2012).

73   Gerges, N., Rak, J. & Jabado, N. New technologies for the detection of circulating tumour cells. *British medical bulletin* **94**, 49-64, doi:10.1093/bmb/ldq011 (2010).

74   McKenzie, S. & Williams, L. *Clinical laboratory hematology*. (Prentice Hall, 2014).

75   Li, P. *et al.* Acoustic separation of circulating tumor cells. *Proc Natl Acad Sci U S A* **112**, 4970-4975, doi:10.1073/pnas.1504484112 (2015).

76   Ding, X. *et al.* Cell separation using tilted-angle standing surface acoustic waves. *Proc Natl Acad Sci U S A* **111**, 12992-12997, doi:10.1073/pnas.1413325111 (2014).

77   Zharov, V. P., Galanzha, E. I., Shashkov, E. V., Khlebtsov, N. G. & Tuchin, V. V. In vivo photoacoustic flow cytometry for monitoring of circulating single cancer cells and contrast agents. *Opt Lett* **31**, 3623-3625, doi:10.1364/OL.31.003623 (2006).

78   Phillips, K. G. *et al.* Quantification of cellular volume and sub-cellular density fluctuations: comparison of normal peripheral blood cells and circulating tumor cells identified in a breast cancer patient. *Frontiers in oncology* **2** (2012).

79   Jin, C. *et al.* Technologies for label-free separation of circulating tumor cells: from historical foundations to recent developments. *Lab on a Chip* **14**, 32-44 (2014).

80   Cima, I. *et al.* Label-free isolation of circulating tumor cells in microfluidic devices: Current research and perspectives. *Biomicrofluidics* **7**, 11810, doi:10.1063/1.4780062 (2013).

81   Vona, G. *et al.* Isolation by size of epithelial tumor cells: a new method for the immunomorphological and molecular characterization of circulating tumor cells. *The American journal of pathology* **156**, 57-63 (2000).

82   Hou, J. M. *et al.* Circulating Tumor Cells as a Window on Metastasis Biology in Lung Cancer. *Am J Pathol* **178**, 989-996, doi:10.1016/j.ajpath.2010.12.003 (2011).

83   De Giorgi, V. *et al.* Application of a filtration-and isolation-by-size technique for the detection of circulating tumor cells in cutaneous melanoma. *Journal of Investigative Dermatology* **130**, 2440-2447 (2010).

84   Desitter, I. *et al.* A new device for rapid isolation by size and characterization of rare circulating tumor cells. *Anticancer Res* **31**, 427-441 (2011).

85   Zheng, S. *et al.* Membrane microfilter device for selective capture, electrolysis and genomic analysis of human circulating tumor cells. *J Chromatogr A* **1162**, 154-161, doi:10.1016/j.chroma.2007.05.064 (2007).

86   Lin, H. K. *et al.* Portable filter-based microdevice for detection and characterization of circulating tumor cells. *Clinical cancer research : an official journal of the American Association for Cancer Research* **16**, 5011-5018, doi:10.1158/1078-0432.CCR-10-1105 [doi] (2010).

87   Zheng, S. *et al.* 3D microfilter device for viable circulating tumor cell (CTC) enrichment from blood. *Biomed Microdevices* **13**, 203-213, doi:10.1007/s10544-010-9485-3 (2011).

88   Hosokawa, M. *et al.* Size-selective microcavity array for rapid and efficient detection of circulating tumor cells. *Analytical chemistry* **82**, 6629-6635 (2010).

89   Lim, L. S. *et al.* Microsieve lab-chip device for rapid enumeration and fluorescence in situ hybridization of circulating tumor cells. *Lab Chip* **12**, 4388-4396, doi:10.1039/c2lc20750h (2012).

90   Tan, S. J. *et al.* Versatile label free biochip for the detection of circulating tumor cells from peripheral blood in cancer patients. *Biosensors & bioelectronics* **26**, 1701-1705, doi:10.1016/j.bios.2010.07.054 (2010).

91   Zhou, M. D. *et al.* Separable bilayer microfiltration device for viable label-free enrichment of circulating tumour cells. *Sci Rep* **4**, 7392, doi:10.1038/srep07392 (2014).

92   Di Carlo, D., Irimia, D., Tompkins, R. G. & Toner, M. Continuous inertial focusing, ordering, and separation of particles in microchannels. *Proceedings of the National Academy of Sciences of the United States of America* **104**, 18892-18897, doi:0704958104 [pii] (2007).

93   Russom, A. *et al.* Differential inertial focusing of particles in curved low-aspect-ratio microchannels. *New journal of physics* **11**, 075025 (2009).

94   Choi, S., Ku, T., Song, S., Choi, C. & Park, J. K. Hydrophoretic high-throughput selection of platelets in physiological shear-stress range. *Lab Chip* **11**, 413-418, doi:10.1039/c0lc00148a (2011).

95   Davis, J. A. *et al.* Deterministic hydrodynamics: taking blood apart. *Proc Natl Acad Sci U S A* **103**, 14779-14784, doi:10.1073/pnas.0605967103 (2006).

96   Lee, A. *et al.* All-in-one centrifugal microfluidic device for size-selective circulating tumor cell isolation with high purity. *Anal Chem* **86**, 11349-11356, doi:10.1021/ac5035049 (2014).

97   Eramo, A. *et al.* Identification and expansion of the tumorigenic lung cancer stem cell population. *Cell death and differentiation* **15**, 504-514, doi:10.1038/sj.cdd.4402283 (2008).

98   Kim, T. H., Yoon, H. J., Stella, P. & Nagrath, S. Cascaded spiral microfluidic device for deterministic and high purity continuous separation of circulating tumor cells. *Biomicrofluidics* **8**, 064117, doi:10.1063/1.4903501 (2014).

164

99   Sollier, E. *et al.* Size-selective collection of circulating tumor cells using Vortex technology. *Lab on a Chip* **14**, 63-77, doi:10.1039/c3lc50689d (2014).

100   Hyun, K. A., Kwon, K., Han, H., Kim, S. I. & Jung, H. I. Microfluidic flow fractionation device for label-free isolation of circulating tumor cells (CTCs) from breast cancer patients. *Biosensors & bioelectronics* **40**, 206-212, doi:10.1016/j.bios.2012.07.021 (2013).

101   Warkiani, M. E. *et al.* Slanted spiral microfluidics for the ultra-fast, label-free isolation of circulating tumor cells. *Lab Chip* **14**, 128-137, doi:10.1039/c3lc50617g (2014).

102   Warkiani, M. E. *et al.* An ultra-high-throughput spiral microfluidic biochip for the enrichment of circulating tumor cells. *Analyst* **139**, 3245-3255, doi:10.1039/c4an00355a (2014).

103   Khoo, B. L. *et al.* Clinical validation of an ultra high-throughput spiral microfluidics for the detection and enrichment of viable circulating tumor cells. *PLoS One* **9**, e99409, doi:10.1371/journal.pone.0099409 (2014).

104   Becker, F. F. *et al.* Separation of human breast cancer cells from blood by differential dielectric affinity. *Proceedings of the National Academy of Sciences of the United States of America* **92**, 860-864 (1995).

105   Shim, S. *et al.* Antibody-independent isolation of circulating tumor cells by continuous-flow dielectrophoresis. *Biomicrofluidics* **7**, 11807, doi:10.1063/1.4774304 (2013).

106   Choi, H. *et al.* A label-free DC impedance-based microcytometer for circulating rare cancer cell counting. *Lab Chip* **13**, 970-977, doi:10.1039/c2lc41376k (2013).

107   Cheung, K. J. *et al.* Polyclonal breast cancer metastases arise from collective dissemination of keratin 14-expressing tumor cell clusters. *Proc Natl Acad Sci U S A* **113**, E854-863, doi:10.1073/pnas.1508541113 (2016).

108   Marrinucci, D. *et al.* Cytomorphology of circulating colorectal tumor cells: a small case series. *Journal of oncology* **2010** (2010).

109   Gossett, D. R. *et al.* Label-free cell separation and sorting in microfluidic systems. *Analytical and bioanalytical chemistry* **397**, 3249-3267, doi:10.1007/s00216-010-3721-9 (2010).

110   Yu, Z. T., Aw Yong, K. M. & Fu, J. Microfluidic blood cell sorting: now and beyond. *Small* **10**, 1687-1703, doi:10.1002/smll.201302907 (2014).

111   Stott, S. L. *et al.* Isolation and characterization of circulating tumor cells from patients with localized and metastatic prostate cancer. *Sci Transl Med* **2**, 25ra23, doi:2/25/25ra23 [pii]10.1126/scitranslmed.3000403 (2010).

112   Fan, Z. H. & Beebe, D. J. Lab on a chip and circulating tumor cells. *Lab Chip* **14**, 12-13, doi:10.1039/c3lc90125d (2014).

113   Yoon, H. J. *et al.* Tunable Thermal-Sensitive Polymer-Graphene Oxide Composite for Efficient Capture and Release of Viable Circulating Tumor Cells. *Adv Mater*, doi:10.1002/adma.201600658 (2016).

114   Hodgkinson, C. L. *et al.* Tumorigenicity and genetic profiling of circulating tumor cells in small-cell lung cancer. *Nat Med* **20**, 897-903, doi:10.1038/nm.3600 (2014).

115   Yu, M. *et al.* Ex vivo culture of circulating breast tumor cells for individualized testing of drug susceptibility. *Science* **345**, 216-220 (2014).

116   Cayrefourcq, L. *et al.* Establishment and characterization of a cell line from human circulating colon cancer cells. *Cancer Res* **75**, 892-901, doi:10.1158/0008-5472.CAN-14-2613 (2015).

117   Alix-Panabières, C. & Pantel, K. Challenges in circulating tumour cell research. *Nature Reviews Cancer* **14**, 623-631 (2014).

118   Joosse, S. A., Gorges, T. M. & Pantel, K. Biology, detection, and clinical implications of circulating tumor cells. *EMBO molecular medicine* **7**, 1-11 (2015).

119   Zhang, Z., Ramnath, N. & Nagrath, S. Current Status of CTCs as Liquid Biopsy in Lung Cancer and Future Directions. *Front Oncol* **5**, 209, doi:10.3389/fonc.2015.00209 (2015).

120   de Bono, J. S. *et al.* Circulating tumor cells predict survival benefit from treatment in metastatic castration-resistant prostate cancer. *Clin Cancer Res* **14**, 6302-6309, doi:10.1158/1078-0432.CCR-08-0872 (2008).

121   Smirnov, D. A. *et al.* Global gene expression profiling of circulating tumor cells. *Cancer Res* **65**, 4993-4997, doi:10.1158/0008-5472.CAN-04-4330 (2005).

122   Leversha, M. A. *et al.* Fluorescence in situ hybridization analysis of circulating tumor cells in metastatic prostate cancer. *Clin Cancer Res* **15**, 2091-2097, doi:10.1158/1078-0432.CCR-08-2036 (2009).

123   Attard, G. *et al.* Characterization of ERG, AR and PTEN gene status in circulating tumor cells from patients with castration-resistant prostate cancer. *Cancer Res* **69**, 2912-2918, doi:10.1158/0008-5472.CAN-08-3667 (2009).

124   Chimonidou, M., Kallergi, G., Georgoulias, V., Welch, D. R. & Lianidou, E. S. Breast cancer metastasis suppressor-1 promoter methylation in primary breast tumors and corresponding circulating tumor cells. *Mol Cancer Res* **11**, 1248-1257, doi:10.1158/1541-7786.MCR-13-0096 (2013).

125   Chimonidou, M., Strati, A., Malamos, N., Georgoulias, V. & Lianidou, E. S. SOX17 promoter methylation in circulating tumor cells and matched cell-free DNA isolated from plasma of patients with breast cancer. *Clin Chem* **59**, 270-279, doi:10.1373/clinchem.2012.191551 (2013).

126   Malara, N. *et al.* Folic acid functionalized surface highlights 5-methylcytosine-genomic content within circulating tumor cells. *Small* **10**, 4324-4331, doi:10.1002/smll.201400498 (2014).

127   Riethdorf, S. & Pantel, K. Advancing personalized cancer therapy by detection and characterization of circulating carcinoma cells. *Ann N Y Acad Sci* **1210**, 66-77, doi:10.1111/j.1749-6632.2010.05779.x (2010).

128   Yu, M. *et al.* Cancer therapy. Ex vivo culture of circulating breast tumor cells for individualized testing of drug susceptibility. *Science* **345**, 216-220, doi:10.1126/science.1253533 (2014).

129   Cristofanilli, M. *et al.* Circulating Tumor Cells: A Novel Prognostic Factor for Newly Diagnosed Metastatic Breast Cancer. *Journal of Clinical Oncology* **23**, 1420-1430, doi:10.1200/jco.2005.08.140 (2005).

130   Yagata, H. *et al.* Evaluation of circulating tumor cells in patients with breast cancer: multi-institutional clinical trial in Japan. *Int J Clin Oncol* **13**, 252-256, doi:10.1007/s10147-007-0748-9 (2008).

131   Kurihara, T. *et al.* Detection of circulating tumor cells in patients with pancreatic cancer: a preliminary result. *J Hepatobiliary Pancreat Surg* **15**, 189-195, doi:10.1007/s00534-007-1250-5 (2008).

132   Jonathan, D. Rapid translation of circulating tumor cell biomarkers into clinical practice: technology development, clinical needs and regulatory requirements. *Lab on a Chip* **14**, 24-31 (2014).

133   Paterlini-Brechot, P. & Benali, N. L. Circulating tumor cells (CTC) detection: clinical impact and future directions. *Cancer letters* **253**, 180-204 (2007).

134   Liu, Z. *et al.* Rapid isolation of cancer cells using microfluidic deterministic lateral displacement structure. *Biomicrofluidics* **7**, 11801, doi:10.1063/1.4774308 (2013).

135   Sun, J. *et al.* Double spiral microchannel for label-free tumor cell separation and enrichment. *Lab on a Chip* **12**, 3952-3960 (2012).

136   Karabacak, N. M. *et al.* Microfluidic, marker-free isolation of circulating tumor cells from blood samples. *Nature protocols* **9**, 694-710 (2014).

137   Silberberg, G. S. a. A. Behaviour of macroscopic rigid spheres in Poiseuille flow. *Journal of Fluid Mechanics* **14**, 22, doi:10.1017/S0022112062001111 (1962).

138   G, S. & A, S. Radial Particle Displacements in Poiseuille Flow of Suspensions. *Nature* **189**, 209-210, doi:10.1038/189209a0 (1961).

139   Lee, W., Amini, H., Stone, H. A. & Di Carlo, D. Dynamic self-assembly and control of microfluidic particle crystals. *Proceedings of the National Academy of Sciences* **107**, 22413-22418, doi:10.1073/pnas.1010297107 (2010).

140   ASMOLOV, E. S. The inertial lift on a spherical particle in a plane Poiseuille flow at large channel Reynolds number. *Journal of Fluid Mechanics* **381**, 63-87, doi:doi:10.1017/S0022112098003474 (1999).

141   Gossett, D. R. & Carlo, D. D. Particle Focusing Mechanisms in Curving Confined Flows. *Analytical Chemistry* **81**, 8459-8465, doi:10.1021/ac901306y (2009).

142   Martel, J. M. & Toner, M. Particle Focusing in Curved Microfluidic Channels. *Sci. Rep.* **3**, doi:10.1038/srep03340 (2013).

143   Liu, S. & Wicha, M. S. Targeting breast cancer stem cells. *Journal of clinical oncology : official journal of the American Society of Clinical Oncology* **28**, 4006-4012, doi:10.1200/JCO.2009.27.5388
JCO.2009.27.5388 [pii] (2010).

144   Rahib, L. *et al.* Projecting cancer incidence and deaths to 2030: the unexpected burden of thyroid, liver, and pancreas cancers in the United States. *Cancer Res* **74**, 2913-2921, doi:10.1158/0008-5472.can-14-0155 (2014).

145   Hezel, A. F., Kimmelman, A. C., Stanger, B. Z., Bardeesy, N. & Depinho, R. A. Genetics and biology of pancreatic ductal adenocarcinoma. *Genes & development* **20**, 1218-1249, doi:10.1101/gad.1415606 (2006).

146   Kuzu, U. B. *et al.* The diagnostic value of brush cytology alone and in combination with tumor markers in pancreaticobiliary strictures. *Gastroenterology research and practice* **2015**, 580254, doi:10.1155/2015/580254 (2015).

147   Lee, J. G. & Leung, J. Tissue sampling at ERCP in suspected pancreatic cancer. *Gastrointestinal endoscopy clinics of North America* **8**, 221-235 (1998).

148   Noh, K. W. & Wallace, M. B. Endoscopic ultrasound-guided fine-needle aspiration in the diagnosis and staging of pancreatic adenocarcinoma. *MedGenMed : Medscape general medicine* **7**, 15 (2005).

149   Pantel, K., Brakenhoff, R. H. & Brandt, B. Detection, clinical relevance and specific biological properties of disseminating tumour cells. *Nature reviews. Cancer* **8**, 329-340, doi:10.1038/nrc2375 (2008).

150   Allard, W. J. *et al.* Tumor cells circulate in the peripheral blood of all major carcinomas but not in healthy subjects or patients with nonmalignant diseases. *Clinical cancer research : an official journal of the American Association for Cancer Research* **10**, 6897-6904, doi:10.1158/1078-0432.ccr-04-0378 (2004).

151   Rhim, A. D. *et al.* EMT and dissemination precede pancreatic tumor formation. *Cell* **148**, 349-361, doi:10.1016/j.cell.2011.11.025 (2012).

152   Youngwirth, L. M. *et al.* Nationwide trends and outcomes associated with neoadjuvant therapy in pancreatic cancer: An analysis of 18 243 patients. *Journal of surgical oncology*, doi:10.1002/jso.24630 (2017).

153   de Geus, S. W. *et al.* Neoadjuvant therapy versus upfront surgery for resected pancreatic adenocarcinoma: A nationwide propensity score matched analysis. *Surgery* **161**, 592-601, doi:10.1016/j.surg.2016.08.040 (2017).

154   Paterlini-Brechot, P. & Benali, N. L. Circulating tumor cells (CTC) detection: clinical impact and future directions. *Cancer letters* **253**, 180-204, doi:10.1016/j.canlet.2006.12.014 (2007).

155   Jin, C. *et al.* Technologies for label-free separation of circulating tumor cells: from historical foundations to recent developments. *Lab on a chip* **14**, 32-44, doi:10.1039/c3lc50625h (2014).

156   Lara, O., Tong, X., Zborowski, M. & Chalmers, J. J. Enrichment of rare cancer cells through depletion of normal cells using density and flow-through, immunomagnetic cell separation. *Experimental hematology* **32**, 891-904, doi:10.1016/j.exphem.2004.07.007 (2004).

157   Riethdorf, S. *et al.* Detection of circulating tumor cells in peripheral blood of patients with metastatic breast cancer: a validation study of the CellSearch system.

Clinical cancer research : an official journal of the American Association for Cancer Research **13**, 920-928, doi:10.1158/1078-0432.ccr-06-1695 (2007).

158 Cohen, S. J. *et al.* Prognostic significance of circulating tumor cells in patients with metastatic colorectal cancer. *Ann Oncol* **20**, 1223-1229, doi:10.1093/annonc/mdn786 (2009).

159 Hayes, D. F. *et al.* Circulating tumor cells at each follow-up time point during therapy of metastatic breast cancer patients predict progression-free and overall survival. *Clinical cancer research : an official journal of the American Association for Cancer Research* **12**, 4218-4224, doi:10.1158/1078-0432.ccr-05-2821 (2006).

160 Krebs, M. G. *et al.* Evaluation and prognostic significance of circulating tumor cells in patients with non-small-cell lung cancer. *Journal of clinical oncology : official journal of the American Society of Clinical Oncology* **29**, 1556-1563, doi:10.1200/JCO.2010.28.7045 (2011).

161 Moreno, J. G. *et al.* Circulating tumor cells predict survival in patients with metastatic prostate cancer. *Urology* **65**, 713-718, doi:10.1016/j.urology.2004.11.006 (2005).

162 Bidard, F. C. *et al.* Circulating tumor cells in locally advanced pancreatic adenocarcinoma: the ancillary CirCe 07 study to the LAP 07 trial. *Annals of oncology : official journal of the European Society for Medical Oncology / ESMO* **24**, 2057-2061, doi:10.1093/annonc/mdt176 (2013).

163 Wellner, U., Brabletz, T. & Keck, T. ZEB1 in Pancreatic Cancer. *Cancers* **2**, 1617-1628 (2010).

164 Budd, G. T. *et al.* Circulating tumor cells versus imaging—predicting overall survival in metastatic breast cancer. *Clinical Cancer Research* **12**, 6403-6409 (2006).

165 Tjensvoll, K., Nordgård, O. & Smaaland, R. Circulating tumor cells in pancreatic cancer patients: Methods of detection and clinical implications. *International Journal of Cancer* **134**, 1-8 (2014).

166 Serrano, M. J., Sanchez-Rovira, P., Delgado-Rodriguez, M. & Gaforio, J. J. Detection of circulating tumor cells in the context of treatment: prognostic value in breast cancer. *Cancer Biol Ther* **8**, 671-675 (2009).

167 Nelson, N. J. Circulating tumor cells: will they be clinically useful? *J Natl Cancer Inst* **102**, 146-148, doi:10.1093/jnci/djq016 (2010).

168 Botteri, E. *et al.* Modeling the relationship between circulating tumour cells number and prognosis of metastatic breast cancer. *Breast Cancer Res Treat* **122**, 211-217, doi:10.1007/s10549-009-0668-7 (2010).

169 Luo, M., Brooks, M. & Wicha, M. S. Epithelial-mesenchymal plasticity of breast cancer stem cells: implications for metastasis and therapeutic resistance. *Curr Pharm Des* **21**, 1301-1310 (2015).

170   Di Palma, S. & Bodenmiller, B. Unraveling cell populations in tumors by single-cell mass cytometry. *Curr Opin Biotechnol* **31**, 122-129, doi:10.1016/j.copbio.2014.07.004 (2015).

171   Nakshatri, H., Srour, E. F. & Badve, S. Breast cancer stem cells and intrinsic subtypes: controversies rage on. *Curr Stem Cell Res Ther* **4**, 50-60 (2009).

172   Johnson, E. S., Anand, R. K. & Chiu, D. T. Improved detection by ensemble-decision aliquot ranking of circulating tumor cells with low numbers of a targeted surface antigen. *Anal Chem* **87**, 9389-9395, doi:10.1021/acs.analchem.5b02241 (2015).

173   Phillips, K. G., Kuhn, P. & McCarty, O. J. Physical biology in cancer. 2. The physical biology of circulating tumor cells. *Am J Physiol Cell Physiol* **306**, C80-88, doi:10.1152/ajpcell.00294.2013 (2014).

174   Hur, S. C., Mach, A. J. & Di Carlo, D. High-throughput size-based rare cell enrichment using microscale vortices. *Biomicrofluidics* **5**, 22206, doi:10.1063/1.3576780 (2011).

175   Mohamed, H. *et al.* Development of a rare cell fractionation device: application for cancer detection. *IEEE Trans Nanobioscience* **3**, 251-256 (2004).

176   Kumar, A., Bhanja, A., Bhattacharyya, J. & Jaganathan, B. G. Multiple roles of CD90 in cancer. *Tumour Biol* **37**, 11611-11622, doi:10.1007/s13277-016-5112-0 (2016).

177   Zhu, L., Zhang, W., Wang, J. & Liu, R. Evidence of CD90+CXCR4+ cells as circulating tumor stem cells in hepatocellular carcinoma. *Tumour Biol* **36**, 5353-5360, doi:10.1007/s13277-015-3196-6 (2015).

178   Zhu, J., Thakolwiboon, S., Liu, X., Zhang, M. & Lubman, D. M. Overexpression of CD90 (Thy-1) in pancreatic adenocarcinoma present in the tumor microenvironment. *PLoS One* **9**, e115507, doi:10.1371/journal.pone.0115507 (2014).

179   Foygel, K. *et al.* Detection of pancreatic ductal adenocarcinoma in mice by ultrasound imaging of thymocyte differentiation antigen 1. *Gastroenterology* **145**, 885-894 e883, doi:10.1053/j.gastro.2013.06.011 (2013).

180   Siegel, R. L., Miller, K. D. & Jemal, A. Cancer statistics, 2016. *CA Cancer J Clin* **66**, 7-30, doi:10.3322/caac.21332 (2016).

181   Lockhart, A. C., Rothenberg, M. L. & Berlin, J. D. Treatment for pancreatic cancer: current therapy and continued progress. *Gastroenterology* **128**, 1642-1654 (2005).

182   Sawicka, E., Mirończuk, A., Wojtukiewicz, M. Z. & Sierko, E. Chemoradiotherapy for locally advanced pancreatic cancer patients: is it still an open question? *Contemporary Oncology* **20**, 102 (2016).

183   Herreros-Villanueva, M. & Bujanda, L. Non-invasive biomarkers in pancreatic cancer diagnosis: what we need versus what we have. *Annals of translational medicine* **4** (2016).

184   Sieuwerts, A. M. *et al.* Anti-epithelial cell adhesion molecule antibodies and the detection of circulating normal-like breast tumor cells. *Journal of the National Cancer Institute* **101**, 61-66, doi:10.1093/jnci/djn419 [doi] (2009).

185   Königsberg, R. *et al.* Detection of EpCAM positive and negative circulating tumor cells in metastatic breast cancer patients. *Acta Oncologica* **50**, 700-710 (2011).

186   Murlidhar, V., Rivera-Baez, L. & Nagrath, S. Affinity Versus Label-Free Isolation of Circulating Tumor Cells: Who Wins? *Small* **12**, 4450-4463, doi:10.1002/smll.201601394 (2016).

187   Hyun, K.-A. & Jung, H.-I. Advances and critical concerns with the microfluidic enrichments of circulating tumor cells. *Lab on a Chip* **14**, 45-56 (2014).

188   Nagrath, S., Jack, R. M., Sahai, V. & Simeone, D. M. Opportunities and Challenges for Pancreatic Circulating Tumor Cells. *Gastroenterology* **151**, 412-426 (2016).

189   Kulemann, B. *et al.* Circulating tumor cells found in patients with localized and advanced pancreatic cancer. *Pancreas* **44**, 547-550 (2015).

190   Catenacci, D. V. *et al.* Acquisition of portal venous circulating tumor cells from patients with pancreaticobiliary cancers by endoscopic ultrasound. *Gastroenterology* **149**, 1794-1803. e1794 (2015).

191   Bobek, V., Gurlich, R., Eliasova, P. & Kolostova, K. Circulating tumor cells in pancreatic cancer patients: enrichment and cultivation. *World Journal of Gastroenterology: WJG* **20**, 17163 (2014).

192   Gao, Y. *et al.* Clinical significance of pancreatic circulating tumor cells using combined negative enrichment and immunostaining-fluorescence in situ hybridization. *Journal of Experimental & Clinical Cancer Research* **35**, 66 (2016).

193   Kulemann, B. *et al.* KRAS mutations in pancreatic circulating tumor cells: a pilot study. *Tumor Biology* **37**, 7547-7554 (2016).

194   Cappelletti, V. *et al.* Circulating Biomarkers for Prediction of Treatment. *J Natl Cancer Inst Monogr* **2015**, 51 (2015).

195   Kalluri, R. & Weinberg, R. A. The basics of epithelial-mesenchymal transition. *The Journal of clinical investigation* **119**, 1420-1428, doi:10.1172/JCI39104 [doi] (2009).

196   Karamitopoulou, E. Role of epithelial-mesenchymal transition in pancreatic ductal adenocarcinoma: is tumor budding the missing link? *Front Oncol* **3**, 221, doi:10.3389/fonc.2013.00221 (2013).

197   Roche. *Ventana DISCOVERY ULTRA*, <http://www.ventana.com/product/page?view=discoveryultra> (

198   Villa-Diaz, L. G. *et al.* Synthetic polymer coatings for long-term growth of human embryonic stem cells. *Nat Biotechnol* **28**, 581-583, doi:10.1038/nbt.1631 (2010).

199   McShane, L. M. *et al.* REporting recommendations for tumor MARKer prognostic studies (REMARK). *Breast Cancer Res Treat* **100**, 229-235, doi:10.1007/s10549-006-9242-8 (2006).

200   Pasquinelli, A. E., Hunter, S. & Bracht, J. MicroRNAs: a developing story. *Curr Opin Genet Dev* **15**, 200-205, doi:10.1016/j.gde.2005.01.002 (2005).

201   Gregory, P. A. *et al.* The miR-200 family and miR-205 regulate epithelial to mesenchymal transition by targeting ZEB1 and SIP1. *Nat Cell Biol* **10**, 593-601, doi:10.1038/ncb1722 (2008).

202   Burk, U. *et al.* A reciprocal repression between ZEB1 and members of the miR-200 family promotes EMT and invasion in cancer cells. *EMBO Rep* **9**, 582-589, doi:10.1038/embor.2008.74 (2008).

203   Di Carlo, D., Irimia, D., Tompkins, R. G. & Toner, M. Continuous inertial focusing, ordering, and separation of particles in microchannels. *Proceedings of the National Academy of Sciences* **104**, 18892-18897, doi:10.1073/pnas.0704958104 (2007).

204   Wendel, M. *et al.* Fluid biopsy for circulating tumor cell identification in patients with early-and late-stage non-small cell lung cancer: a glimpse into lung cancer biology. *Physical biology* **9**, 016005, doi:10.1088/1478-3967/9/1/016005 (2012).

205   Ruiz, C. *et al.* Limited genomic heterogeneity of circulating melanoma cells in advanced stage patients. *Physical biology* **12**, 016008, doi:10.1088/1478-3975/12/1/016008 (2015).

206   Talasaz, A. H. *et al.* Isolating highly enriched populations of circulating epithelial cells and other rare cells from blood using a magnetic sweeper device. *Proc Natl Acad Sci U S A* **106**, 3970-3975, doi:10.1073/pnas.0813188106

        0813188106 [pii] (2009).

207   Zhang, L. *et al.* The identification and characterization of breast cancer CTCs competent for brain metastasis. *Science translational medicine* **5**, 180ra148, doi:10.1126/scitranslmed.3005109 [doi] (2013).

208   Pailler, E. *et al.* Detection of circulating tumor cells harboring a unique ALK rearrangement in ALK-positive non-small-cell lung cancer. *Journal of clinical oncology : official journal of the American Society of Clinical Oncology* **31**, 2273-2281, doi:10.1200/JCO.2012.44.5932 (2013).

209   Maioli, E. *et al.* Critical Appraisal of the MTT Assay in the Presence of Rottlerin and Uncouplers. *Biological procedures online* **11**, 227-240 (2009).